THE ASTROPHYSICAL JOURNAL SUPPLEMENT SERIES, 71:817–869, 1989 December

EVOLUTIONARY POPULATION SYNTHESIS IN STELLAR SYSTEMS. I. A GLOBAL APPROACH

ALBERTO BUZZONI
Osservatorio Astronomico di Brera, Milano, Italy
Received 1988 December 1; accepted 1989 May 12

ABSTRACT

A new grid of 450 theoretical models for old simple stellar populations (SSPs) is presented. Evolutionary synthesis explores the influence of relevant parameters such as age, chemical composition, initial mass function, and stellar mass loss, on the integrated spectral energy distribution (SED). Ages range between 4 and 18 Gyr, and the metallicity Z ranges from 0.0001 to 0.03, with helium content $Y = 0.23$ and 0.25, respectively. Three values are considered for the initial mass function, assumed as a power law, $N_{(M)} \propto M^{-s}$; $s = 1.35$, 2.35, and 3.35.

The computational code takes into account in a quantitative way the contributions from all the relevant stellar evolutionary phases according to the theory of the stellar evolution. Thus late stages in the life of low-mass stars, such as the horizontal branch and the asymptotic and post–asymptotic giant branches, are accounted for. Furthermore, a simplified treatment for the evolution of the horizontal branch is developed, and the influence of different morphologies are investigated.

Colors and magnitudes in the Johnson *UBVRIJK* system are also reproduced, allowing a self-consistent comparison with the observations of real stellar systems.

Subject headings: galaxies: stellar content — stars: evolution

I. INTRODUCTION

Stellar luminous matter is known to carry the main information describing the structure of the universe. In fact, even inferences on the likely existence of dark matter in the galaxies stem directly from the careful interpretation of features due to the stellar component.

It is fair to say, therefore, that stars play a major role in marking the different hierarchical scale of aggregation in the universe, since they are the basic building blocks of galaxies and other clusters. In this sense the proper comprehension of the evolutionary status of stellar populations is an unavoidable step toward the understanding of the features of the stellar aggregates as a function of cosmic time. This is why evolutionary population synthesis (EPS) enters in an effective way a variety of problems involving stellar systems under different approaches.

This work is intended to contribute in a basic way to all the problems involving EPS. Its main purpose is to explore the influence of a set of primary parameters, such as the age, the chemical composition, and the initial mass function (IMF) on the expected integral spectral energy distribution (SED), carefully accounting for the requirements stemming from the theory of stellar evolution.

This is an important point, since previous works on EPS systematically missed, in our opinion, a realistic description of the evolutionary scenario by ignoring the contribution from stars in some important stages of their life, such as the horizontal branch (HB), the asymptotic giant branch (AGB), and the post–asymptotic giant branch (PAGB) (Tinsley and Gunn 1976, hereafter TG76; Tinsley 1978; Gunn, Stryker, and Tinsley 1981; Bruzual 1983; Arimoto and Yoshii 1986; Pickles 1985*a*). In some cases this lack was partially compensated for by means of qualitative or semiempirical corrections (Sil'chenko 1983): we believe that a detailed accounting for these stars is now an unavoidable requirement to correctly infer the overall properties of the stellar systems. In this paper, the first of a series of three, we present a new grid of EPS models and focus our attention on the detailed description of the theory and of the operational procedure set up. In what follows, § II is devoted to the theoretical framework and § III to the detailed description of the link of the different stellar evolutionary phases; § IV deals with the model atmospheres and § V with the photometric calibration, in order to calculate colors to be compared with the observations. Finally, in § VI some relevant numerical details of the models are presented, and in § VII we summarize our conclusions.

On the basis of these models, Paper II will discuss the present evolutionary status of the real stellar systems (galaxies and globular clusters). This work will be extended in Paper III, where a detailed application of the present EPS models to the study of the distant galaxies and the related cosmological problems will be attempted.

II. THEORY

a) *Strategy and Basic Requirements*

A crucial requirement to be fulfilled in the EPS is the correct evaluation of the partition of the stars among the different evolutionary branches in the H-R diagram. We know that star counts must be proportional to the lifetimes in all the post–main-sequence (PMS) phases, while they depend primarily on the IMF in the main sequence (MS). Two different procedures have then to be followed, and continuity on the H-R diagram has to be ensured. In this section we will stress some relevant points of the theory, first sketched by

TG76 and then widely discussed in Renzini (1981), Buzzoni (1982), Renzini and Buzzoni (1983*a*, *b*; 1986, hereafter RB86).

In the case of a single generation of coeval and chemically homogeneous stars (which we call a simple stellar population [SSP]), we adopt an IMF in the canonical form:

$$\delta N = N_{(M)}\delta M = AM^{-s}\delta M, \tag{1}$$

with the Salpeter exponent $s = 2.35$ for the empirical counts in the solar neighborhood. If $\delta M \ll M$, the right-hand side of this equation gives the number of stars on the MS about the mass M, per bin of width δM. The coefficient A in equation (1) is a normalization factor possibly related to the star formation rate (SFR), which depends on time. Since we are considering single burst populations, for which the SFR is virtually a δ-function, A is a constant related to the total number of stars ($N_{\rm tot}$) or the total mass ($M_{\rm tot}$) of the SSP in a simple way:

$$A = (1-s)\frac{N_{\rm tot}}{\left[M^{1-s}\right]_{M_l}^{M_u}}, \quad s \neq 1, \tag{2a}$$

$$A = \frac{N_{\rm tot}}{\ln\left(M_u/M_l\right)}, \qquad s = 1, \tag{2b}$$

or

$$A = (2-s)\frac{M_{\rm tot}}{\left[M^{2-s}\right]_{M_l}^{M_u}}, \quad s \neq 2, \tag{3a}$$

$$A = \frac{M_{\rm tot}}{\ln\left(M_u/M_l\right)}, \qquad s = 2, \tag{3b}$$

where M_u and M_l are the masses of the upper and lower cutoffs of the IMF.

If the mass of the stars at some relevant points in the H-R diagram (for example, at the turnoff point [TO]) is a function of the time, we can write equation (1) as

$$\delta N = AM^{-s}\left|\frac{dM}{dt}\right|\delta t. \tag{4}$$

Equation (4) rests on the basic assumption that the time interval δt is short enough to ensure a variation δM on mass M such as $\delta M \ll M$. It is worth emphasizing the fully new and powerful inferences stemming from an application of equation (4) to the PMS star counts. In fact, if we consider, for instance, the dependence on time of the mass of the stars evolving across the TO, i.e., $dM_{\rm TO}/dt$, we find from the models that it is of the same order as $M_{\rm TO}/T$, where T is the age of the population for a given $M_{\rm TO}$. Moreover, the PMS evolutionary lifetime, $t_{\rm PMS}$, for a star of mass $M_{\rm TO}$ is always much shorter than T (the ratio $t_{\rm PMS}/T$ ranges between $\frac{1}{3}$ and $\frac{1}{5}$; see, for instance, RB86). This means, in other words, that the difference δM in the initial mass between dying stars and those leaving the TO at a given age can be evaluated as $\delta M = t_{\rm PMS}(dM_{\rm TO}/dt) \sim M_{\rm TO}(t_{\rm PMS}/T)$, thus ensuring that $\delta M/M \ll 1$.

We conclude that in a SSP we are dealing at any time with a PMS evolution of stars of initial mass nearly identical to $M_{\rm TO}$. Thus equation (4) provides the right partition of the stars along the different evolutionary branches, once we divide them into discrete bins of known duration δt. We can also write

$$\delta N_{\rm PMS} = b\,\delta t_{\rm PMS}, \tag{5}$$

where

$$b = AM_{\rm TO}^{-s}\left|\frac{dM_{\rm TO}}{dt}\right| \tag{6}$$

is the "evolutionary flux" of the SSP.

Another important quantity, equivalent to b but more useful in the practical application, is the "specific evolutionary flux" defined as

$$B = b/L_{\rm tot}, \tag{7}$$

where $L_{\rm tot}$ is the total (bolometric) luminosity of a SSP having a given b flux. Since $L_{\rm tot}$ scales with the same value of A as b does, their ratio is an intrinsic parameter of the SSP allowing a direct link between stars counts and evolutionary lifetimes for real populations of integral observed luminosity L_*:

$$N_{\rm PMS} = BL_*t_{\rm PMS}. \tag{8}$$

As shown in RB86, B does not depend very strongly on the other parameters, and it can be regarded almost as a cosmic constant. Its value is about $1.7 \pm 0.4\ 10^{-11}\ L_\odot^{-1}\ {\rm yr}^{-1}$.

Concerning the inner consistency of the EPS models, there is another important condition to be fulfilled. Equation (5) implies that the contribution in bolometric luminosity coming from the stars in the PMS phases ($L_{\rm PMS}$) is given by

$$L_{\rm PMS} = b\int^{\rm PMS} L_t\,dt, \tag{9}$$

where L_t is taken over the evolutionary track of a star of mass $M_{\rm TO}$. The physical meaning of equation (9) is that the PMS luminosity of a SSP is simply proportional to the nuclear (and gravitational) fuel available to stars having $M = M_{\rm TO}$. This condition, originally stated in TG76 and now known as the "fuel consumption theorem" (FCT; RB86), is a powerful tool to check the consistency of the monochromatic contribution from stars in some exotic phases, such as, for instance, the AGB. In these cases we can reinforce our approximate knowledge of the evolutionary path of the stars in the H-R diagram by means of the constraints on their fuel available, which is usually rather well known from the stellar models.

b) SSPs and Real Stellar Populations

Theoretical SSPs closely resemble the real cases of single burst SFRs, but in principle all arbitrary complex histories can be constructed by properly combining these basic models.

It could be asked whether or not it is correct to identify a single burst SFR, producing stars in a short (but finite) time, with a virtually instantaneous generation of a theoretical SSP. In a general way a real stellar population observed at the time T and at the wavelength λ is the convolution of some SSPs weighted by their SFR. Obviously, if SFR $= \delta_{(T)}$, by definition the population is a SSP.

In the general case that the SFR $\neq 0$ in a "short" time $\tau \ll T$, our δ-function simplification holds as long as the expected variation of the SSP *at the relevant wavelength of observation* can be supposed to be negligible over the age interval $[T-\tau, T]$. This condition is usually fairly well satisfied. Complications can arise only when approaching the creation event (as $T \to \tau$) or in the case of a sudden phase transition in the overall evolutionary status over time scales comparable to τ.

Another question, which deserves more attention in comparing theoretical and observed SEDs, concerns the stochastic fluctuations in the emitted flux due to the discreteness of the real stellar populations. Stochastic fluctuations could play a role, for instance, in globular clusters, despite their some 10^5 stars, a number apparently large enough to ensure a smooth contribution to the total SED (Buzzoni 1988).

Let us assume a sample of $N_{\rm tot}$ stars each having individual luminosity l_i at a given wavelength λ; the Poissonian uncertainty δl_i related to the luminosity l_i of the ith star is expected to be $\delta l_i = l_i$. Summing up over all stars, we get

$$\frac{\delta L_{\rm tot}}{L_{\rm tot}} = \frac{\left(\sum l_i^2\right)^{1/2}}{\sum l_i}, \tag{10}$$

where $L_{\rm tot}$ is the total luminosity of the population at that λ. As a particular case, if all the stars have the same luminosity l, we have

$$\frac{\delta L_{\rm tot}}{L_{\rm tot}} = \frac{1}{\sqrt{N_{\rm tot}}}. \tag{11}$$

A generalization of equations (10) and (11) provides

$$\frac{\delta L_{\rm tot}}{L_{\rm tot}} = \frac{\left(\sum l_i^2\right)^{1/2}}{\sum l_i} = \frac{1}{\sqrt{N_{\rm eff}}}, \tag{12}$$

where $N_{\rm eff}$ can be regarded as the effective number of stars emitting at that wavelength. By definition $N_{\rm eff}$ can never exceed $N_{\rm tot}$, and it is a function of λ depending on the distribution in luminosity and color of the stars of the population. Functions $N_{{\rm eff}(\lambda)}$ are a direct result of our computation, and they provide a useful way to estimate the intrinsic fluctuation in the SED of SSPs.

In Figure 1 we show the synthetic *C-M* diagrams for a SSP closely resembling a typical globular cluster, and the derived function for $N_{\rm eff}$ is displayed in Figure 2. Here $N_{\rm eff}$ has to be scaled for the total bolometric luminosity (in solar units) of the SSP. From the figure one clearly sees that there is a dramatic cutoff in the number of contributors at the short wavelengths ($\lambda \leq 2000$ Å), so that in this range we have to

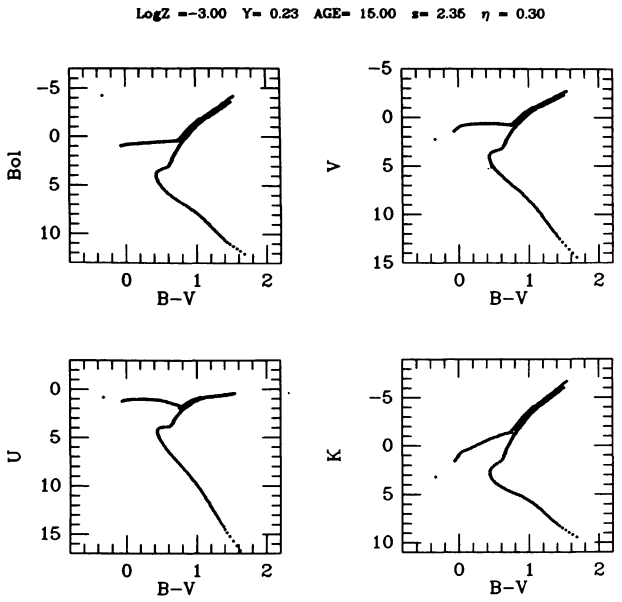

FIG. 1.—*C-M* diagrams for a SSP model resembling a typical globular cluster. Above the figure are noted the distinctive parameters adopted. The diagrams display only the locus of the isochrone and not the number distribution of the stars along it. The isolated point at $B-V=-0.33$ represents the PAGB stars.

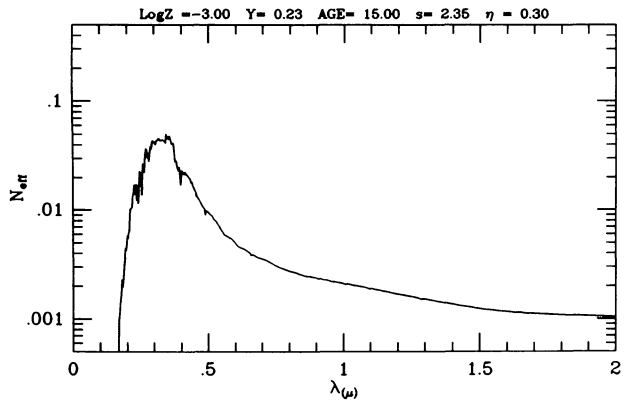

FIG. 2.—Effective number of contributors to the synthetic SED for the SSP displayed in Fig. 1. In order to match real SSPs, $N_{\rm eff}$ has to be scaled for the total bolometric luminosity (in solar units).

expect a large intrinsic spread among clusters *with the same distinctive parameters*. Also, more quiescent color indices such as $U-B$ and $B-V$ are estimated to suffer an intrinsic uncertainty of ± 0.02 and ± 0.05 mag, respectively, assuming a total luminosity of $10^5\ L_\odot$, and an even larger spread is expected for $V-K$: ± 0.11 mag.

The function $N_{{\rm eff}(\lambda)}$ is also a measure of the "opacity" of the stellar systems. From Figure 2 one sees, for example, that there are more than 40 times as many effective contributors to the U band as to the K band. As a result, looking at our hypothetical cluster, we should expect a highly crowded stellar field in the ultraviolet, while a more contrasted plot would

come out in the infrared with just a few bright objects embedded in a faint background. This could help in optimizing the observation of the innermost regions in the core of the globular clusters or in the bulge of the galaxies.

III. INGREDIENTS FOR EPS

An effective approach to EPS requires mainly two sets of data to be properly linked: (1) we need a set of isochrones providing a good representation of the distribution of the stars in the H-R diagram, and (2) we should be able to reproduce the SED of each star along the isochrone in order to take into account all the possible contributors to the total light of the population.

Concerning the isochrones and remembering what is stated in § II, we must ensure continuity in luminosity, temperature, and star counts between the MS (plus subgiant branch [SGB]) and the red giant branch (RGB) and the subsequent phases, for which we use evolutionary tracks at constant mass.

Since we are interested in fully exploring the influence of some primary parameters on the synthetic SED, we organized the grid of the computed models as follows. Metallicity ranges between $0.0001 \leq Z \leq 0.03$. Helium abundance roughly mimics an enrichment in the primeval chemical mixture, with $Y = 0.23$ for the metal-poor populations and $Y = 0.25$ for $Z \geq 0.01$. The first value fits well the theoretical expectations of the big bang nucleosynthesis (Wagoner 1973; Boesgaard and Steigman 1985) and the abundance estimates of globular clusters (Buzzoni *et al.* 1983). The latter ($Y = 0.25$) is probably a realistic estimate of the helium abundance for intermediate and solar-like metallicities. For the sake of homogeneity we have retained this value also for super metal-rich populations, although an enhancement to $Y = 0.30$ would perhaps have been more suitable. However, in this case, an increase of less than 1% is expected, for instance, in the TO temperature of the isochrones, and minor changes are induced in the overall photometric properties of the populations. Three different exponents for the IMF are considered in the range $1.35 \leq s \leq 3.35$. Furthermore, the effects due to stellar mass loss and the morphology of the HB (see later) have been investigated, since they modulate in a not negligible way the synthetic SED. Mass loss is parameterized by means of the coefficient η (Reimers 1975): it ranges from 0.3 to 0.5, around its commonly accepted value of 0.4 resulting from the empirical calibration on Galactic globular clusters (Fusi Pecci and Renzini 1976, 1978).

Ages of the models are chosen to cover old SSPs, dominated by low-mass stars (typically less than 1.3 $M_\odot$): they span from 4 to 18 Gyr. This ensures a great homogeneity in the evolutionary features of the SSPs, since evolution of the stars along the RGB and beyond always takes place with a degenerate He core. It also enables the growth of the RGB and HB as they are known in the Galactic globular clusters. Moreover, a quiescent final fading of the stars as white dwarfs is always expected, avoiding the disruptive supernova event. This age range is also convenient for the study of the galaxies: if we assume present elliptical galaxies to be described by our older models, the evolutionary sequences enable us to follow their evolution back in time until redshift $z \simeq 2$ in a $(H_0, q_0) = (50, 0)$ cosmology.

TABLE 1

GRID FOR CALCULATED SSP MODELS

CHEMICAL COMPOSITION (Z, Y)	AGE (Gyr)							
	4	5	6	8	10	12.5	15	18
(0.0001, 0.23)	...	...	...	x	x	x	x	x
(0.001, 0.23)	...	...	...	x	x	x	x	x
(0.01, 0.25)	x	x	x	x	x	x	x	...
(0.017, 0.25)	x	x	x	x	x	x	x	...
(0.03, 0.25)	x	x	x	x	x	x	x	...

NOTE.—IMF: $s = 1.35, 2.35, 3.35$. Mass loss: $\eta = 0.3$–0.5. HB morphology: R-HB, I-HB, B-HB for age = 8, 10, 12.5, 15, 18; R-HB for age = 4, 5, 6.

In total, more than 450 synthetic models have been calculated as summarized in Table 1, following the procedure described in the next sections to link all the different stellar evolutionary phases.

a) *Main Sequence*

In constructing the models, we used the wide set of isochrones published by VandenBerg and collaborators (VandenBerg 1983, 1985; VandenBerg and Bell 1985; VandenBerg and Laskarides 1987). This set is commonly accepted as the most effective in reproducing the observed features of the *C-M* diagrams of the globular clusters. In particular it seems to account properly for the influence of the stellar convection, increasing the mixing-length parameter α in order to fit the colors of the observed TO and RGB in the clusters. The basic difference between this new set and the most popular one used so far in EPS, i.e., the Yale isochrones (Ciardullo and Demarque 1977), is the fact that by increasing α from 1.0 (as previously used) to 1.5–1.6, stars become slightly bluer. The effect of increasing the efficiency in the convection mimics an increase in the mass of the convective envelope of the stars, thus increasing the effective gravity. This forces stars to reach thermodynamic equilibrium at lower radii and slightly higher temperatures. The shift becomes important where a large convective envelope is present, namely, around the TO for the low-mass stars ($M < 1.5\ M_\odot$) and at the base of the RGB. It increases for high-metallicity mixtures owing to the direct influence of the opacity on the radiative gradient, which constrains convection.

Relevant consequences are induced in the EPS models. It is well known, for instance, that the MS stars are believed to be the main contributors to the short-wavelength emission of the galaxies, since the stars around the TO are usually among the bluest members of a SSP. In fact the comparison of the observed and theoretical SEDs around the 4000 Å break is a very popular procedure to estimate the age of the elliptical galaxies (O'Connell 1980; Pickles 1985*a*; Pickles and Van der Kruit 1988). Therefore, it is clear that synthetic models that miss the right blueness of the MS are expected to underestimate the true age of the galaxies, since younger isochrones are required to fit the observed SED.

Because of their wide spread in temperature, MS stars are effective contributors to all the different bands of the total SED. In particular, the near-infrared could be modulated by

the red dwarfs, especially in the cases of a steep IMF. Since VandenBerg's isochrones start at $M_{bol} \sim +7$ and do not cover the faint tail of the MS, we extended them beyond $M_{bol} \sim +11$ by means of the set of evolutionary tracks for red dwarfs calculated by the same authors (VandenBerg, Hartwick, and Alexander 1983). This choice, among the different sets of tracks available (e.g., Copeland, Jensen, and Jørgensen 1970; Sienkiewicz 1982; Neece 1984; D'Antona and Mazzitelli 1985), has been made essentially for the sake of homogeneity, since the computational code, and in particular the treatment of the opacity, in these stellar models are the same as in VandenBerg's isochrones. This is an important requirement for allowing a good match in temperature between the two sets.

Red dwarfs are almost unevolved stars, and they are still expected to populate the ZAMS; nevertheless, in order to ensure continuity, a little enhancement has been necessary, slightly increasing luminosity and temperature of the dwarfs from their location on the ZAMS. A lower cutoff in mass at $M_l = 0.1\ M_\odot$ has always been adopted for the MS: this should account for the limit envisaged, for instance, for the red dwarfs in the globular clusters (Drukier, Fahlman, and Richer 1988 find $M_l \leq 0.18\ M_\odot$ in M13). It is worth noting that M_l has to be regarded as an effective lower limit for the IMF that compensates for the simplified power law assumed. Tests performed by varying M_l ensure that its influence on the synthetic SED of the SSP is negligible, since only M_{tot} (and then the M/L ratio) is affected.

b) *The Post–Main-Sequence Link*

In accounting for the PMS evolution, great care must be taken to match evolved stars correctly with the bulk of the SSP represented by the MS. Continuity in the star counts has to be guaranteed in order to avoid fatal misinterpretations of the contribution from the bright stars. PMS phases provide roughly two-thirds of the bolometric light of a SSP. They radiate mainly in the infrared, but their contribution at the short wavelengths cannot be neglected when we try to discriminate the age of a SSP from the study of its SED in the blue. Correct scaling of the PMS rests on the basic relations sketched in § II*a*: in particular, by means of equation (5) we are able to convert the extremely thin spread in mass into star counts, through the IMF. As we noted in the previous discussion, the only (crucial) quantity to be known in this regard is the evolutionary flux b. This provides the right scale factor, since it contains the information on the total mass of the SSP, through the constant A of equations (2) and (3). In a sequence of models, A remains constant with varying age, and the evolutionary flux is modulated only by the factor $M_{TO}^{-s}|dM_{TO}/dt|$, which is time-dependent. For the TO derivative we have used an analytical expression which accounts for both VandenBerg's and Yale's isochrones in the range of Table 1. We note in this regard that the systematic differences between the two sets of isochrones do not strongly affect this relation, since the mixing-length parameter works only in the outer layers of low-mass stars and not in their radiative cores, where the nuclear clock resides. Equation (6) can be written as

$$b = AM_{TO}^{-s}(-\theta 10^{\nu-9\theta} t^{\theta-1})\ \mathrm{yr}^{-1}, \qquad (13)$$

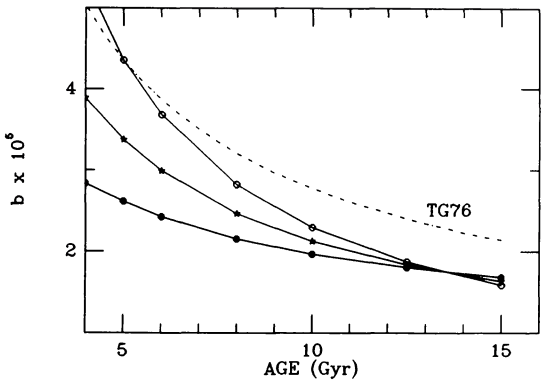

FIG. 3.—Evolutionary flux for a unitary SSP. Models with $(Z, Y) = (0.017, 0.25)$ and three different exponents for the IMF law are assumed: $s = 1.35$ (*open circles*), 2.35 (*stars*), and 3.35 (*filled circles*). For comparison the dot-dash line displays the b-function as derived from TG76 assuming $s = 2.35$ (see text for discussion).

where

$$\theta = 0.467Z + 0.035Y - 0.286,$$

$$\nu = (0.116 - 0.05Y)\log Z + 0.016\log^2 Z - 0.92Y + 0.609,$$

and M_{TO} (in solar units) is estimated directly from the isochrones at the given age t (in years). Figure 3 shows the evolutionary flux of the unitary SSP (i.e., a SSP having $A = 1$) for different distinctive parameters. Also reported in the figure is the evolutionary flux for $s = 2.35$ as derived from TG76 and based on the isochrones by Hejlesen *et al.* (1972). The systematic difference in comparison with TG76 almost entirely resides in the value for M_{TO}, which in Hejlesen's isochrones is $\sim 7\%$ lower than the value given by VandenBerg for the age range considered here. As a direct consequence, TG76 models are expected to overestimate the contribution of all the PMS phases, in particular that of the red giant stars. On the other hand, by a fortunate coincidence, this partially compensates for the lack in their inclusion of HB and AGB stars: two basic ingredients which are taken into account in our code.

c) *Red Giant Branch*

The RGB has been inserted using the wide grid of tracks by Sweigart and Gross (1978). They almost entirely cover the range of the grid of isochrones and follow stars until the tip of their RGB evolution. However, Sweigart and Gross's models were calculated for a mixing-length parameter $\alpha = 1$, since they were an extension of the tracks by Mengel *et al.* (1979) that formed the base for the Yale isochrones. In practice, we simply retained the linear slope of the $\log L$–$\log T$ relation of the RGBs and adjusted the offsets to match VandenBerg's isochrones. Thus the new RGBs become

$$\log T = (-0.13\log Z - 0.092)\log L + \text{offset}. \qquad (14)$$

Evolutionary lifetimes, as well as the value of the luminosity at the tip of the RGB, (L_{fl}), just before the onset of the He burning phase, were maintained as in Sweigart and Gross

(1978). To ease the calculation of our grid of SSP also for intermediate cases, we have analytically fitted both these quantities so that the luminosity function $\Phi_{\log L}$ for a SSP can be written as

$$\Phi_{(\log L)} = b(\ln 10)\,\varepsilon \times 10^{\varepsilon \log L + \zeta}, \tag{15}$$

where

$$\varepsilon = \frac{(-5.05-0.53\log Z)(M_{\rm TO}/3.16)^8 + 0.565Y - 0.11\log Z - 2.732}{\log L_{\rm fl}},$$

$$\zeta = \left(\frac{M_{\rm TO}}{2.63}\right)^8 - 0.773Y - 0.058\log Z + 9.154 + \left(\frac{M_{\rm TO}}{0.5}\right)^{-8},$$

and $\log L_{\rm fl}$ is set by

$$\log L_{\rm fl} = (0.75Y - 0.3)\,M_{\rm TO} + 0.09\log Z - 1.12Y + 3.93. \tag{16}$$

d) *Stellar Mass Loss*

To understand better the role of mass loss in our context, we have to remember that this phenomenon involves the outer layers of the stars, removing fresh fuel from their envelopes. Thus, as soon as the nuclear burning proceeds outward, the evolution is abruptly truncated: this is believed to occur in the AGB phase, as we will see later.

In red giants the mass loss is not expected to affect photometric features of the evolution strongly, but, since the mechanism involves the stellar envelope, the actual mass of the stars reaching the subsequent HB phase is slightly reduced. Moreover, one might guess that mass loss works in different way on each RGB star because of little individual peculiarities, so that the final HB mass should scatter around a mean value. Mass loss was implemented in our models following the relations stated by Reimers (1975). Its rate is assumed to depend on radiation pressure and gravity as

$$\frac{dM}{dt} = -4\times 10^{-13}\eta\frac{L}{gR}\ (M_\odot\ \mathrm{yr})^{-1}, \tag{17}$$

where η is a tuning factor, of the order of the unity, and the other quantities are to be expressed in solar units. Recalling equation (5), we can rearrange equation (17) for our specific aims, evidencing the luminosity function $\Phi_{(\log L)}$ and the actual mass of the stars in RGB:

$$dM = 13.5\frac{\eta\Phi}{bM}10^{1.5\log L}T^{-2}d\log L. \tag{18}$$

A numerical integration of equation (18) over the whole RGB will provide the total mass removed by the stellar wind. This turns out to be usually of the order of $(\eta/2)M_\odot$ for stars in the old SSPs involved here. It is worth emphasizing that the η parameter may be an (unknown) function of some other quantities. Since stellar wind is driven essentially by the opacity of the stellar envelope, one might expect η to increase with increasing metallicity.

In what follows, η will be considered as a parameterized mean value, keeping in mind the possibility that a convenient spread around this value could be present.

e) *Horizontal Branch*

Among the different evolutionary phases of low-mass stars, the HB is certainly one of the most intriguing to be fully understood. A variety of evolutionary tracks are already available, covering a large spread in total mass and metallicity, and computational details seem to be rather well under control (Sweigart and Gross 1976; Seidel, Demarque, and Weinberg 1987; Sweigart 1987). Nevertheless, difficulties still arise in explaining the HB morphology as it is seen, for instance, in the globular clusters. Two requirements need to be fulfilled to reproduce the observations: (1) slightly lower masses than the TO mass and (2) a spread in the actual mass of the HB stars.

Point 1 is easily satisfied once mass loss is taken into account, as previously discussed; point 2 is related to the well-known "second parameter dilemma" and is at present not clearly understood (Sandage and Wildey 1967; Rood 1973; Fusi Pecci and Renzini 1978; Caputo 1983; Crocker, Rood, and O'Connell 1988). Despite our poor knowledge of the mechanism(s) involved, some pertinent statements can be made:

1. Independently of the mechanism at work, the net effect is a spread in color (and then in temperature) along the HB observed in some globular clusters.
2. This effect could be induced by a spread in the actual mass of the stars. The sense is that stars of lower mass populate the HB at the bluer colors.
3. Assuming the real HB to be conveniently described by a distribution of the stars along the ZAHB (Iben and Rood 1970), a narrower spread in mass is required to produce a given spread in color when metallicity increases.
4. HB morphology in the globular clusters seems to be related to the metallicity of the population in the sense that the HB becomes bluer with decreasing Z (but there are some remarkable exceptions dealing with the second-parameter problem: we mention, for instance, the classical cases of NGC 7006 or NGC 6752). Moreover, at the present, no direct observation can support this trend to be effective also for metal-rich populations, say close to the solar values.

Since we believe that simply ignoring the HB problem would be dangerous, we proceed as follows. The reliable knowledge of the evolutionary lifetimes ($t_{\rm HB}$) provides us the total number of stars to be distributed in the HB of each SSP at every age. From Sweigart and Gross (1976) we find

$$\log t_{\rm HB} = \mu\left(\frac{0.54}{M}\right)^6 + \xi, \tag{19}$$

where

$$\mu = 0.761M_c - 0.02\log Z - 0.432 + (0.63 - 0.6M_c)\,Y$$

and

$$\xi = -3.769M_c + 0.02 \log Z + (3.6M_c - 2.21)Y + 9.986.$$

Here t_{HB} is in years and M_c is the He core mass from RGB (Sweigart and Gross 1978):

$$M_c = -0.023M_{TO} - 0.221Y - 0.009 \log Z + 0.534. \quad (20)$$

Let us consider now three typical HB temperature distributions observed in the Galactic globular clusters: a blue HB like that of NGC 6752, a spread HB as in M3, and a red clump as in 47 Tucanae. Now, the big question is, how do these HBs evolve back in time? From a purely formal point of view we can write

$$g_{(\log T')} d \log T' = f_{(\log T)} h_{(\log T, \log T')} d \log T. \quad (21)$$

Equation (21) says that the HB distribution $g_{(\log T')}$ at the age $\tau = t - \delta t$ is evolved in respect to the reference $f_{(\log T)}$ at the time t following these prescriptions:

1. There is a shift redward, due to the fact that young stars are systematically more massive, and therefore they populate preferentially the red edge of the HB at lower temperatures. Thus $\log T' = \log T - \delta \log T$, and the shift $\delta \log T$ is estimated as

$$\delta \log T = \frac{d \log T}{dM} \frac{dM_{TO}}{dt} \delta t, \quad (22)$$

where the first derivative is computed on the basis of the ZAHB models and the second derivative is evaluated at the TO.

2. There is a rebinning effect induced by the function $h_{(\log T, \log T')}$ in equation (21), which behaves like a Jacobian in projecting a bin of width $d \log T$ at the time t into a bin $d \log T'$ wide at the time τ. Explicitly,

$$d \log T' = h_{(\log T, \log T')} d \log T$$

$$= \left[\frac{\partial M}{\partial \log T} \Big/ \frac{\partial M}{\partial \log T'} \right] d \log T. \quad (23)$$

Derivatives are calculated on the ZAHB. Once the new distribution $g_{(\log T')}$ is obtained from $f_{(\log T)}$, normalization to the new total number of stars proceeds via equation (19) by means of the evolutionary flux b. Figure 4 sketches the evolution suggested for the HB of the metal-poor SSP of Figure 1. According to Sweigart and Gross (1976) and Sweigart (1987), a useful expression relating M and $\log T$ along the ZAHB is

$$M = \frac{\alpha}{1 - (T_{lim}/T)^{10}} (\log T - 3.90) + \text{offset}, \quad (24)$$

where

$$\alpha = (0.457 - 0.23 \log^2 Z) M_c - 0.4 \log Z - 0.64$$

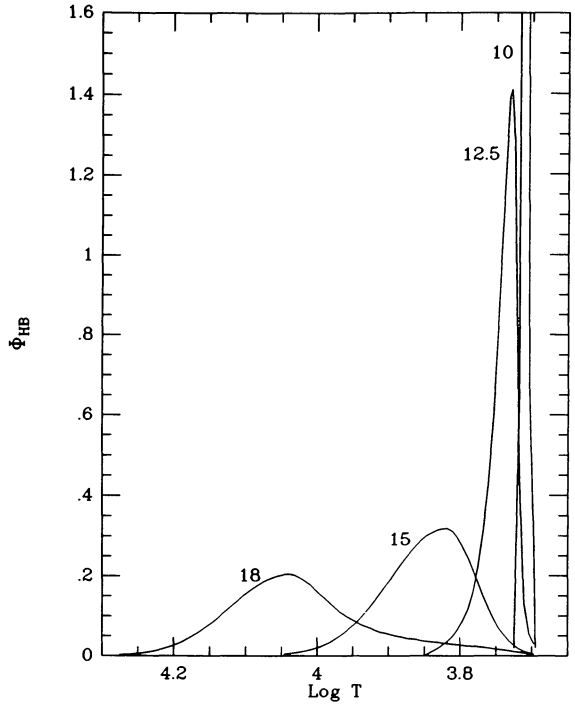

FIG. 4.—Evolution of the HB morphology with time for the SSP displayed in Fig. 1. Labels refer to the age (in Gyr). Distributions are in relative units.

and

$$T_{lim} = 4600 \times 10^{-0.01 \log Z}.$$

It is worth noting that the whole procedure described never requires the exact knowledge of the offset in the M–$\log T$ relation, since only its derivative is involved. Furthermore, no special hypotheses are needed for the mechanism(s) leading to the spread in HB. The only constraint in this sense is that it must work in the same way at any time.

In conclusion, in this purely heuristic approach, the unknown second parameter only works by imposing the starting reference function $f_{(\log T)}$ and an offset to the M–$\log T$ relation such as is required to link the "mean" HB mass with the stellar mass at the RGB tip. One could argue that an arbitrary degree of freedom is introduced, since the HB evolutionary tracks already constrain the M–$\log T$ relation. We point out, on the other hand, that (1) some arbitrariness is introduced at the highest conservative level to preserve all the other HB features suggested by the theory, and (2) the present theory of stellar evolution is not able to reproduce properly the observed HB morphologies: we believe it is not so arbitrary to state that a tuneup is needed in the theory!

f) *Asymptotic Giant Branch*

There are basically two problems to be solved to insert AGB evolution correctly in the SSP models: (1) we do not know the detailed path of the stars along the AGB for the various combinations of age and chemical composition, and

(2) stellar evolution can be strongly affected by some new mechanisms—for instance mass loss—that introduce additional degrees of freedom to be parameterized and explored.

At the present, a very limited data base of AGB evolutionary tracks is available: this is because of the great difficulty in properly reconstructing the whole structure of these stars, since their two sources of energy, the H and He burning shells, work under very peculiar conditions and some abrupt instabilities can arise (thermal pulses). Essentially all our theoretical advances concerning the AGB evolution of low-mass stars arise from the works by Gingold (1974, 1976), Paczyński (1970, 1971, 1975), and Iben (1982), who provided some quantitative hints about the evolutionary lifetimes and the expected luminosity function for stars of different chemical composition. In particular, Gingold and Iben let Population II stars ($Z = 0.001$) evolve with masses between 0.5 and 0.7 $M_\odot$, while Paczyński provided a useful relation between core mass and luminosity for Population I stars ($Z = 0.03$). This relation accounts fairly for the path of the stars along the upper part of the AGB, when thermal pulses occur.

Some relevant contributions, providing a better understanding of the inner structure of the AGB stars and in particular of their nucleosynthesis and energetics, also came from Iben and Renzini (1982*a*, *b*, 1983) and Renzini and Voli (1981). This facilitates the setting of reasonable constraints to the contribution of the AGB stars to a SSP via the FCT.

Insertion of the AGB in our models proceeds as follows:

1. A smooth path superposed on the RGB was assumed in the H-R diagram: then the $\log L$–$\log T$ relation for the branch is given by equation (14). This simplification slightly underestimates the temperature of the AGB, since in observed *C-M* diagrams it lies to the left of the RGB. This is not a serious problem, because the difference in color is usually less than 0.2 mag in $B - V$ at the base of the AGB, and it vanishes near the tip. No attempt to fit blueward excursions of the stars due to thermal pulses has been made: the extremely short time spent by stars at the high temperatures ($\log T > 4$) is quite negligible (less than 10^5 yr over $\sim 15 \times 10^6$ yr for the whole AGB evolution, or $\sim 0.7\%$).

2. Transition between the early AGB (EAGB) and thermal pulse phase occurs at the luminosity L_p. From Iben and Truran (1978) and Iben and Renzini (1983) we calculate

$$\log L_p = 0.19 \log M_{\rm TO} + \log (0.075 M_{\rm TO} - 0.015) + 4.641. \quad (25)$$

3. A flat bolometric luminosity function is assumed for the EAGB, starting from the HB level. The subsequent onset of thermal pulses induces a change in the evolutionary rate, and stars move in the upper part of the AGB twice as fast as in the EAGB. During the thermal pulses the luminosity function $\Phi_{(\log L)}$ follows from the mass-luminosity relation by Paczyński (1971):

$$\Phi_{(\log L)} = 4.1 \times 10^6 b. \quad (26)$$

It is worth noting that the simplified treatment of the EAGB because of the lack of information from stellar evolutionary models does not strongly affect the reliability of the procedure adopted. Indeed, even if it can be recognized that the true AGB luminosity function shows an exponential fading (see, for instance, Cohen *et al.* 1981 and Richer 1981 for observations in the Magellanic Clouds), the adopted flat distribution properly averages the true path. What counts in this regard is in fact a safe accounting for the fuel available to the stars (Buzzoni 1982): *this naturally constrains the evolutionary rate, whatever the shape adopted for the* t–$\log L$ *relation.*

4. All over the AGB evolutionary path, stellar mass loss has been taken into account following the procedure previously described. Mass loss plays an important role here, since it removes fresh fuel from the stellar envelope strongly affecting the PAGB mass and the final fading of the stars. In practice, AGB evolution with mass loss was followed step by step and stopped as soon as the actual envelope mass (i.e., the difference between the actual total mass and the *C-O* core) fell below the critical value given by equation (33) in Renzini and Voli (1981; their case A, with superwind parameter $b = 1$).

g) Post–Asymptotic Giant Branch

The fast ejection of most of the stellar envelope (the so-called "superwind phase") leads to a rapid escape of the stars away from the AGB to the opposite side of the H-R diagram. PAGB evolution of low-mass stars is believed to coincide with the planetary nebula event, being the nebula formed by the lost envelope (see, for instance, Wood and Cahn 1977). Stars in the PAGB can reach very high temperatures ($T > 10^5$ K), and they spend most of their fuel above $T = 20{,}000$ K. The associated energetics is not relevant (RB86 find just $\sim 1\%$ at the most in the bolometric emission of an old SSP), but it is remarkable to note that this light is emitted mainly in the far-UV, at wavelengths shorter than 2000 Å. Here the PAGB might contribute in a more effective way to the SED of a SSP. Basically, the treatment of the PAGB was computed following Paczyński's (1970, 1971) models, displaying evolution for three relevant masses (i.e., 0.6, 0.8, and 1.2 $M_\odot$). Photometric contribution was assumed to occur mainly around the highest temperature ($T_{\rm max}$) reached by the stars:

$$\log T_{\rm max} = 2.26 \log M_f + 5.65, \quad (27)$$

where M_f is the actual mass (in solar units) of the stars leaving the AGB after ejection of their envelope. Blackbody radiation was adopted, since no model atmospheres are available for these high temperatures, and in any case the strong ionization ensures a good Planckian approximation. The normalization to the SED of the SSP was accomplished via the FCT, assuming fuel F to be

$$F_{(M)} = 7.6 \times 10^{-5} M_f^{-5.22} \quad (28)$$

(Paczyński 1971), where F is in equivalent hydrogen solar masses. In practice, converting equation (28) into solar luminosities released per year (remembering that 1 g of hydrogen releases 6×10^{18} ergs), we obtain via equation (9) the proper

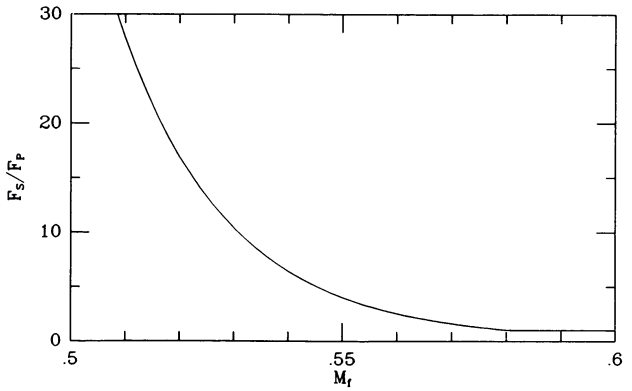

FIG. 5.—Increase of the PAGB bolometric contribution to the synthetic models of SSPs. The curve extrapolates the ratio between the fuel available to the PAGB stars according to Schönberner (1979, 1981) (F_s) and that available according to Paczyński (1971) models (F_p).

value for the bolometric luminosity contributed to the rest of the SSP and also the scaling factor for the blackbody.

To compute the overall contribution of the PAGB to the SEDs of our models, we had often to extrapolate equation (28) in order to infer the expected emission of stars with remnant masses slightly lower than 0.6 $M_\odot$; this assumes a smooth trend for the mass-fuel relation. Comparing equation (28) with the equivalent one derived from the models by Schönberner (1979, 1981), we notice an abrupt increase in the fuel for $M_f < 0.54\ M_\odot$ due to the significant increase in the lifetimes for his model at the lowest mass (0.546 $M_\odot$). Elsewhere the two relations agree fairly well. Had one relied on this, hypothetical fit of the trend envisaged by Schönberner's tracks for low masses provided

$$F_{(M)} = 7\times10^{-11}M_f^{-30.8}, \qquad (29)$$

with F in the same units as in equation (28) (RB86). The ratio of the two relations is displayed in Figure 5. Just a glance at the figure illustrates how dramatically the role of the PAGB would change: in fact, a slight decrease in M_f would transform the stars into very strong UV emitters, even providing the major contribution to the total bolometric light of a SSP(!). This easily explains why PAGB stars are such fascinating candidates invoked to account for the UV excess in the elliptical galaxies (Barbaro and Olivi 1989; Bertelli, Chiosi, and Bertola 1989; Bertola 1988; Burstein *et al.* 1988). We prefer deferring to Paper II a more careful and extensive discussion of this exciting point. We remark, however, that this abrupt increase in the PAGB contribution and the induced "UV catastrophe" fully rest on the *extrapolation of a trend* suggested only by the extreme model in Schönberner's sequence. We are inclined at the present to assume a more prudent and conservative position relying on Paczyński's models, since only a direct calculation of a grid of PAGB evolutionary tracks for $M_f < 0.55\ M_\odot$ will be able to clarify the problem decisively. In our models, the PAGB is confined to a more modest (although not negligible) role inside the SSPs.

IV. MODEL ATMOSPHERES

There is a further fundamental step to be accomplished in order to obtain the synthetic SED of a SSP after having properly assembled its isochrone: we need to know the contribution of each individual star to the SED of the whole population. Among the various stellar libraries available we choose the sets of theoretical model atmospheres by Kurucz (1979) and Bell and Gustafsson (1978, hereafter BG78). Other useful empirical sets provided SEDs for selected stellar spectral types (O'Connell 1973; Jacoby, Hunter, and Christian 1984; Pickles 1985*b*). The main reason for our choice resides in the fact that theoretical grids directly match the SSP isochrones, which were assembled in the (log L, log T)-space. This enabled us to overcome some crucial problems like that of the bolometric correction (BC) of the stellar atmospheres, allowing also a convenient coverage of the H-R diagram, through the basic parameters (T, g,[Fe/H]) minimizing interpolation inside the grids.

The bolometric correction directly enters in scaling the contribution of the single stars to the total SED. It is well known that it is a function of the temperature of the stars, but we still have some trouble in firmly defining its quantitative trend empirically, especially for cold and hot stars, owing to the problem of reconstructing their emission out of the visible window. In contrast, this is a very easy job for the theoretical models, which are naturally normalized by Boltzmann's law.

Moreover, using theoretical model atmospheres, we overcame the uncertainties related to the calibration of the empirical spectral types with the effective temperatures. In principle this could affect the results in a not negligible way, since once again stars at the two extremes of the spectral scale are usually badly calibrated in temperature.

The major limit of the theoretical atmospheres is that in general they cannot take into account all the elements present in the chemical mixture. Thus, due to their limited (although wide) set of opacities implemented, they are usually expected to underestimate blanketing effects. We shall return in detail to this question in § V.

Another weak point is that there are no models for super metal-rich stars (i.e, $Z > Z_\odot$): both Kurucz and BG78 grids assume [Fe/H] ≤ 0. This is a serious problem for the empirical libraries too, since most of the stars in the solar neighborhood have [Fe/H] < 0.

On the other hand, no serious problem seems to arise from the fixed helium abundance in the theoretical grids ($Y = 0.30$). In fact helium is expected to affect continuum emission very marginally (being a weak e^- donor), and only its own absorption lines are influenced.

The link of the theoretical atmospheres with our SSP models was accomplished according to the following prescriptions:

1. Both Kurucz and BG78 grids have been regrided to the same wavelengths, in the sense that BG78 models were readjusted to Kurucz wavelengths. The spectral resolution for Kurucz models ranges from 25 Å for $\lambda < 5000$ Å to 100 Å or more in the red and infrared. The BG78 grid is coarser, ranging from 50 Å in the ultraviolet to 400 Å in the near-infrared. Obviously the net resolution of the synthetic SED is limited by the BG78 grid.

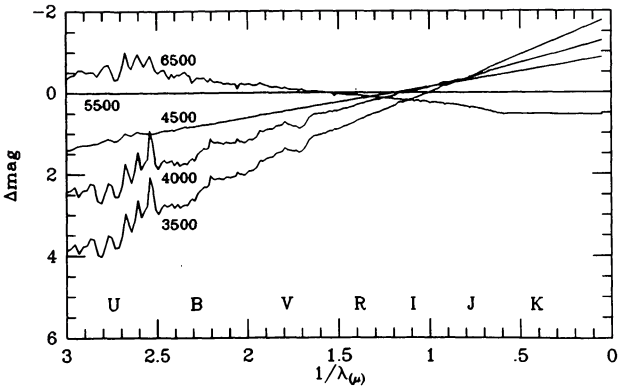

FIG. 6.—Monochromatic magnitude difference for some model atmospheres. Curves are labeled with their temperatures. A model at $T = 5500$ K is taken as reference. Johnson's bands are marked at the bottom. The linear trend with $1/\lambda$, which made possible the extrapolation of the models in wavelengths and in temperature, is evident.

2. Since the BG78 published grid covers only the range $3300 < \lambda < 10{,}800$ Å, an extrapolation was made to extend it in wavelength. This has been done using the Kurucz grid as a reference. It is known that a nearly linear relation exists between monochromatic magnitude differences of two stars plotted against $1/\lambda$ (Mendoza and Johnson 1965; Golay 1974). The slope of the line is related to their difference in effective temperature, so that we can write

$$m_1 - m_2 = \alpha(1/\lambda) + \beta \tag{30}$$

and

$$\alpha = C\left(\frac{1}{T_1} - \frac{1}{T_2}\right)^{\gamma}. \tag{31}$$

The subscripts 1 and 2 refer to the two stars ($T_2 > T_1$ to avoid problems with the exponent in eq. [31]). For the blackbody and also in our calculations, γ turns to be around unity, but we have retained it for the sake of generality. Using equations (30) and (31), we were able to extrapolate all the BG78 models confidently by properly comparing them with Kurucz grid via a least-squares procedure. Figure 6 gives some examples.

3. The same procedure was used also to extrapolate a number of models down to $T < 4000$ K. This extended the BG78 grid, since the available atmospheres are not able to reproduce cold stars either at the tip of the RGB and AGB or at the faint tail of the MS. Of course, the extrapolation procedure did not allow us to reproduce details and features of the spectra induced by the decrease in temperature (new absorption lines, molecular bands, etc.). This means, for instance, that carbon stars, possibly present at the tip of the AGB, have been considered here as normal AGB members.

4. The choice of the interpolation grid for each star along the isochrones was determined by its effective temperature. For $T > 50{,}000$ K a blackbody was assumed; in the range $50{,}000 > T > 5500$ K we used the Kurucz grid, while the BG78 grid covered the range $5500 > T > 4000$ K. At lower temperatures we used the extrapolated models.

5. Interpolation into the grids was made linearly in [Fe/H], log T, and log g wherever possible.

It is worth emphasizing that synthesized SEDs in our models are not intended to reproduce detailed features of the spectra such as absorption lines and molecular bands. The only information we can retain from them concerns low-resolution features, such as the continuum and the main spectral breaks (the Balmer discontinuity, for instance). Nevertheless, our procedure potentially enables the implementation of a variety of spectral indices once a careful calibration on the stellar framework has been pursued. In this sense some attempts are in progress to refine synthesis of the most popular indices in the UV, in the visible, and in the infrared (cf., for instance, Spinrad and Taylor 1969*a*, *b*; Whitford 1973, 1977; Faber 1973; O'Connell 1973; Faber, Burstein, and Dressler 1977; Aaronson, Frogel, and Persson 1978; Frogel *et al.* 1978; Burstein 1979; Rose 1985; Boulade, Rose, and Vigroux 1988).

V. PHOTOMETRIC CALIBRATION AND COLORS

The last step to be carefully accounted for in constructing our EPS models concerns the calculation of synthetic colors from their SEDs. This is an important requirement because photometry is usually much more convenient than spectrophotometry, often providing equivalent synthetic information about the stellar systems observed. A lot of care has to be taken in computing magnitudes and colors from the models and confidently comparing them with the observations. In fact, a number of complications arise, leading in principle to dangerous misinterpretations of the observations.

However, it is important to realize in this regard that the use of the theoretical grids of stellar atmospheres radically reverses the aim of this comparison, now performed *to check* self-consistency of the theoretical framework and *not to calibrate it*.

a) *Reproducing the Photometric System*

A first major problem concerned the careful reproduction of the features of Johnson's photometric system. Reduction of the observed magnitudes back to the standard system is usually fairly well performed through comparison with reference objects: this is not usually the case for the theoretical magnitudes and colors.

Some remarkable biases in this sense have been evidenced by Ažusienis and Straižys (1969), Kurucz (1979), Buser and Kurucz (1978), and Buser (1978*a*, *b*). Buser (1978*a*), for instance, has shown that using Matthews and Sandage (1963) response functions for Johnson *UBV* filters to compute theoretical colors, one would introduce a systematic drift depending on the SED to be convolved. He proposed, then, a revised photometric system, adopting B and V filters from Ažusienis and Straižys (1969) and a new profile for the U filter (called U_3 in his work). When applied to the Vilnius spectral catalog (Straižys and Sviderskiene 1972), this system works much better in reproducing Johnson's empirical *UBV* photometry, and we adopted it also in our work, so that we use the V, B_3, and U_3 combination. Moreover, in order to refine the red

TABLE 2

MODIFIED RESPONSE CURVES FOR R AND I BANDS

λ (Å)	R_B	I_B
5200	0.000	...
5400	0.021	...
5600	0.121	...
5800	0.256	...
6000	0.408	...
6200	0.529	...
6400	0.659	...
6600	0.778	...
6800	0.888	0.000
7000	0.985	0.002
7200	1.000	0.043
7400	0.971	0.107
7600	0.892	0.195
7800	0.741	0.308
8000	0.579	0.454
8200	0.452	0.541
8400	0.261	0.637
8600	0.178	0.750
8800	0.102	0.858
9000	0.071	0.949
9200	0.037	1.000
9400	0.019	0.986
9600	0.000	0.939
9800	...	0.888
10000	...	0.793
10200	...	0.719
10400	...	0.599
10600	...	0.524
10800	...	0.408
11000	...	0.340
11200	...	0.277
11400	...	0.194
11600	...	0.151
11800	...	0.088
12000	...	0.000
λ_{eff}	7175	9455
σ (Å)	755	980

magnitudes, we extended Buser's (1978*a*) procedure to Johnson R and I bands.

Thus the Vilnius spectral catalog was taken as a reference, and convolution with the original R and I filters (Johnson 1965) was performed. An iterative algorithm slightly changed the response curves, minimizing the systematic trends in the differences between computed and standard colors for each spectral types, as given by Johnson (1966). In shaping the filter response, we constrained the algorithm in order to avoid arbitrarily induced bimodalities in the transmission profiles or drastic changes in the effective wavelengths or in the pass-bands. A good solution was obtained with the new response curves reported in Table 2 and displayed in Figure 7.

As shown in Figures 8*a*–8*d*, standard colors are well reproduced by the new set of filters, and any systematic trend with color is removed. Unfortunately, this refinement cannot be applied to the J and K bands because of the lack of a convenient set of reference infrared spectra. Thus we have been necessarily forced to adopt the canonical response curves for these bands (Johnson 1965).

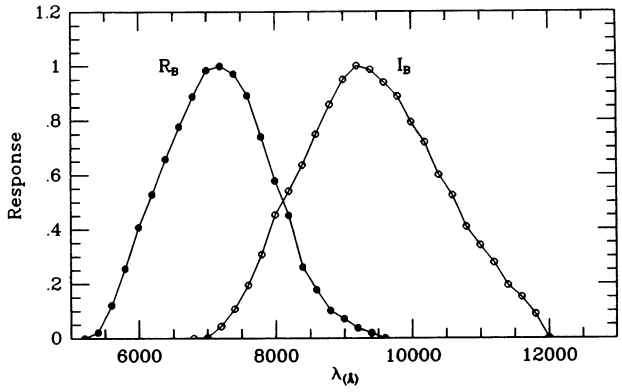

FIG. 7.—Modified response curves for Johnson R and I bands

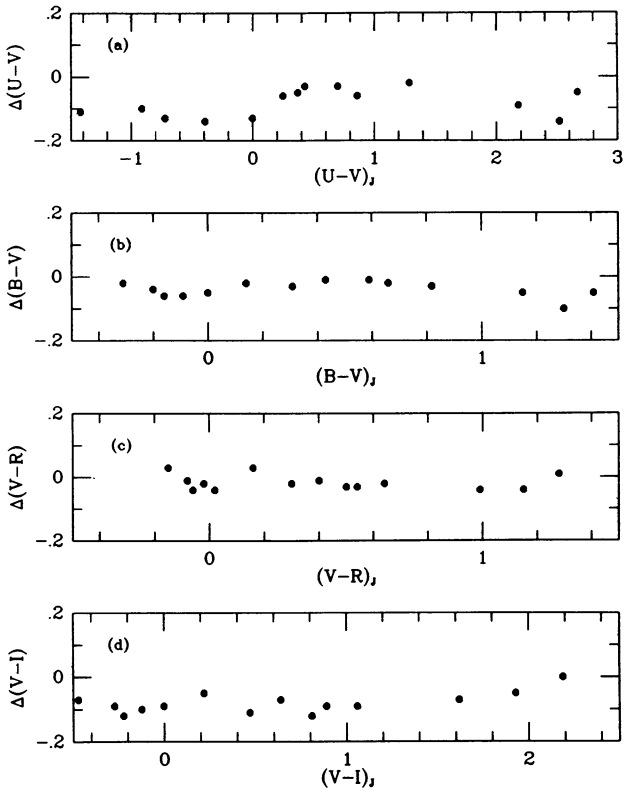

FIG. 8.—Color residuals of the reconstructed photometric system. The Vilnius spectral catalog (Straižys and Sviderskienė 1972) is taken as the reference for the SED of the different spectral types. Residuals are in the sense (Johnson minus this paper).

b) *Flux Calibration*

A further warning concerns the calibrating fluxes which provide the zero points for the magnitude scales. The first natural choice in this sense would be to refer to the flux of Vega, usually taken as a photometric standard candle.

Despite the accuracy of this approach, we decided to revise it slightly in order to obtain a better match with the observa-

TABLE 3

ABSOLUTE CALIBRATION OF THE PHOTOMETRY FOR A 0.0 MAGNITUDE STAR

Band	λ_{eff} (μm)	f_λ (ergs s^{-1} cm^{-2} Å^{-1})	f_ν (W m^{-2} Hz^{-1})
U	0.36	4.45E−9	1.92E−23
B.....	0.44	6.25E−9	4.04E−23
V.....	0.55	3.53E−9	3.56E−23
R.....	0.70	1.62E−9	2.65E−23
I.....	0.90	7.31E−10	1.98E−23
J.....	1.25	2.98E−10	1.55E−23
K.....	2.20	4.98E−11	0.80E−23

TABLE 4

VEGA MAGNITUDE AND COLORS

Colors	Oke and Schild 1970 (T = 9660 K)	Hayes and Latham 1975 (T = 9400 K)	Tüg *et al.* 1977
V	0.01	0.00	−0.02
$U-V$	0.04	0.09	...
$B-V$	0.01	0.03	0.02
$V-R$	0.01	0.02	...
$V-I$	0.01	0.03	...
$V-J$	0.02	0.05	...
$V-K$	0.02	0.06	...

tions. As a matter of fact, magnitudes rest in practice on the concept of a *mean A0 V star* instead of one single primary standard candle. Thus we preferred to readjust our calibration according to the Johnson's (1966) temperature scale for the A0 V type (to which an effective temperature $T_{eff} = 9850$ is attributed), retaining only the V flux calibration from Vega, as it follows from the work by Hayes and Latham (1975). Table 3 reports the calibration fluxes eventually adopted in our synthetic photometry. The values reported in the table stem from the direct convolution of the Kurucz model atmosphere at (T_{eff}, log g,[Fe/H]) = (9850,4.0,0) with the adopted filter responses. Table 4 compares the derived colors and magnitudes of Vega according to the calibrations by different authors (Oke and Schild 1970; Hayes and Latham 1975; Tüg, White, and Lockwood 1977). In order to calculate colors over the whole relevant range in wavelength, the observed absolute fluxes have been properly fitted with Kurucz models. According to Code *et al.* (1976) and Kurucz (1979), Vega calibration by Oke and Schild (1970) is fairly well represented by a model atmosphere with $T_{eff} = 9660$, while a lower temperature (T_{eff} = 9400) better matches the calibration by Hayes and Latham (1975).

As a general result of the whole procedure discussed, we conclude that uncertainties in reproducing *absolute* stellar colors should be around ± 0.05 mag for $B-V$ and $V-R$, while they rise to about ± 0.1 mag for $U-V$, $V-I$, $V-J$, and $V-K$. For the infrared colors the most relevant sources of uncertainty arise from the lack of correction of the filter response for the air mass and the intrinsic difficulties in calibrating the zero points for these bands (Campins, Rieke, and Lebofsky 1985).

Despite all of the intrinsic technical and numerical uncertainties, it is nevertheless clear that the minimization of the systematic trends in the color residuals, as shown in Figure 8, ensures a safe self-consistency of the adopted system. Thus *differences* in magnitudes and colors between different synthetic SSP models should be much more reliable than quoted above: we estimate relative uncertainties of ± 0.02 mag for $\Delta(B-V)$, $\Delta(V-R)$, and $\Delta(V-I)$ and ± 0.05 mag for $\Delta(U-V)$, $\Delta(V-J)$, and $\Delta(V-K)$.

c) *Bolometric Corrections and Temperature Scales*

The only exhaustive work covering the whole range of spectral types and assembling in a coherent way colors, BCs, and temperatures still remains that of Johnson (1966). However, many subsequent studies provided relevant contributions to some specific class of stars suggesting somehow updates to his original calibration. Johnson's work is essentially confirmed in what concerns the empirical stellar colors for the different spectral types, and we will refer to it as a comparison reference for our results. On the other hand, bolometric and temperature scales deserve a more detailed discussion, since some relevant alternatives are to be considered.

Some uncertainties in this sense surely arise for early-type stars. Here Johnson's calibration seems to predict temperatures and bolometric corrections that are too low (in their absolute value) because of the lack of reliable information about the UV emission of these stars. An important improvement in this regard comes from the work by Code *et al.* (1976), who collected space observations at short wavelengths and measured absolute fluxes for a number of B–A stars. Their calibration seems to be the most reliable at the present for hot stars, and it merges with Johnson's scale around the A0 type.

On the opposite side, cold stars still remain an open question. Johnson's BC–spectral type relation is fairly well confirmed by many authors (cf., for instance, Lee 1970; Flower 1977; and Frogel, Persson, and Cohen 1980) and also his BC–log T relation holds. Nevertheless, some relevant discrepancies are evidenced by Ridgway *et al.* (1980), who reconsidered the temperature calibration for red giant stars (later than K type). On the basis of measurements of stellar radii by lunar occultation and multicolor photometry, they find a clear difference between derived effective and observed IR color temperatures. The difference seems to be important for very cold stars (with spectral type later than M0), increasing with decreasing temperature, and is of the order of 10% around M5 III (with T_{eff} hotter than T_c). No explicit causes are identified by the authors to account for such a great discrepancy, which they conclude to be real. Since their IR temperatures match previous calibrations fairly well (and no abnormal blanketing is found to affect colors), the only reasonable source of the discrepancy could reside in some perverse systematic biases affecting the measure of the stellar radii. No revisions are given in the paper about the BCs: if Johnson's scale is assumed to be valid for a given spectral type, one should

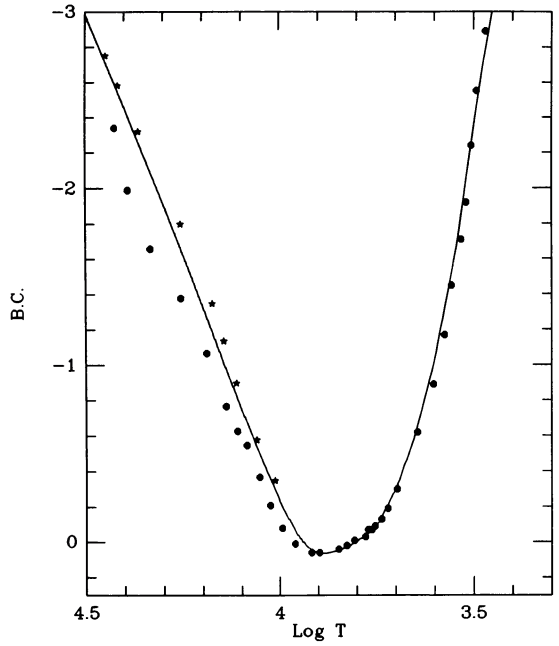

FIG. 9.—Calibration of BC vs. temperature. Our adopted theoretical relation for class V stars and [Fe/H] = 0 (*solid line*) is compared with that of Johnson (1966) (*filled circles*). Stars mark the alternative most confident calibration for hot stars as derived by Code *et al.* (1976).

expect again a substantial discrepancy in the colors, since a larger absolute flux must be spent at wavelengths shorter than V.

In conclusion, we agree with the incoming evidence for a slight increase in the temperature scale for M stars, as supported also by theory (Tsuji 1978), but the true amount of this increase is probably much less than that envisaged by Ridgway *et al.* (1980). In our opinion Johnson's (1966) data are still to be regarded as a safe source for BC and $T_{\rm eff}$, keeping in mind, however, that his temperature scale for late-type stars should be probably increased by some percent. In Figure 9 we report our BC–log T relation compared with the assumed empirical scale. Here BCs are in the sense $(M_{\rm bol} - V)$ and are normalized such that BC $= -0.07$ for the Sun. This value stems from the V calibration of Table 3 and an assumed $M_{\rm bol\odot} = 4.72$ and $L_\odot = 3.89 \times 10^{33}$ ergs s^{-1}. The overall agreement with our calibration confirms that a proper weight of the contribution of the stars with different temperatures to the synthetic SED has been achieved in the models.

d) *Dependence on Chemical Composition*

It is important to check the behavior of our calibration as a function of the metallicity. Unfortunately, in this case a comparison with the observations becomes difficult because of the relative scarcity of stars with nonsolar chemical composition (in particular with $Z > Z_\odot$). Nevertheless, this step cannot be dismissed, since it is known that the adopted stellar model atmospheres slightly underestimate blanketing effects, and a quantitative evaluation of the related uncertainty is needed.

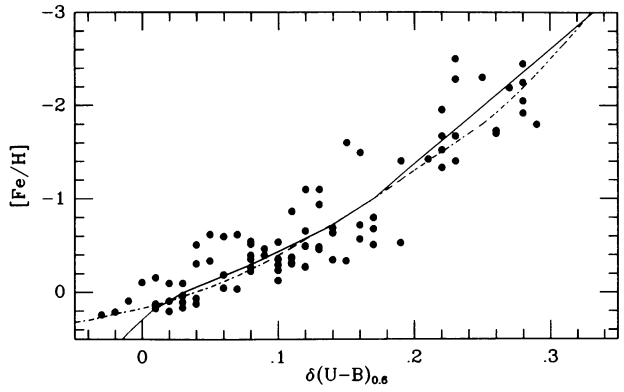

FIG. 10.—Calibration of Sandage's (1969) $\delta(U-B)_{0.6}$ index. Our adopted theoretical relation (*solid line*) is compared with the original data by Carney (1979) (*filled circles*) and with the relation proposed by Sandage and Fouts (1988) (*dot-dash line*). See text for discussion.

The proper account for blanketing effects in calculating theoretical model atmospheres is known to be not a simple task. We would argue in this sense that a deterministic solution of the problem is probably unattainable both because of the virtually infinite combinations involving the partition of the heavy elements in the chemical mixtures and because of the detailed knowledge required for their contribution to the opacity. A remarkable attempt to approach the problem is due, for instance, to Magain (1983), who tried to compensate for such a lack of opacity by means of an artificial enhancement of the metals in the chemical mixture of the atmospheres. After calibration on the Sun via the data by Labs and Neckel (1970), his procedure seems to be very effective in reproducing *UBV* colors for some standard stars of spectral type F5 V–G0 V. Unfortunately, the method fails out of this range because of its too critical assumptions constraining the physical conditions in the atmospheres. Concerning our problem, therefore, we preferred to avoid any manipulation of the data on the basis of more or less physical justifications, merely warning that the problem does exist.

On the other hand, it is worth noting that our adopted flux calibration *partially compensates for the blueness* of the stellar model atmospheres, since the zero points in the magnitudes rest on a standard candle (Kurucz model for a mean A0 V star) which suffers, in principle, from the same effect. However, just to outline an alternative and quantitative approach to the question, we could estimate *a posteriori* the virtual enhancement in the metallicity required to account fully for the lack of opacity in the theoretical atmospheres. A stringent test in this sense involves the $\delta(U-B)_{0.6}$ index as defined by Sandage (1969). In practice,

$$\delta(U-B)_{0.6} = (U-B)_{\rm Hyades} - (U-B)_*, \qquad (32)$$

where both $U-B$ colors on the right-hand side of the equation are calculated on the MS of the population at $B-V = 0.6$. For the Hyades, Sandage (1969) found $(U-B)_{\rm Hyades} = 0.13$, so that $\delta(U-B)_{0.6} = 0$ for this value. This photometric index is clearly related to the blanketing vector in the color-color diagram of a stellar population.

A direct calibration of $\delta(U-B)_{0.6}$ with stellar metallicity has been provided by Carney (1979) and Cameron (1985) and summarized by Sandage and Fouts (1988). Original data from Carney (1979) (excluding binary stars) are reported in Figure 10, together with the relation tabulated by Sandage and Fouts (1988) and that derived from the theoretical atmospheres.

On the basis of this comparison the [Fe/H] associated with $\delta(U-B)_{0.6}=0$ in our relation is 0.3. This agrees with a supersolar metallicity for the Hyades. A similar value (i.e., [Fe/H] = 0.38) was found by Nissen (1970), while a subsequent discussion and revision of his data by Hardorp (1978, 1980) and Nissen and Gustafsson (1978) led to a present accepted range of $0.13 < [Fe/H] < 0.17$. The exact value of the metallicity depends on the color assumed for the Sun, $(B-V)_\odot$ commonly ranging from 0.62 to 0.68 (see Hardorp 1980 for a detailed discussion). In our system the Sun has $(B-V)_\odot = 0.62$, and this implies that we have to compare our estimate of the Hyades' metallicity with the quoted upper limit of 0.17 (also confirmed by Sandage and Fouts's relation) and then with $\Delta[Fe/H] \sim 0.13$. On the other hand, no relevant differences are evident at metallicities near to or lower than the solar value between our relation and that reported by Sandage and Fouts (1988), while a little discrepancy ($\Delta[Fe/H] \sim 0.1$) still arises, comparing with $\delta(U-B)_{0.6}$ as derived by Johnson's (1966) color calibration (for a fiducial [Fe/H] = 0).

In conclusion, a possible overestimate of 20%–30% seems to occur in reproducing [Fe/H] (or Z in a first approximation) for metal-rich populations, while no relevant discrepancies should affect the metal-poor stars. This agrees with the expected trend, since underestimating blanketing, we need higher metallicities to reproduce the observations.

However, in order to infer the uncertainties related to the SSP models, the above-mentioned values are certainly an upper limit, since isochrone paths still (correctly) account for Z. Thus, as a safe limit, we could state, for instance, that the SED of a given real SSP of solar metallicity (i.e., $Z=0.017$) should be reproduced by an equivalent model with $0.017 < Z \leq 0.022$. No corrections for such effects are applied on the grid of models presented here.

VI. THE MODELS

The whole grid of computed models of SSPs is displayed in Tables 5A–5O and 6A–6O, while for a selected sample of models listed in Table 7 we give the synthetic spectra in Tables 8A and 8B and in Figures 11–20.

Calculations in Tables 5 and 6 are arranged in order of increasing metal abundance and, for a given Z, in order of decreasing power-law exponent (s) of the IMF. Each table of the sequence from A to O is divided into two panels exploring increasing values of the mass-loss parameter η. In the series of Table 5, evolution is followed assuming a red HB (R-HB) for the 15 Gyr models, while intermediate (I-HB) and blue (B-HB) morphologies are taken into account in the series of Table 6. As discussed in § III, the three smoothed reference temperature distributions adopted are peaked respectively just blueward of the RGB at the HB luminosity level (R-HB), at $\log T = 3.82$ with a tail until $\log T = 4.05$ (I-HB) and at $\log T = 4.3$ with a tail until $\log T = 4.6$ (B-HB). These distributions are always referred to models with age $t=15$ Gyr and are taken as starting points for time evolution as previously explained. Due to the quick bunching to the red of the young HBs, no remarkable differences in the morphologies are present for $t \leq 8$ Gyr, and then early evolution is followed only in the case of R-HBs until $t=4$ Gyr. For $Z \leq 0.001$ evolution is stopped at $t=8$ Gyr owing to the lack of isochrones for younger metal-poor populations.

For each sequence of models we give relevant values for the stellar masses along the isochrones (at the TO point, at the RG tip, and in the PAGB phase, in that order), the specific evolutionary flux B as defined from equation (7), and the synthetic magnitudes and colors. Bolometric magnitudes in each sequence are normalized to the model at $t=15$ Gyr in order to provide a consistent luminosity evolution for SSPs with time. Bolometric partition of the contributions from the different stellar evolutionary phases is also reported, and finally the mass-to-light ratio M/L is calculated in bolometric and in Johnson B, V, and K bands. Solar colors as defined for a G2 V star in Johnson (1966) are adopted for the translation of L. It is worth stressing that this M/L is in fact a lower limit, since only the actual bright mass is accounted for in the ratio.

Tables 8A and 8B report detailed SEDs for the selected SSPs listed in Table 7: all the models are scaled to $L_{tot}=10^{10}$ $L_\odot$, and logarithms of the flux (per unit of wavelength) are given for optimizing numerical display.

Each synthetic spectrum is also displayed in the series of Figures 11–20 (*upper panels*), together with the monochromatic contributions from the different stellar evolutionary phases (*lower panels*).

VII. SUMMARY AND FUTURE DEVELOPMENTS

In this work we have presented the computational code and the final results concerning the construction of synthetic SEDs for old SSPs. A wide set of combinations among relevant parameters such as age, metallicity, IMF, and stellar mass-loss efficiency have been quantitatively explored, carefully accounting for the prescriptions stemming from the theory of the stellar evolution. The most relevant improvements are concerned with the treatment of the PMS evolutionary phases, present in the models until the planetary nebula event. Particular care has been given to the description of the HB, and a simplified model for its evolution with time has been developed.

A detailed discussion about theoretical reproducibility of the standard photometric systems to enable a proper comparison of theoretical and empirical magnitudes and colors is also given. The Johnson system is reproduced within ± 0.05 mag for $B-V$ and $V-R$ colors, and ± 0.10 mag for $U-V$, $V-I$, $V-J$, $V-K$, and an even better accuracy is achieved by using colors in a differential way.

Relevant quantities and general information about more than 450 models of SSPs are displayed, and a subsample of 10 synthetic spectra is detailed. This paper is the first step in a more extensive work which is intended to address the global problem of the study of the stellar populations and its implications for the evolutionary status of the stellar systems. In the subsequent papers of this series we will then extend the discussion and applications of this grid of models.

TABLE 5

RELEVANT PROPERTIES FOR SSP MODELS WITH RED HORIZONTAL BRANCH

A.

	Z	[Fe/H]	Y	s	η	
	0.0001	-2.27	0.23	3.35	0.30	
		R-HB				
AGE (Gyr)	18.0	15.0	12.5	10.0	8.0	
Mto	0.75	0.79	0.82	0.88	0.93	
Mrt	0.67	0.72	0.77	0.83	0.91	
Mpn	0.53	0.55	0.56	0.59	0.63	
B	1.30	1.30	1.26	1.25	1.25	
Bol	0.07	0.00	-0.11	-0.21	-0.30	
Bol-V	-0.49	-0.47	-0.46	-0.39	-0.27	
U-V	0.77	0.74	0.71	0.62	0.43	
B-V	0.74	0.72	0.69	0.63	0.52	
V-R	0.73	0.71	0.70	0.65	0.55	
V-I	1.28	1.25	1.23	1.14	0.97	
V-J	1.80	1.77	1.74	1.62	1.39	
V-K	2.49	2.46	2.43	2.29	2.06	
% MS	.477	.483	.485	.486	.464	
% SGB	.077	.064	.064	.046	.033	
% RGB	.270	.260	.245	.237	.233	
% HB	.070	.069	.066	.065	.064	
% AGB	.103	.121	.138	.164	.205	
% PAGB	.003	.002	.002	.001	.001	
M/Lbol	6.60	6.30	6.20	5.80	4.90	
M/Lb	10.75	9.89	9.38	7.79	5.32	
M/Lv	9.72	9.11	8.88	7.79	5.89	
M/Lk	3.69	3.56	3.57	3.56	3.33	

	Z	[Fe/H]	Y	s	η	
	0.0001	-2.27	0.23	3.35	0.50	
Mto	0.75	0.79	0.82	0.88	0.93	
Mrt	0.59	0.65	0.71	0.79	0.88	
Mpn	0.48	0.51	0.52	0.55	0.59	
B	1.35	1.35	1.30	1.29	1.30	
Bol	0.07	0.00	-0.11	-0.21	-0.29	
Bol-V	-0.48	-0.46	-0.45	-0.38	-0.28	
U-V	0.75	0.72	0.69	0.60	0.45	
B-V	0.72	0.70	0.68	0.62	0.52	
V-R	0.72	0.70	0.69	0.64	0.55	
V-I	1.26	1.24	1.22	1.13	0.98	
V-J	1.78	1.75	1.72	1.60	1.40	
V-K	2.46	2.43	2.39	2.27	2.03	
% MS	.493	.499	.503	.504	.482	
% SGB	.080	.066	.067	.047	.034	
% RGB	.279	.269	.254	.246	.242	
% HB	.078	.073	.069	.067	.067	
% AGB	.066	.089	.105	.133	.173	
% PAGB	.005	.004	.003	.002	.002	
M/Lbol	6.90	6.60	6.40	6.00	5.00	
M/Lb	10.94	10.08	9.51	7.91	5.48	
M/Lv	10.07	9.45	9.08	7.98	6.07	
M/Lk	3.93	3.80	3.79	3.72	3.52	

TABLE 5—*Continued*

B.

	Z	[Fe/H]	Y	s	η	
	0.0001	-2.27	0.23	2.35	0.30	
		R-HB				
AGE (Gyr)	18.0	15.0	12.5	10.0	8.0	
Mto	0.75	0.79	0.82	0.88	0.93	
Mrt	0.67	0.72	0.77	0.83	0.91	
Mpn	0.53	0.55	0.56	0.59	0.63	
B	1.67	1.66	1.61	1.60	1.56	
Bol	0.13	0.00	-0.16	-0.32	-0.51	
Bol-V	-0.40	-0.39	-0.37	-0.29	-0.18	
U-V	0.71	0.68	0.65	0.57	0.38	
B-V	0.70	0.68	0.66	0.60	0.48	
V-R	0.68	0.67	0.65	0.59	0.49	
V-I	1.19	1.16	1.13	1.03	0.85	
V-J	1.67	1.64	1.60	1.45	1.21	
V-K	2.33	2.29	2.25	2.08	1.84	
% MS	.332	.342	.341	.343	.332	
% SGB	.098	.081	.082	.058	.040	
% RGB	.345	.332	.314	.304	.291	
% HB	.090	.088	.084	.083	.080	
% AGB	.132	.155	.177	.210	.255	
% PAGB	.004	.003	.002	.002	.001	
M/Lbol	2.40	2.20	2.00	1.80	1.40	
M/Lb	3.47	3.09	2.71	2.14	1.35	
M/Lv	3.25	2.95	2.64	2.20	1.55	
M/Lk	1.43	1.35	1.25	1.22	1.07	

	Z	[Fe/H]	Y	s	η	
	0.0001	-2.27	0.23	2.35	0.50	
Mto	0.75	0.79	0.82	0.88	0.93	
Mrt	0.59	0.65	0.71	0.79	0.88	
Mpn	0.48	0.51	0.52	0.55	0.59	
B	1.74	1.73	1.69	1.68	1.64	
Bol	0.13	0.00	-0.15	-0.32	-0.50	
Bol-V	-0.39	-0.37	-0.35	-0.28	-0.18	
U-V	0.68	0.66	0.63	0.54	0.39	
B-V	0.68	0.67	0.64	0.58	0.48	
V-R	0.67	0.65	0.64	0.58	0.49	
V-I	1.16	1.14	1.11	1.01	0.85	
V-J	1.64	1.61	1.57	1.43	1.21	
V-K	2.28	2.24	2.20	2.04	1.79	
% MS	.345	.356	.357	.359	.349	
% SGB	.103	.084	.086	.060	.042	
% RGB	.360	.346	.329	.318	.305	
% HB	.101	.094	.089	.087	.084	
% AGB	.085	.115	.136	.173	.217	
% PAGB	.006	.005	.004	.003	.002	
M/Lbol	2.50	2.30	2.10	1.80	1.50	
M/Lb	3.52	3.15	2.74	2.09	1.45	
M/Lv	3.36	3.03	2.72	2.18	1.66	
M/Lk	1.55	1.45	1.35	1.26	1.20	

TABLE 5—*Continued*

C.

	Z 0.0001	[Fe/H] -2.27	Y 0.23	s 1.35	η 0.30	
AGE (Gyr)	18.0	R-HB 15.0	12.5	10.0	8.0	
Mto	0.75	0.79	0.82	0.88	0.93	
Mrt	0.67	0.72	0.77	0.83	0.91	
Mpn	0.53	0.55	0.56	0.59	0.63	
B	1.86	1.84	1.80	1.77	1.71	
Bol	0.19	0.00	-0.21	-0.44	-0.70	
Bol-V	-0.38	-0.36	-0.35	-0.27	-0.15	
U-V	0.69	0.67	0.64	0.55	0.36	
B-V	0.69	0.67	0.65	0.58	0.47	
V-R	0.67	0.65	0.63	0.58	0.48	
V-I	1.16	1.13	1.10	1.00	0.82	
V-J	1.63	1.60	1.56	1.41	1.15	
V-K	2.28	2.24	2.20	2.03	1.78	
% MS	.257	.271	.268	.275	.270	
% SGB	.108	.089	.090	.064	.044	
% RGB	.384	.368	.350	.336	.318	
% HB	.100	.097	.094	.091	.088	
% AGB	.147	.171	.197	.232	.279	
% PAGB	.004	.003	.003	.002	.001	
M/Lbol	1.00	0.90	0.80	0.70	0.60	
M/Lb	1.41	1.22	1.05	0.80	0.56	
M/Lv	1.33	1.18	1.04	0.84	0.65	
M/Lk	0.61	0.56	0.51	0.49	0.47	

	Z 0.0001	[Fe/H] -2.27	Y 0.23	s 1.35	η 0.50	
Mto	0.75	0.79	0.82	0.88	0.93	
Mrt	0.59	0.65	0.71	0.79	0.88	
Mpn	0.48	0.51	0.52	0.55	0.59	
B	1.95	1.93	1.89	1.86	1.80	
Bol	0.19	0.00	-0.20	-0.44	-0.70	
Bol-V	-0.36	-0.34	-0.33	-0.25	-0.15	
U-V	0.67	0.64	0.61	0.53	0.38	
B-V	0.67	0.65	0.63	0.57	0.46	
V-R	0.65	0.64	0.62	0.57	0.47	
V-I	1.13	1.11	1.08	0.98	0.81	
V-J	1.59	1.56	1.52	1.37	1.15	
V-K	2.22	2.19	2.14	1.98	1.72	
% MS	.269	.283	.281	.288	.284	
% SGB	.114	.093	.095	.067	.046	
% RGB	.403	.385	.368	.353	.336	
% HB	.113	.105	.100	.097	.093	
% AGB	.095	.128	.152	.192	.239	
% PAGB	.006	.005	.004	.003	.002	
M/Lbol	1.10	1.00	0.80	0.70	0.60	
M/Lb	1.49	1.31	1.02	0.78	0.55	
M/Lv	1.44	1.28	1.02	0.83	0.65	
M/Lk	0.70	0.64	0.53	0.50	0.50	

TABLE 5—*Continued*

D.

	Z	[Fe/H]	Y	s	η	
	0.0010	-1.27	0.23	3.35	0.30	
		R-HB				
AGE (Gyr)	18.0	15.0	12.5	10.0	8.0	
Mto	0.76	0.79	0.83	0.89	0.94	
Mrt	0.65	0.71	0.76	0.82	0.89	
Mpn	0.52	0.53	0.55	0.57	0.59	
B	1.40	1.39	1.38	1.37	1.32	
Bol	0.08	0.00	-0.08	-0.18	-0.32	
Bol-V	-0.62	-0.60	-0.58	-0.57	-0.56	
U-V	0.95	0.92	0.88	0.84	0.82	
B-V	0.82	0.80	0.78	0.76	0.74	
V-R	0.79	0.77	0.76	0.75	0.74	
V-I	1.40	1.38	1.35	1.33	1.31	
V-J	1.98	1.95	1.92	1.89	1.88	
V-K	2.76	2.73	2.69	2.66	2.64	
% MS	.447	.436	.429	.440	.449	
% SGB	.093	.097	.097	.072	.069	
% RGB	.286	.276	.267	.259	.244	
% HB	.070	.068	.067	.066	.063	
% AGB	.102	.121	.137	.160	.174	
% PAGB	.003	.003	.002	.002	.002	
M/Lbol	8.50	8.00	6.80	6.40	6.10	
M/Lb	16.80	15.24	12.49	11.43	10.60	
M/Lv	14.11	13.03	10.88	10.14	9.58	
M/Lk	4.18	3.97	3.44	3.30	3.17	

	Z	[Fe/H]	Y	s	η	
	0.0010	-1.27	0.23	3.35	0.50	
Mto	0.76	0.79	0.83	0.89	0.94	
Mrt	0.55	0.62	0.68	0.76	0.83	
Mpn	0.47	0.49	0.50	0.53	0.55	
B	1.47	1.46	1.44	1.43	1.36	
Bol	0.08	0.00	-0.08	-0.18	-0.33	
Bol-V	-0.59	-0.58	-0.56	-0.54	-0.54	
U-V	0.92	0.89	0.86	0.82	0.80	
B-V	0.80	0.78	0.77	0.74	0.73	
V-R	0.77	0.76	0.75	0.73	0.72	
V-I	1.37	1.35	1.33	1.31	1.29	
V-J	1.94	1.92	1.89	1.86	1.85	
V-K	2.70	2.68	2.64	2.61	2.60	
% MS	.468	.456	.447	.459	.466	
% SGB	.097	.101	.101	.076	.072	
% RGB	.299	.288	.279	.271	.253	
% HB	.081	.074	.071	.069	.066	
% AGB	.049	.075	.098	.122	.141	
% PAGB	.006	.005	.004	.003	.002	
M/Lbol	8.90	8.40	7.10	6.70	6.30	
M/Lb	16.80	15.43	12.68	11.43	10.65	
M/Lv	14.37	13.44	11.15	10.33	9.71	
M/Lk	4.50	4.29	3.69	3.52	3.34	

TABLE 5—*Continued*

E.

	Z	[Fe/H]	Y	s	η	
	0.0010	-1.27	0.23	2.35	0.30	
AGE (Gyr)	18.0	R-HB 15.0	12.5	10.0	8.0	
Mto	0.76	0.79	0.83	0.89	0.94	
Mrt	0.65	0.71	0.76	0.82	0.89	
Mpn	0.52	0.53	0.55	0.57	0.59	
B	1.75	1.74	1.70	1.68	1.65	
Bol	0.14	0.00	-0.15	-0.32	-0.50	
Bol-V	-0.52	-0.51	-0.50	-0.49	-0.47	
U-V	0.90	0.87	0.84	0.81	0.78	
B-V	0.79	0.77	0.75	0.73	0.71	
V-R	0.75	0.74	0.73	0.71	0.70	
V-I	1.31	1.29	1.28	1.26	1.23	
V-J	1.85	1.83	1.81	1.79	1.76	
V-K	2.59	2.56	2.54	2.52	2.48	
% MS	.307	.298	.296	.313	.309	
% SGB	.115	.120	.118	.088	.085	
% RGB	.358	.344	.330	.319	.307	
% HB	.088	.085	.083	.081	.079	
% AGB	.128	.150	.169	.197	.218	
% PAGB	.004	.003	.003	.002	.002	
M/Lbol	2.80	2.60	2.20	1.90	1.70	
M/Lb	4.91	4.44	3.65	3.07	2.65	
M/Lv	4.24	3.90	3.27	2.80	2.46	
M/Lk	1.47	1.39	1.19	1.03	0.94	

	Z	[Fe/H]	Y	s	η	
	0.0010	-1.27	0.23	2.35	0.50	
Mto	0.76	0.79	0.83	0.89	0.94	
Mrt	0.55	0.62	0.68	0.76	0.83	
Mpn	0.47	0.49	0.50	0.53	0.55	
B	1.86	1.84	1.80	1.77	1.73	
Bol	0.14	0.00	-0.15	-0.32	-0.51	
Bol-V	-0.48	-0.47	-0.47	-0.46	-0.45	
U-V	0.87	0.84	0.82	0.79	0.76	
B-V	0.77	0.75	0.74	0.72	0.70	
V-R	0.73	0.72	0.71	0.70	0.69	
V-I	1.28	1.26	1.25	1.23	1.21	
V-J	1.80	1.78	1.77	1.74	1.72	
V-K	2.51	2.49	2.47	2.45	2.42	
% MS	.326	.315	.312	.330	.323	
% SGB	.122	.127	.124	.093	.089	
% RGB	.380	.364	.347	.336	.321	
% HB	.103	.094	.089	.086	.083	
% AGB	.062	.095	.123	.152	.180	
% PAGB	.007	.006	.005	.004	.003	
M/Lbol	3.00	2.70	2.30	2.00	1.80	
M/Lb	4.98	4.36	3.68	3.11	2.72	
M/Lv	4.38	3.90	3.32	2.86	2.55	
M/Lk	1.63	1.48	1.29	1.13	1.04	

TABLE 5—*Continued*

F.

	Z	[Fe/H]	Y	s	η	
	0.0010	-1.27	0.23	1.35	0.30	
		R-HB				
AGE (Gyr)	18.0	15.0	12.5	10.0	8.0	
Mto	0.76	0.79	0.83	0.89	0.94	
Mrt	0.65	0.71	0.76	0.82	0.89	
Mpn	0.52	0.53	0.55	0.57	0.59	
B	1.93	1.91	1.87	1.84	1.81	
Bol	0.20	0.00	-0.20	-0.44	-0.68	
Bol-V	-0.49	-0.49	-0.48	-0.48	-0.46	
U-V	0.89	0.86	0.83	0.81	0.79	
B-V	0.78	0.77	0.75	0.73	0.71	
V-R	0.74	0.73	0.72	0.71	0.69	
V-I	1.29	1.27	1.26	1.25	1.22	
V-J	1.82	1.80	1.78	1.77	1.74	
V-K	2.54	2.52	2.51	2.50	2.46	
% MS	.238	.230	.232	.251	.244	
% SGB	.125	.130	.128	.095	.092	
% RGB	.395	.378	.362	.348	.337	
% HB	.096	.093	.090	.088	.087	
% AGB	.141	.165	.185	.215	.239	
% PAGB	.005	.004	.003	.003	.002	
M/Lbol	1.20	1.00	0.90	0.80	0.60	
M/Lb	2.03	1.67	1.47	1.28	0.93	
M/Lv	1.77	1.47	1.31	1.17	0.86	
M/Lk	0.64	0.54	0.49	0.44	0.34	

	Z	[Fe/H]	Y	s	η	
	0.0010	-1.27	0.23	1.35	0.50	
Mto	0.76	0.79	0.83	0.89	0.94	
Mrt	0.55	0.62	0.68	0.76	0.83	
Mpn	0.47	0.49	0.50	0.53	0.55	
B	2.06	2.03	1.98	1.94	1.91	
Bol	0.20	0.00	-0.21	-0.45	-0.69	
Bol-V	-0.45	-0.45	-0.45	-0.44	-0.43	
U-V	0.86	0.84	0.81	0.79	0.77	
B-V	0.76	0.75	0.74	0.72	0.70	
V-R	0.71	0.71	0.70	0.69	0.68	
V-I	1.25	1.24	1.23	1.22	1.19	
V-J	1.76	1.75	1.74	1.72	1.70	
V-K	2.45	2.44	2.43	2.42	2.39	
% MS	.254	.245	.245	.266	.257	
% SGB	.134	.138	.135	.100	.097	
% RGB	.421	.402	.383	.368	.354	
% HB	.114	.104	.098	.094	.091	
% AGB	.069	.105	.134	.167	.198	
% PAGB	.008	.007	.005	.004	.003	
M/Lbol	1.30	1.10	0.90	0.80	0.70	
M/Lb	2.08	1.74	1.41	1.22	1.04	
M/Lv	1.84	1.56	1.28	1.12	0.98	
M/Lk	0.73	0.62	0.51	0.46	0.41	

TABLE 5—*Continued*
G.

		Z	[Fe/H]	Y	s	η		
		0.0100	-0.25	0.25	3.35	0.30		
AGE (Gyr)	R-HB 15.0	12.5	10.0	8.0		6.0	5.0	4.0
Mto	0.87	0.91	0.97	1.02		1.08	1.14	1.20
Mrt	0.75	0.82	0.89	0.97		1.07	1.13	1.22
Mpn	0.53	0.55	0.57	0.59		0.61	0.63	0.65
B	1.41	1.38	1.38	1.35		1.34	1.32	1.26
Bol	0.00	-0.10	-0.20	-0.31		-0.45	-0.54	-0.67
Bol-V	-0.91	-0.88	-0.84	-0.80		-0.77	-0.74	-0.72
U-V	1.25	1.21	1.15	1.09		1.03	0.99	0.94
B-V	0.92	0.90	0.88	0.85		0.82	0.80	0.77
V-R	0.89	0.88	0.86	0.84		0.81	0.80	0.78
V-I	1.61	1.59	1.55	1.51		1.47	1.44	1.41
V-J	2.30	2.27	2.22	2.17		2.12	2.08	2.05
V-K	3.23	3.20	3.14	3.07		3.01	2.97	2.94
% MS	.455	.441	.429	.410		.386	.383	.380
% SGB	.077	.088	.084	.093		.103	.101	.102
% RGB	.276	.263	.256	.244		.233	.225	.211
% HB	.067	.066	.066	.064		.064	.062	.060
% AGB	.121	.139	.165	.187		.213	.228	.245
% PAGB	.003	.002	.002	.002		.001	.001	.001
M/Lbol	10.90	10.60	8.80	8.10		7.20	6.60	5.90
M/Lb	30.86	28.66	22.52	19.43		16.34	14.31	12.21
M/Lv	23.63	22.35	17.88	15.87		13.72	12.23	10.74
M/Lk	4.54	4.42	3.74	3.54		3.23	2.99	2.70

		Z	[Fe/H]	Y	s	η		
		0.0100	-0.25	0.25	3.35	0.50		
Mto	0.87	0.91	0.97	1.02		1.08	1.14	1.20
Mrt	0.63	0.71	0.80	0.89		1.00	1.07	1.16
Mpn	0.48	0.50	0.51	0.53		0.56	0.58	0.60
B	1.49	1.45	1.45	1.43		1.41	1.38	1.33
Bol	0.00	-0.10	-0.20	-0.31		-0.45	-0.55	-0.68
Bol-V	-0.86	-0.84	-0.80	-0.76		-0.72	-0.70	-0.67
U-V	1.24	1.20	1.14	1.08		1.02	0.98	0.93
B-V	0.91	0.90	0.87	0.84		0.81	0.79	0.76
V-R	0.88	0.87	0.84	0.82		0.80	0.78	0.76
V-I	1.58	1.56	1.52	1.48		1.44	1.42	1.38
V-J	2.25	2.23	2.18	2.13		2.07	2.04	2.00
V-K	3.16	3.13	3.07	3.01		2.94	2.91	2.86
% MS	.481	.464	.452	.432		.407	.402	.402
% SGB	.082	.093	.088	.098		.108	.106	.108
% RGB	.292	.276	.270	.256		.246	.236	.223
% HB	.074	.070	.070	.068		.067	.066	.063
% AGB	.065	.093	.116	.143		.169	.188	.203
% PAGB	.005	.004	.004	.003		.002	.002	.002
M/Lbol	11.50	11.10	9.30	8.50		7.50	6.90	6.20
M/Lb	30.81	28.93	22.72	19.47		16.11	14.28	12.14
M/Lv	23.81	22.56	18.22	16.05		13.65	12.33	10.77
M/Lk	4.88	4.76	4.06	3.78		3.43	3.18	2.91

TABLE 5—*Continued*

H.

		Z	[Fe/H]	Y	s	η		
		0.0100	-0.25	0.25	2.35	0.30		
AGE (Gyr)	R-HB 15.0	12.5	10.0	8.0	6.0	5.0	4.0
Mto	0.87	0.91	0.97	1.02	1.08	1.14	1.20
Mrt	0.75	0.82	0.89	0.97	1.07	1.13	1.22
Mpn	0.53	0.55	0.57	0.59	0.61	0.63	0.65
B	1.80	1.76	1.72	1.66	1.62	1.58	1.52
Bol	0.00	-0.15	-0.34	-0.53	-0.77	-0.92	-1.12
Bol-V	-0.80	-0.78	-0.76	-0.73	-0.71	-0.70	-0.68
U-V	1.20	1.17	1.11	1.07	1.01	0.98	0.93
B-V	0.89	0.88	0.86	0.84	0.81	0.79	0.77
V-R	0.85	0.84	0.83	0.81	0.79	0.78	0.77
V-I	1.52	1.50	1.48	1.45	1.43	1.41	1.39
V-J	2.17	2.15	2.12	2.08	2.05	2.03	2.00
V-K	3.07	3.03	3.00	2.96	2.93	2.90	2.88
% MS	.307	.294	.291	.279	.260	.262	.259
% SGB	.097	.110	.102	.112	.121	.118	.119
% RGB	.352	.333	.318	.299	.282	.270	.254
% HB	.086	.084	.081	.079	.077	.075	.072
% AGB	.154	.176	.205	.229	.257	.273	.295
% PAGB	.004	.003	.002	.002	.002	.001	.001
M/Lbol	3.40	3.00	2.50	2.20	1.80	1.60	1.30
M/Lb	8.46	7.26	5.83	4.90	3.83	3.31	2.59
M/Lv	6.66	5.77	4.72	4.04	3.25	2.86	2.28
M/Lk	1.48	1.33	1.12	1.00	0.82	0.74	0.61

		Z	[Fe/H]	Y	s	η		
		0.0100	-0.25	0.25	2.35	0.50		
Mto	0.87	0.91	0.97	1.02	1.08	1.14	1.20
Mrt	0.63	0.71	0.80	0.89	1.00	1.07	1.16
Mpn	0.48	0.50	0.51	0.53	0.56	0.58	0.60
B	1.93	1.87	1.84	1.77	1.73	1.68	1.62
Bol	0.00	-0.16	-0.34	-0.54	-0.77	-0.93	-1.13
Bol-V	-0.73	-0.72	-0.70	-0.68	-0.65	-0.65	-0.63
U-V	1.18	1.15	1.10	1.05	1.00	0.97	0.92
B-V	0.88	0.87	0.85	0.83	0.80	0.79	0.76
V-R	0.83	0.82	0.81	0.79	0.78	0.77	0.75
V-I	1.48	1.47	1.44	1.42	1.39	1.38	1.35
V-J	2.11	2.09	2.06	2.03	1.99	1.98	1.94
V-K	2.96	2.95	2.91	2.87	2.83	2.82	2.78
% MS	.331	.312	.312	.297	.278	.279	.276
% SGB	.104	.117	.109	.119	.129	.126	.127
% RGB	.378	.355	.340	.318	.301	.286	.271
% HB	.096	.090	.088	.084	.082	.080	.077
% AGB	.085	.119	.146	.177	.207	.228	.248
% PAGB	.007	.005	.005	.004	.003	.002	.002
M/Lbol	3.60	3.20	2.70	2.30	1.90	1.70	1.40
M/Lb	8.32	7.26	5.91	4.85	3.79	3.36	2.64
M/Lv	6.61	5.82	4.82	4.03	3.24	2.90	2.34
M/Lk	1.63	1.45	1.25	1.08	0.90	0.81	0.68

TABLE 5—*Continued*

		Z	[Fe/H]	Y	s	η		
		0.0100	-0.25	0.25	1.35	0.30		
AGE (Gyr)	R-HB 15.0	12.5	10.0	8.0	6.0	5.0	4.0
Mto	0.87	0.91	0.97	1.02	1.08	1.14	1.20
Mrt	0.75	0.82	0.89	0.97	1.07	1.13	1.22
Mpn	0.53	0.55	0.57	0.59	0.61	0.63	0.65
B	1.99	1.93	1.87	1.81	1.76	1.71	1.64
Bol	0.00	-0.21	-0.47	-0.72	-1.05	-1.26	-1.52
Bol-V	-0.78	-0.76	-0.75	-0.73	-0.72	-0.71	-0.71
U-V	1.19	1.16	1.11	1.07	1.02	1.00	0.95
B-V	0.89	0.88	0.86	0.84	0.82	0.80	0.78
V-R	0.84	0.84	0.82	0.81	0.80	0.79	0.78
V-I	1.51	1.49	1.48	1.46	1.44	1.43	1.41
V-J	2.15	2.13	2.11	2.08	2.06	2.05	2.03
V-K	3.04	3.02	3.00	2.97	2.95	2.93	2.91
% MS	.237	.225	.226	.217	.202	.204	.200
% SGB	.105	.119	.110	.120	.128	.125	.126
% RGB	.388	.367	.348	.326	.306	.292	.275
% HB	.095	.092	.089	.086	.083	.081	.078
% AGB	.170	.194	.224	.249	.279	.297	.319
% PAGB	.004	.003	.003	.002	.002	.002	.001
M/Lbol	1.30	1.20	0.90	0.80	0.60	0.50	0.50
M/Lb	3.18	2.85	2.08	1.78	1.30	1.05	1.04
M/Lv	2.50	2.27	1.68	1.47	1.09	0.90	0.90
M/Lk	0.57	0.53	0.40	0.36	0.27	0.23	0.23
		Z	[Fe/H]	Y	s	η		
		0.0100	-0.25	0.25	1.35	0.50		
Mto	0.87	0.91	0.97	1.02	1.08	1.14	1.20
Mrt	0.63	0.71	0.80	0.89	1.00	1.07	1.16
Mpn	0.48	0.50	0.51	0.53	0.56	0.58	0.60
B	2.15	2.07	2.02	1.94	1.88	1.83	1.77
Bol	0.00	-0.22	-0.47	-0.74	-1.06	-1.27	-1.53
Bol-V	-0.71	-0.70	-0.69	-0.67	-0.66	-0.66	-0.64
U-V	1.17	1.15	1.10	1.06	1.01	0.98	0.94
B-V	0.88	0.87	0.85	0.83	0.81	0.79	0.77
V-R	0.82	0.82	0.81	0.80	0.78	0.78	0.76
V-I	1.46	1.46	1.44	1.42	1.40	1.39	1.37
V-J	2.07	2.07	2.05	2.02	2.00	1.99	1.97
V-K	2.92	2.92	2.89	2.87	2.85	2.84	2.81
% MS	.257	.241	.244	.233	.217	.217	.216
% SGB	.114	.127	.118	.128	.137	.133	.135
% RGB	.421	.393	.375	.349	.328	.312	.295
% HB	.106	.100	.097	.092	.090	.087	.084
% AGB	.094	.132	.162	.194	.225	.249	.269
% PAGB	.008	.006	.005	.004	.003	.002	.002
M/Lbol	1.40	1.20	1.00	0.80	0.70	0.60	0.50
M/Lb	3.18	2.67	2.17	1.67	1.42	1.20	0.96
M/Lv	2.52	2.14	1.77	1.39	1.21	1.03	0.85
M/Lk	0.65	0.55	0.47	0.37	0.33	0.28	0.24

TABLE 5—*Continued*

J.

		Z	[Fe/H]	Y	s	η		
		0.0170	-0.02	0.25	3.35	0.30		
AGE (Gyr)	R-HB 15.0	12.5	10.0	8.0	6.0	5.0	4.0
Mto	0.94	0.98	1.02	1.08	1.14	1.20	1.27
Mrt	0.81	0.87	0.95	1.03	1.13	1.20	1.29
Mpn	0.54	0.56	0.58	0.59	0.62	0.64	0.65
B	1.30	1.32	1.31	1.30	1.28	1.24	1.21
Bol	0.00	-0.06	-0.17	-0.27	-0.41	-0.53	-0.65
Bol-V	-1.04	-0.99	-0.94	-0.90	-0.85	-0.85	-0.82
U-V	1.38	1.33	1.26	1.19	1.12	1.08	1.04
B-V	0.97	0.94	0.92	0.88	0.85	0.84	0.81
V-R	0.94	0.92	0.89	0.87	0.84	0.83	0.81
V-I	1.70	1.66	1.62	1.57	1.53	1.52	1.49
V-J	2.43	2.38	2.32	2.27	2.21	2.20	2.16
V-K	3.42	3.35	3.28	3.22	3.15	3.14	3.09
% MS	.501	.478	.441	.427	.400	.407	.402
% SGB	.058	.062	.085	.087	.098	.090	.093
% RGB	.252	.251	.241	.234	.224	.212	.201
% HB	.060	.062	.061	.060	.059	.057	.056
% AGB	.126	.145	.170	.189	.217	.232	.248
% PAGB	.002	.002	.002	.002	.001	.001	.001
M/Lbol	12.40	11.10	10.20	9.40	8.20	7.50	6.80
M/Lb	41.44	34.46	29.69	25.42	20.60	18.67	16.01
M/Lv	30.30	25.90	22.73	20.19	16.82	15.38	13.57
M/Lk	4.89	4.46	4.17	3.92	3.48	3.21	2.97
		Z	[Fe/H]	Y	s	η		
		0.0170	-0.02	0.25	3.35	0.50		
Mto	0.94	0.98	1.02	1.08	1.14	1.20	1.27
Mrt	0.68	0.76	0.86	0.95	1.06	1.14	1.24
Mpn	0.49	0.50	0.52	0.54	0.56	0.58	0.60
B	1.38	1.39	1.38	1.37	1.35	1.31	1.27
Bol	0.00	-0.06	-0.17	-0.28	-0.42	-0.53	-0.65
Bol-V	-0.99	-0.94	-0.89	-0.85	-0.80	-0.79	-0.77
U-V	1.37	1.32	1.25	1.18	1.11	1.07	1.03
B-V	0.96	0.94	0.91	0.88	0.84	0.83	0.81
V-R	0.92	0.90	0.88	0.85	0.83	0.82	0.80
V-I	1.67	1.63	1.59	1.55	1.50	1.48	1.46
V-J	2.39	2.33	2.28	2.22	2.16	2.14	2.11
V-K	3.35	3.28	3.21	3.15	3.07	3.06	3.02
% MS	.530	.504	.465	.451	.423	.433	.423
% SGB	.061	.066	.090	.092	.104	.095	.098
% RGB	.266	.265	.254	.247	.236	.225	.213
% HB	.065	.066	.064	.064	.063	.061	.059
% AGB	.073	.096	.124	.144	.172	.185	.206
% PAGB	.004	.004	.003	.003	.002	.002	.001
M/Lbol	13.10	11.80	10.80	9.90	8.70	7.90	7.10
M/Lb	41.43	34.99	29.75	25.56	20.68	18.43	15.97
M/Lv	30.57	26.30	22.98	20.31	17.04	15.33	13.53
M/Lk	5.26	4.83	4.50	4.20	3.80	3.45	3.16

TABLE 5—*Continued*

K.

		Z	[Fe/H]	Y	s	η		
		0.0170	-0.02	0.25	2.35	0.30		
AGE (Gyr)	R-HB 15.0	12.5	10.0	8.0	6.0	5.0	4.0
Mto	0.94	0.98	1.02	1.08	1.14	1.20	1.27
Mrt	0.81	0.87	0.95	1.03	1.13	1.20	1.29
Mpn	0.54	0.56	0.58	0.59	0.62	0.64	0.65
B	1.73	1.71	1.66	1.63	1.57	1.53	1.49
Bol	0.00	-0.14	-0.33	-0.51	-0.76	-0.92	-1.11
Bol-V	-0.90	-0.87	-0.84	-0.81	-0.79	-0.79	-0.76
U-V	1.32	1.27	1.22	1.15	1.09	1.06	1.02
B-V	0.93	0.91	0.89	0.86	0.84	0.82	0.80
V-R	0.89	0.87	0.85	0.84	0.82	0.81	0.80
V-I	1.59	1.57	1.54	1.51	1.48	1.47	1.45
V-J	2.27	2.24	2.20	2.17	2.13	2.12	2.09
V-K	3.22	3.18	3.14	3.09	3.06	3.05	3.01
% MS	.337	.324	.291	.284	.266	.269	.265
% SGB	.076	.079	.106	.107	.118	.108	.111
% RGB	.336	.326	.307	.294	.275	.263	.249
% HB	.081	.080	.078	.076	.073	.071	.069
% AGB	.167	.189	.216	.238	.267	.289	.306
% PAGB	.003	.003	.002	.002	.001	.001	.001
M/Lbol	3.80	3.30	2.80	2.40	2.00	1.70	1.50
M/Lb	10.76	8.92	7.23	5.86	4.71	3.93	3.31
M/Lv	8.16	6.89	5.69	4.74	3.88	3.30	2.83
M/Lk	1.58	1.39	1.19	1.04	0.87	0.75	0.67

		Z	[Fe/H]	Y	s	η		
		0.0170	-0.02	0.25	2.35	0.50		
Mto	0.94	0.98	1.02	1.08	1.14	1.20	1.27
Mrt	0.68	0.76	0.86	0.95	1.06	1.14	1.24
Mpn	0.49	0.50	0.52	0.54	0.56	0.58	0.60
B	1.87	1.84	1.78	1.75	1.68	1.65	1.59
Bol	0.00	-0.15	-0.34	-0.52	-0.77	-0.93	-1.12
Bol-V	-0.83	-0.81	-0.78	-0.75	-0.73	-0.72	-0.70
U-V	1.30	1.26	1.21	1.14	1.08	1.05	1.01
B-V	0.92	0.90	0.88	0.86	0.83	0.81	0.79
V-R	0.87	0.85	0.84	0.82	0.80	0.79	0.78
V-I	1.55	1.53	1.50	1.47	1.44	1.43	1.41
V-J	2.21	2.18	2.15	2.11	2.07	2.05	2.03
V-K	3.12	3.08	3.04	3.00	2.96	2.94	2.92
% MS	.363	.348	.311	.303	.284	.289	.283
% SGB	.082	.085	.114	.114	.126	.116	.118
% RGB	.362	.350	.328	.315	.295	.283	.266
% HB	.088	.087	.083	.081	.078	.077	.074
% AGB	.099	.126	.160	.183	.214	.233	.257
% PAGB	.006	.005	.004	.003	.003	.002	.002
M/Lbol	4.10	3.50	3.00	2.60	2.10	1.90	1.60
M/Lb	10.78	8.87	7.26	6.01	4.64	4.08	3.31
M/Lv	8.26	6.92	5.77	4.86	3.86	3.46	2.86
M/Lk	1.76	1.53	1.32	1.16	0.95	0.87	0.73

TABLE 5—*Continued*

L.

		Z	[Fe/H]	Y	s	η		
		0.0170	-0.02	0.25	1.35	0.30		
AGE (Gyr)	R-HB 15.0	12.5	10.0	8.0		6.0	5.0	4.0
Mto	0.94	0.98	1.02	1.08		1.14	1.20	1.27
Mrt	0.81	0.87	0.95	1.03		1.13	1.20	1.29
Mpn	0.54	0.56	0.58	0.59		0.62	0.64	0.65
B	1.93	1.90	1.83	1.79		1.71	1.67	1.62
Bol	0.00	-0.20	-0.46	-0.71		-1.04	-1.26	-1.51
Bol-V	-0.88	-0.86	-0.84	-0.82		-0.81	-0.80	-0.79
U-V	1.30	1.26	1.22	1.16		1.10	1.07	1.04
B-V	0.92	0.91	0.89	0.87		0.84	0.83	0.81
V-R	0.88	0.87	0.85	0.84		0.82	0.82	0.81
V-I	1.57	1.55	1.53	1.51		1.49	1.48	1.47
V-J	2.25	2.22	2.20	2.17		2.14	2.14	2.12
V-K	3.19	3.17	3.13	3.10		3.08	3.07	3.05
% MS	.262	.253	.224	.219		.203	.206	.203
% SGB	.084	.086	.114	.114		.125	.115	.117
% RGB	.374	.360	.337	.322		.300	.287	.271
% HB	.090	.088	.085	.083		.080	.078	.075
% AGB	.187	.208	.237	.260		.291	.313	.333
% PAGB	.004	.003	.002	.002		.002	.001	.001
M/Lbol	1.50	1.30	1.00	0.90		0.70	0.60	0.50
M/Lb	4.13	3.48	2.58	2.24		1.68	1.41	1.15
M/Lv	3.16	2.69	2.03	1.80		1.38	1.18	0.97
M/Lk	0.63	0.55	0.43	0.39		0.31	0.26	0.22

		Z	[Fe/H]	Y	s	η		
		0.0170	-0.02	0.25	1.35	0.50		
Mto	0.94	0.98	1.02	1.08		1.14	1.20	1.27
Mrt	0.68	0.76	0.86	0.95		1.06	1.14	1.24
Mpn	0.49	0.50	0.52	0.54		0.56	0.58	0.60
B	2.10	2.05	1.97	1.92		1.85	1.81	1.74
Bol	0.00	-0.21	-0.47	-0.72		-1.05	-1.26	-1.52
Bol-V	-0.80	-0.79	-0.77	-0.75		-0.74	-0.73	-0.73
U-V	1.29	1.25	1.20	1.14		1.09	1.06	1.02
B-V	0.91	0.90	0.88	0.86		0.83	0.82	0.80
V-R	0.86	0.85	0.84	0.82		0.81	0.80	0.79
V-I	1.53	1.51	1.49	1.47		1.45	1.44	1.43
V-J	2.17	2.16	2.13	2.11		2.08	2.07	2.06
V-K	3.07	3.05	3.03	3.00		2.97	2.96	2.95
% MS	.285	.274	.241	.236		.218	.224	.219
% SGB	.091	.094	.123	.123		.135	.124	.126
% RGB	.407	.390	.363	.347		.324	.311	.291
% HB	.099	.096	.092	.089		.086	.084	.081
% AGB	.112	.140	.177	.202		.235	.255	.282
% PAGB	.007	.006	.005	.004		.003	.002	.002
M/Lbol	1.60	1.40	1.10	0.90		0.70	0.60	0.50
M/Lb	4.06	3.48	2.64	2.08		1.56	1.31	1.07
M/Lv	3.13	2.72	2.10	1.68		1.30	1.10	0.92
M/Lk	0.70	0.62	0.48	0.40		0.32	0.27	0.23

TABLE 5—*Continued*

M.

		Z	[Fe/H]	Y	s	η		
		0.0300	0.23	0.25	3.35	0.30		
AGE (Gyr)	R-HB 15.0	12.5	10.0	8.0	6.0	5.0	4.0
Mto	1.00	1.04	1.08	1.14	1.20	1.26	1.34
Mrt	0.86	0.93	1.01	1.09	1.20	1.27	1.36
Mpn	0.54	0.56	0.58	0.60	0.62	0.65	0.65
B	1.27	1.26	1.30	1.29	1.27	1.24	1.24
Bol	0.00	-0.09	-0.15	-0.26	-0.40	-0.51	-0.61
Bol-V	-1.13	-1.09	-1.03	-0.98	-0.93	-0.91	-0.87
U-V	1.50	1.44	1.37	1.29	1.21	1.16	1.12
B-V	1.00	0.97	0.94	0.91	0.88	0.86	0.84
V-R	0.96	0.94	0.92	0.89	0.86	0.85	0.83
V-I	1.75	1.71	1.66	1.62	1.57	1.55	1.51
V-J	2.51	2.47	2.40	2.34	2.28	2.25	2.21
V-K	3.54	3.49	3.41	3.34	3.27	3.23	3.18
% MS	.512	.500	.441	.427	.406	.402	.393
% SGB	.052	.052	.082	.083	.089	.085	.083
% RGB	.245	.240	.239	.232	.222	.213	.207
% HB	.058	.058	.059	.059	.058	.057	.056
% AGB	.130	.149	.177	.198	.224	.243	.259
% PAGB	.002	.002	.002	.001	.001	.001	.001
M/Lbol	14.30	14.20	12.20	10.90	10.30	9.50	8.30
M/Lb	53.37	49.69	39.30	32.62	28.63	25.45	21.04
M/Lv	37.96	36.33	29.54	25.20	22.74	20.59	17.34
M/Lk	5.49	5.50	4.81	4.38	4.22	3.96	3.49

		Z	[Fe/H]	Y	s	η		
		0.0300	0.23	0.25	3.35	0.50		
Mto	1.00	1.04	1.08	1.14	1.20	1.26	1.34
Mrt	0.72	0.81	0.91	1.00	1.13	1.21	1.31
Mpn	0.49	0.51	0.52	0.54	0.56	0.58	0.60
B	1.35	1.33	1.37	1.36	1.34	1.32	1.31
Bol	0.00	-0.09	-0.15	-0.26	-0.40	-0.50	-0.61
Bol-V	-1.08	-1.04	-0.98	-0.93	-0.88	-0.85	-0.82
U-V	1.49	1.44	1.37	1.29	1.20	1.16	1.11
B-V	0.99	0.97	0.94	0.91	0.87	0.85	0.83
V-R	0.95	0.93	0.90	0.88	0.85	0.83	0.82
V-I	1.72	1.69	1.64	1.59	1.54	1.51	1.49
V-J	2.47	2.43	2.35	2.30	2.23	2.20	2.16
V-K	3.47	3.42	3.33	3.26	3.19	3.15	3.10
% MS	.542	.528	.467	.451	.430	.428	.416
% SGB	.055	.055	.087	.088	.094	.091	.088
% RGB	.260	.253	.253	.245	.236	.227	.219
% HB	.062	.061	.063	.062	.061	.060	.060
% AGB	.078	.101	.128	.150	.177	.193	.215
% PAGB	.004	.003	.003	.003	.002	.002	.001
M/Lbol	15.10	14.90	12.90	11.50	10.90	10.10	8.80
M/Lb	53.33	49.80	39.68	32.86	28.67	25.37	21.11
M/Lv	38.28	36.41	29.83	25.39	22.98	20.72	17.56
M/Lk	5.90	5.88	5.23	4.75	4.59	4.29	3.81

TABLE 5—*Continued*

N.

		Z	[Fe/H]	Y	s	η		
		0.0300	0.23	0.25	2.35	0.30		
AGE (Gyr)	R-HB 15.0	12.5	10.0	8.0		6.0	5.0	4.0
Mto	1.00	1.04	1.08	1.14		1.20	1.26	1.34
Mrt	0.86	0.93	1.01	1.09		1.20	1.27	1.36
Mpn	0.54	0.56	0.58	0.60		0.62	0.65	0.65
B	1.70	1.68	1.65	1.61		1.57	1.52	1.50
Bol	0.00	-0.15	-0.32	-0.51		-0.74	-0.91	-1.08
Bol-V	-0.99	-0.96	-0.93	-0.90		-0.87	-0.86	-0.84
U-V	1.43	1.38	1.33	1.26		1.18	1.14	1.11
B-V	0.96	0.94	0.92	0.89		0.86	0.85	0.83
V-R	0.91	0.90	0.88	0.86		0.84	0.83	0.82
V-I	1.64	1.61	1.59	1.56		1.53	1.51	1.49
V-J	2.36	2.32	2.29	2.25		2.21	2.19	2.16
V-K	3.35	3.31	3.27	3.23		3.18	3.16	3.13
% MS	.349	.339	.292	.286		.269	.269	.269
% SGB	.068	.068	.102	.102		.106	.102	.097
% RGB	.328	.318	.304	.290		.275	.261	.251
% HB	.077	.076	.075	.073		.071	.069	.068
% AGB	.174	.197	.225	.248		.277	.298	.314
% PAGB	.003	.003	.002	.002		.001	.001	.001
M/Lbol	4.20	3.80	3.20	2.70		2.30	2.00	1.70
M/Lb	13.28	11.48	9.23	7.37		5.94	5.07	4.15
M/Lv	9.80	8.63	7.07	5.80		4.81	4.14	3.46
M/Lk	1.69	1.54	1.31	1.12		0.97	0.85	0.73

		Z	[Fe/H]	Y	s	η		
		0.0300	0.23	0.25	2.35	0.50		
Mto	1.00	1.04	1.08	1.14		1.20	1.26	1.34
Mrt	0.72	0.81	0.91	1.00		1.13	1.21	1.31
Mpn	0.49	0.51	0.52	0.54		0.56	0.58	0.60
B	1.84	1.80	1.78	1.73		1.68	1.64	1.61
Bol	0.00	-0.15	-0.33	-0.51		-0.75	-0.91	-1.09
Bol-V	-0.92	-0.89	-0.86	-0.84		-0.81	-0.79	-0.78
U-V	1.42	1.38	1.32	1.25		1.17	1.13	1.10
B-V	0.96	0.94	0.91	0.89		0.86	0.84	0.82
V-R	0.90	0.88	0.86	0.85		0.83	0.81	0.80
V-I	1.61	1.58	1.55	1.52		1.49	1.47	1.45
V-J	2.30	2.26	2.23	2.19		2.15	2.12	2.10
V-K	3.25	3.21	3.17	3.13		3.08	3.05	3.03
% MS	.376	.363	.314	.306		.289	.290	.288
% SGB	.074	.073	.109	.109		.114	.110	.104
% RGB	.354	.341	.327	.312		.296	.282	.269
% HB	.084	.082	.081	.079		.077	.075	.073
% AGB	.106	.136	.165	.191		.222	.240	.264
% PAGB	.006	.005	.004	.003		.003	.002	.002
M/Lbol	4.50	4.10	3.40	2.90		2.50	2.20	1.80
M/Lb	13.34	11.61	9.11	7.49		6.11	5.18	4.12
M/Lv	9.84	8.73	7.04	5.89		4.94	4.27	3.46
M/Lk	1.86	1.71	1.43	1.24		1.09	0.97	0.80

TABLE 5—*Continued*

O.

		Z	[Fe/H]	Y	s	η		
		0.0300	0.23	0.25	1.35	0.30		
AGE (Gyr)	R-HB 15.0	12.5	10.0	8.0	6.0	5.0	4.0	
Mto	1.00	1.04	1.08	1.14	1.20	1.26	1.34	
Mrt	0.86	0.93	1.01	1.09	1.20	1.27	1.36	
Mpn	0.54	0.56	0.58	0.60	0.62	0.65	0.65	
B	1.90	1.86	1.82	1.77	1.71	1.66	1.63	
Bol	0.00	-0.21	-0.45	-0.70	-1.03	-1.24	-1.48	
Bol-V	-0.98	-0.95	-0.94	-0.92	-0.90	-0.89	-0.88	
U-V	1.41	1.37	1.32	1.26	1.19	1.15	1.12	
B-V	0.95	0.94	0.92	0.89	0.87	0.85	0.84	
V-R	0.90	0.89	0.88	0.86	0.85	0.84	0.83	
V-I	1.62	1.60	1.59	1.56	1.54	1.53	1.52	
V-J	2.33	2.30	2.28	2.25	2.23	2.21	2.20	
V-K	3.33	3.29	3.27	3.24	3.21	3.20	3.18	
% MS	.273	.265	.223	.220	.207	.208	.209	
% SGB	.075	.074	.109	.108	.112	.107	.102	
% RGB	.367	.353	.334	.318	.300	.284	.273	
% HB	.086	.085	.083	.080	.078	.075	.074	
% AGB	.195	.219	.248	.271	.302	.324	.340	
% PAGB	.003	.003	.002	.002	.002	.001	.001	
M/Lbol	1.60	1.40	1.10	1.00	0.80	0.70	0.60	
M/Lb	4.97	4.19	3.20	2.78	2.14	1.82	1.54	
M/Lv	3.70	3.15	2.45	2.19	1.72	1.49	1.27	
M/Lk	0.65	0.57	0.45	0.42	0.34	0.29	0.25	

		Z	[Fe/H]	Y	s	η		
		0.0300	0.23	0.25	1.35	0.50		
Mto	1.00	1.04	1.08	1.14	1.20	1.26	1.34	
Mrt	0.72	0.81	0.91	1.00	1.13	1.21	1.31	
Mpn	0.49	0.51	0.52	0.54	0.56	0.58	0.60	
B	2.07	2.02	1.96	1.91	1.85	1.80	1.76	
Bol	0.00	-0.21	-0.46	-0.71	-1.03	-1.24	-1.49	
Bol-V	-0.89	-0.87	-0.86	-0.84	-0.82	-0.81	-0.80	
U-V	1.40	1.36	1.31	1.25	1.18	1.14	1.11	
B-V	0.95	0.93	0.91	0.89	0.86	0.85	0.83	
V-R	0.88	0.87	0.86	0.85	0.83	0.82	0.82	
V-I	1.58	1.56	1.55	1.52	1.50	1.48	1.48	
V-J	2.26	2.24	2.22	2.19	2.16	2.14	2.13	
V-K	3.21	3.19	3.16	3.14	3.11	3.08	3.08	
% MS	.297	.287	.242	.238	.224	.227	.227	
% SGB	.082	.080	.118	.117	.121	.117	.110	
% RGB	.400	.383	.362	.344	.324	.309	.294	
% HB	.095	.092	.090	.087	.084	.082	.080	
% AGB	.120	.152	.184	.210	.244	.263	.287	
% PAGB	.006	.005	.004	.004	.003	.002	.002	
M/Lbol	1.70	1.50	1.20	1.00	0.80	0.70	0.60	
M/Lb	4.86	4.13	3.22	2.58	1.97	1.69	1.41	
M/Lv	3.62	3.13	2.48	2.03	1.60	1.38	1.18	
M/Lk	0.71	0.63	0.51	0.42	0.34	0.31	0.26	

NOTE.—Each table of the sequence from A to O is divided into two panels depending on the value of Reimer's parameter for mass loss (η is 0.3 and 0.5 in the upper and lower panels, respectively). The labels R-HB, I-HB, and B-HB refer to the HB morphology adopted for the 15 Gyr model and evolved at the different ages. Stellar masses are in solar units. The other quantities are defined as follows: M_{to} = stellar mass at the turnoff point; M_{rt} = stellar mass at the tip of the RGB; M_{pn} = stellar mass at the onset of the PAGB phase; B = specific evolutionary flux as defined by eq. (7) (here in units of 10^{-11} yr^{-1} $L_{\odot}^{-1}$; Bol = integral bolometric magnitude of the SSP normalized to the model at t = 15 Gyr; Bol − V = bolometric correction of the SSP. $U-V$, $B-V$, $V-R$, $V-I$, $V-J$, and $V-K$, are synthetic colors in the Johnson system. %MS, %SGB, %RGB, %HB, %AGB, and %PAGB are relative contributions to the bolometric from the different stellar evolutionary phases of the SSP. M/L_{bol}, M/L_b, M/L_v, and M/L_k are the mass-to-light ratios of the SSP calculated in the bolometric and Johnson B, V, and K bands in that order. Masses and luminosities are in solar units. The mass M involves only the actual bright mass of the SSP. The values for M/L are thus lower limits.

TABLE 6

RELEVANT PROPERTIES FOR SSP MODELS WITH INTERMEDIATE AND BLUE HORIZONTAL BRANCH

A.

					Z	[Fe/H]	Y	s	η				
					0.0001	-2.27	0.23	3.35	0.30				
		I-HB							B-HB				
Age (Gyr)	18.0	15.0	12.5	10.0	8.0			18.0	15.0	12.5	10.0	8.0	
Mto	0.75	0.79	0.82	0.88	0.93			0.75	0.79	0.82	0.88	0.93	
Mrt	0.67	0.72	0.77	0.83	0.91			0.67	0.72	0.77	0.83	0.91	
Mpn	0.53	0.55	0.56	0.59	0.63			0.53	0.55	0.56	0.59	0.63	
B	1.33	1.32	1.27	1.26	1.26			1.36	1.35	1.30	1.29	1.28	
Bol	0.07	0.00	-0.11	-0.22	-0.31			0.07	0.00	-0.11	-0.22	-0.32	
Bol-V	-0.48	-0.46	-0.45	-0.38	-0.27			-0.52	-0.50	-0.48	-0.40	-0.27	
U-V	0.72	0.70	0.68	0.60	0.43			0.74	0.71	0.67	0.58	0.40	
B-V	0.69	0.68	0.67	0.62	0.51			0.73	0.70	0.67	0.61	0.49	
V-R	0.70	0.69	0.68	0.64	0.54			0.73	0.71	0.69	0.63	0.53	
V-I	1.25	1.22	1.20	1.12	0.96			1.28	1.25	1.22	1.12	0.94	
V-J	1.76	1.73	1.71	1.60	1.38			1.81	1.77	1.73	1.59	1.35	
V-K	2.46	2.42	2.39	2.27	2.04			2.51	2.47	2.43	2.27	2.02	
% MS	.486	.490	.490	.490	.465			.497	.502	.502	.500	.475	
% SGB	.079	.065	.065	.046	.033			.081	.066	.067	.047	.033	
% RGB	.275	.264	.247	.239	.234			.282	.271	.253	.244	.239	
% HB	.053	.056	.057	.059	.062			.029	.032	.034	.038	.043	
% AGB	.105	.123	.139	.165	.205			.108	.126	.143	.169	.210	
% PAGB	.003	.002	.002	.001	.001			.003	.002	.002	.002	.001	
M/Lbol	6.80	6.40	6.30	5.80	4.90			6.90	6.60	6.40	6.00	5.00	
M/Lb	10.48	9.60	9.28	7.65	5.27			11.45	10.46	9.69	7.98	5.28	
M/Lv	9.92	9.17	8.94	7.72	5.89			10.44	9.81	9.34	8.13	6.01	
M/Lk	3.88	3.72	3.73	3.59	3.39			3.90	3.80	3.75	3.79	3.52	
					Z	[Fe/H]	Y	s	η				
					0.0001	-2.27	0.23	3.35	0.50				
Mto	0.75	0.79	0.82	0.88	0.93			0.75	0.79	0.82	0.88	0.93	
Mrt	0.59	0.65	0.71	0.79	0.88			0.59	0.65	0.71	0.79	0.88	
Mpn	0.48	0.51	0.52	0.55	0.59			0.48	0.51	0.52	0.55	0.59	
B	1.38	1.37	1.32	1.30	1.31			1.42	1.40	1.35	1.33	1.33	
Bol	0.08	0.00	-0.11	-0.22	-0.31			0.08	0.00	-0.11	-0.22	-0.31	
Bol-V	-0.47	-0.45	-0.43	-0.37	-0.27			-0.51	-0.49	-0.47	-0.39	-0.27	
U-V	0.70	0.68	0.66	0.59	0.44			0.72	0.68	0.65	0.56	0.42	
B-V	0.67	0.66	0.66	0.61	0.51			0.72	0.69	0.66	0.59	0.49	
V-R	0.69	0.68	0.67	0.63	0.55			0.72	0.70	0.68	0.62	0.53	
V-I	1.23	1.21	1.19	1.12	0.97			1.27	1.24	1.20	1.11	0.94	
V-J	1.74	1.71	1.69	1.58	1.39			1.79	1.75	1.71	1.57	1.35	
V-K	2.42	2.38	2.36	2.24	2.02			2.48	2.43	2.39	2.24	1.99	
% MS	.504	.507	.508	.507	.483			.518	.521	.521	.519	.492	
% SGB	.082	.067	.067	.047	.034			.084	.069	.069	.048	.035	
% RGB	.285	.273	.256	.247	.243			.293	.280	.263	.253	.248	
% HB	.057	.059	.060	.063	.065			.031	.034	.036	.041	.047	
% AGB	.067	.091	.106	.134	.173			.069	.093	.108	.137	.176	
% PAGB	.005	.004	.003	.002	.002			.005	.004	.003	.002	.002	
M/Lbol	7.00	6.70	6.50	6.00	5.10			7.20	6.80	6.70	6.20	5.10	
M/Lb	10.50	9.77	9.31	7.77	5.49			11.73	10.58	9.96	8.02	5.39	
M/Lv	10.12	9.51	9.06	7.91	6.13			10.80	10.01	9.68	8.33	6.13	
M/Lk	4.10	4.00	3.88	3.79	3.59			4.14	4.02	4.04	3.98	3.69	

TABLE 6—*Continued*

B.

					Z	[Fe/H]	Y	s	η				
					0.0001	-2.27	0.23	2.35	0.30				
		I-HB							B-HB				
Age (Gyr)	18.0	15.0	12.5	10.0	8.0			18.0	15.0	12.5	10.0	8.0	
Mto	0.75	0.79	0.82	0.88	0.93			0.75	0.79	0.82	0.88	0.93	
Mrt	0.67	0.72	0.77	0.83	0.91			0.67	0.72	0.77	0.83	0.91	
Mpn	0.53	0.55	0.56	0.59	0.63			0.53	0.55	0.56	0.59	0.63	
B	1.71	1.69	1.63	1.61	1.57			1.76	1.74	1.69	1.66	1.61	
Bol	0.13	0.00	-0.16	-0.33	-0.52			0.13	0.00	-0.16	-0.34	-0.53	
Bol-V	-0.39	-0.37	-0.35	-0.28	-0.17			-0.44	-0.42	-0.39	-0.30	-0.17	
U-V	0.66	0.64	0.62	0.54	0.37			0.68	0.64	0.61	0.52	0.34	
B-V	0.64	0.63	0.63	0.58	0.47			0.69	0.66	0.63	0.56	0.44	
V-R	0.65	0.64	0.63	0.58	0.49			0.68	0.66	0.64	0.57	0.47	
V-I	1.14	1.12	1.10	1.01	0.84			1.18	1.15	1.11	1.00	0.81	
V-J	1.62	1.59	1.56	1.43	1.19			1.67	1.63	1.58	1.41	1.15	
V-K	2.28	2.24	2.21	2.05	1.82			2.34	2.29	2.24	2.04	1.78	
% MS	.339	.348	.345	.346	.334			.351	.359	.356	.356	.342	
% SGB	.101	.082	.083	.058	.040			.104	.085	.085	.060	.041	
% RGB	.354	.338	.318	.306	.291			.365	.349	.328	.315	.299	
% HB	.068	.071	.073	.076	.077			.037	.041	.043	.049	.054	
% AGB	.135	.158	.179	.212	.257			.139	.163	.185	.218	.263	
% PAGB	.004	.003	.002	.002	.001			.004	.003	.003	.002	.001	
M/Lbol	2.50	2.20	2.00	1.80	1.40			2.50	2.30	2.10	1.80	1.50	
M/Lb	3.39	2.90	2.59	2.09	1.32			3.71	3.26	2.82	2.09	1.38	
M/Lv	3.36	2.90	2.59	2.18	1.54			3.52	3.17	2.82	2.22	1.64	
M/Lk	1.55	1.39	1.27	1.25	1.08			1.53	1.45	1.35	1.28	1.20	
					Z	[Fe/H]	Y	s	η				
					0.0001	-2.27	0.23	2.35	0.50				
Mto	0.75	0.79	0.82	0.88	0.93			0.75	0.79	0.82	0.88	0.93	
Mrt	0.59	0.65	0.71	0.79	0.88			0.59	0.65	0.71	0.79	0.88	
Mpn	0.48	0.51	0.52	0.55	0.59			0.48	0.51	0.52	0.55	0.59	
B	1.79	1.76	1.71	1.69	1.64			1.86	1.83	1.77	1.74	1.68	
Bol	0.14	0.00	-0.16	-0.33	-0.52			0.14	0.00	-0.16	-0.34	-0.53	
Bol-V	-0.37	-0.35	-0.34	-0.27	-0.17			-0.43	-0.40	-0.37	-0.29	-0.17	
U-V	0.63	0.61	0.59	0.52	0.39			0.65	0.62	0.58	0.50	0.36	
B-V	0.62	0.62	0.61	0.57	0.47			0.67	0.64	0.61	0.54	0.44	
V-R	0.63	0.62	0.62	0.57	0.49			0.66	0.64	0.62	0.56	0.46	
V-I	1.11	1.10	1.08	0.99	0.84			1.16	1.13	1.09	0.97	0.80	
V-J	1.58	1.55	1.52	1.40	1.19			1.64	1.60	1.54	1.38	1.14	
V-K	2.22	2.18	2.15	2.01	1.77			2.29	2.24	2.18	1.99	1.72	
% MS	.356	.363	.361	.361	.350			.368	.376	.373	.372	.358	
% SGB	.106	.086	.087	.061	.042			.109	.089	.090	.063	.043	
% RGB	.371	.352	.333	.320	.306			.384	.365	.344	.330	.313	
% HB	.075	.077	.078	.081	.082			.041	.044	.047	.054	.060	
% AGB	.087	.117	.137	.174	.218			.090	.121	.142	.179	.224	
% PAGB	.006	.005	.004	.003	.002			.006	.005	.004	.003	.002	
M/Lbol	2.60	2.30	2.10	1.80	1.50			2.70	2.40	2.20	1.90	1.60	
M/Lb	3.40	2.95	2.64	2.05	1.42			3.90	3.28	2.85	2.14	1.47	
M/Lv	3.43	2.98	2.69	2.16	1.64			3.76	3.25	2.90	2.33	1.75	
M/Lk	1.67	1.51	1.40	1.28	1.21			1.72	1.56	1.47	1.40	1.36	

TABLE 6—*Continued*

C.

					Z	[Fe/H]	Y	s	η				
					0.0001	-2.27	0.23	1.35	0.30				
		I-HB							B-HB				
Age (Gyr)	18.0	15.0	12.5	10.0	8.0			18.0	15.0	12.5	10.0	8.0	
Mto	0.75	0.79	0.82	0.88	0.93			0.75	0.79	0.82	0.88	0.93	
Mrt	0.67	0.72	0.77	0.83	0.91			0.67	0.72	0.77	0.83	0.91	
Mpn	0.53	0.55	0.56	0.59	0.63			0.53	0.55	0.56	0.59	0.63	
B	1.91	1.88	1.82	1.78	1.71			1.98	1.95	1.88	1.84	1.76	
Bol	0.20	0.00	-0.21	-0.46	-0.72			0.20	0.00	-0.21	-0.46	-0.73	
Bol-V	-0.36	-0.34	-0.33	-0.26	-0.14			-0.42	-0.40	-0.37	-0.28	-0.14	
U-V	0.64	0.62	0.60	0.53	0.35			0.66	0.62	0.59	0.50	0.32	
B-V	0.63	0.62	0.61	0.57	0.46			0.67	0.65	0.62	0.55	0.43	
V-R	0.63	0.62	0.61	0.56	0.47			0.66	0.64	0.62	0.55	0.45	
V-I	1.11	1.09	1.07	0.98	0.81			1.15	1.12	1.08	0.96	0.77	
V-J	1.57	1.54	1.51	1.38	1.13			1.63	1.58	1.53	1.36	1.08	
V-K	2.22	2.18	2.15	1.99	1.76			2.29	2.24	2.18	1.98	1.71	
% MS	.264	.276	.270	.276	.270			.274	.286	.280	.286	.278	
% SGB	.111	.091	.092	.064	.044			.115	.094	.095	.066	.045	
% RGB	.394	.375	.354	.339	.319			.409	.389	.367	.350	.328	
% HB	.076	.079	.081	.084	.084			.042	.045	.049	.054	.059	
% AGB	.151	.175	.200	.234	.281			.156	.182	.207	.241	.288	
% PAGB	.004	.003	.003	.002	.001			.004	.004	.003	.002	.002	
M/Lbol	1.10	0.90	0.80	0.70	0.60			1.10	1.00	0.80	0.70	0.60	
M/Lb	1.44	1.14	1.00	0.79	0.55			1.58	1.38	1.04	0.79	0.53	
M/Lv	1.44	1.15	1.02	0.83	0.64			1.52	1.36	1.05	0.85	0.64	
M/Lk	0.70	0.58	0.53	0.50	0.48			0.69	0.65	0.53	0.52	0.50	
					Z	[Fe/H]	Y	s	η				
					0.0001	-2.27	0.23	1.35	0.50				
Mto	0.75	0.79	0.82	0.88	0.93			0.75	0.79	0.82	0.88	0.93	
Mrt	0.59	0.65	0.71	0.79	0.88			0.59	0.65	0.71	0.79	0.88	
Mpn	0.48	0.51	0.52	0.55	0.59			0.48	0.51	0.52	0.55	0.59	
B	2.01	1.97	1.92	1.88	1.81			2.10	2.05	1.99	1.94	1.85	
Bol	0.20	0.00	-0.21	-0.46	-0.72			0.20	0.00	-0.21	-0.46	-0.73	
Bol-V	-0.34	-0.32	-0.31	-0.24	-0.15			-0.40	-0.38	-0.35	-0.26	-0.14	
U-V	0.60	0.60	0.58	0.51	0.37			0.63	0.60	0.56	0.48	0.34	
B-V	0.60	0.60	0.60	0.56	0.46			0.65	0.63	0.60	0.53	0.43	
V-R	0.61	0.61	0.60	0.55	0.47			0.65	0.63	0.60	0.54	0.44	
V-I	1.07	1.06	1.04	0.96	0.80			1.12	1.09	1.05	0.93	0.76	
V-J	1.52	1.50	1.47	1.35	1.13			1.58	1.54	1.49	1.32	1.07	
V-K	2.15	2.12	2.09	1.94	1.70			2.22	2.18	2.11	1.92	1.64	
% MS	.278	.290	.285	.291	.285			.290	.301	.295	.301	.292	
% SGB	.118	.095	.096	.067	.046			.122	.099	.100	.069	.047	
% RGB	.416	.393	.373	.356	.336			.433	.409	.387	.368	.345	
% HB	.084	.086	.088	.091	.090			.046	.049	.053	.060	.066	
% AGB	.098	.131	.154	.193	.240			.102	.136	.160	.199	.246	
% PAGB	.007	.005	.004	.003	.002			.007	.005	.004	.003	.002	
M/Lbol	1.10	1.00	0.90	0.70	0.60			1.20	1.00	0.90	0.70	0.60	
M/Lb	1.37	1.22	1.09	0.77	0.55			1.66	1.33	1.13	0.76	0.53	
M/Lv	1.41	1.26	1.12	0.82	0.65			1.63	1.33	1.16	0.83	0.64	
M/Lk	0.73	0.67	0.62	0.52	0.51			0.79	0.67	0.63	0.54	0.53	

TABLE 6—*Continued*

D.

					Z	[Fe/H]	Y	s	η				
					0.0010	-1.27	0.23	3.35	0.30				
		I-HB							B-HB				
Age (Gyr)	18.0	15.0	12.5	10.0	8.0			18.0	15.0	12.5	10.0	8.0	
Mto	0.76	0.79	0.83	0.89	0.94			0.76	0.79	0.83	0.89	0.94	
Mrt	0.65	0.71	0.76	0.82	0.89			0.65	0.71	0.76	0.82	0.89	
Mpn	0.52	0.53	0.55	0.57	0.59			0.52	0.53	0.55	0.57	0.59	
B	1.44	1.41	1.39	1.37	1.31			1.46	1.44	1.41	1.39	1.32	
Bol	0.09	0.00	-0.09	-0.19	-0.33			0.09	0.00	-0.09	-0.21	-0.36	
Bol-V	-0.63	-0.58	-0.57	-0.56	-0.56			-0.67	-0.64	-0.59	-0.55	-0.55	
U-V	0.87	0.85	0.85	0.83	0.81			0.93	0.86	0.81	0.79	0.80	
B-V	0.76	0.74	0.76	0.75	0.74			0.81	0.77	0.73	0.71	0.73	
V-R	0.77	0.75	0.75	0.74	0.73			0.79	0.77	0.74	0.72	0.73	
V-I	1.38	1.34	1.33	1.32	1.31			1.41	1.38	1.33	1.29	1.30	
V-J	1.96	1.91	1.90	1.89	1.87			2.01	1.96	1.90	1.85	1.86	
V-K	2.75	2.69	2.67	2.65	2.64			2.80	2.75	2.67	2.62	2.63	
% MS	.458	.442	.432	.441	.449			.467	.451	.440	.445	.451	
% SGB	.095	.098	.097	.073	.069			.097	.100	.099	.073	.069	
% RGB	.293	.279	.268	.260	.244			.299	.285	.274	.262	.245	
% HB	.046	.056	.063	.065	.062			.027	.035	.044	.055	.060	
% AGB	.105	.122	.137	.161	.174			.107	.125	.140	.162	.174	
% PAGB	.003	.003	.002	.002	.002			.003	.003	.002	.002	.002	
M/Lbol	8.70	8.10	6.90	6.40	6.10			8.90	8.30	7.00	6.50	6.10	
M/Lb	16.43	14.34	12.33	11.22	10.60			18.26	15.96	12.39	10.89	10.41	
M/Lv	14.57	12.96	10.94	10.05	9.58			15.47	14.03	11.30	10.11	9.49	
M/Lk	4.36	4.10	3.52	3.30	3.17			4.42	4.20	3.64	3.41	3.17	
					Z	[Fe/H]	Y	s	η				
					0.0010	-1.27	0.23	3.35	0.50				
Mto	0.76	0.79	0.83	0.89	0.94			0.76	0.79	0.83	0.89	0.94	
Mrt	0.55	0.62	0.68	0.76	0.83			0.55	0.62	0.68	0.76	0.83	
Mpn	0.47	0.49	0.50	0.53	0.55			0.47	0.49	0.50	0.53	0.55	
B	1.51	1.47	1.45	1.43	1.37			1.55	1.51	1.47	1.44	1.37	
Bol	0.10	0.00	-0.09	-0.20	-0.34			0.10	0.00	-0.10	-0.21	-0.37	
Bol-V	-0.62	-0.56	-0.55	-0.54	-0.54			-0.65	-0.62	-0.56	-0.52	-0.54	
U-V	0.83	0.83	0.84	0.82	0.80			0.90	0.83	0.78	0.78	0.79	
B-V	0.75	0.73	0.75	0.74	0.73			0.80	0.76	0.71	0.71	0.72	
V-R	0.76	0.73	0.74	0.73	0.72			0.78	0.76	0.72	0.71	0.72	
V-I	1.35	1.31	1.32	1.30	1.29			1.39	1.35	1.30	1.27	1.29	
V-J	1.93	1.87	1.87	1.85	1.85			1.97	1.92	1.86	1.82	1.84	
V-K	2.70	2.63	2.62	2.60	2.60			2.75	2.69	2.61	2.57	2.59	
% MS	.484	.462	.449	.459	.466			.494	.473	.458	.463	.467	
% SGB	.100	.103	.101	.076	.072			.103	.105	.103	.076	.072	
% RGB	.309	.292	.279	.271	.253			.316	.300	.285	.273	.254	
% HB	.051	.062	.068	.068	.065			.029	.038	.049	.061	.063	
% AGB	.050	.076	.098	.123	.142			.051	.078	.100	.124	.142	
% PAGB	.006	.005	.004	.003	.002			.006	.005	.004	.003	.002	
M/Lbol	9.20	8.50	7.10	6.70	6.30			9.40	8.70	7.30	6.70	6.30	
M/Lb	17.05	14.64	12.34	11.43	10.65			18.76	16.27	12.34	10.92	10.55	
M/Lv	15.27	13.35	11.05	10.33	9.71			16.04	14.44	11.46	10.14	9.71	
M/Lk	4.78	4.46	3.73	3.55	3.34			4.80	4.57	3.90	3.58	3.37	

TABLE 6—*Continued*

E.

					Z	[Fé/H]	Y	s	η				
					0.0010	-1.27	0.23	2.35	0.30				
		I-HB							B-HB				
Age (Gyr)	18.0	15.0	12.5	10.0	8.0			18.0	15.0	12.5	10.0	8.0	
Mto	0.76	0.79	0.83	0.89	0.94			0.76	0.79	0.83	0.89	0.94	
Mrt	0.65	0.71	0.76	0.82	0.89			0.65	0.71	0.76	0.82	0.89	
Mpn	0.52	0.53	0.55	0.57	0.59			0.52	0.53	0.55	0.57	0.59	
B	1.81	1.77	1.71	1.69	1.65			1.86	1.81	1.76	1.71	1.66	
Bol	0.15	0.00	-0.16	-0.33	-0.51			0.15	0.00	-0.16	-0.35	-0.54	
Bol-V	-0.53	-0.48	-0.48	-0.48	-0.47			-0.57	-0.55	-0.51	-0.47	-0.46	
U-V	0.81	0.80	0.81	0.80	0.78			0.87	0.81	0.76	0.75	0.76	
B-V	0.72	0.71	0.74	0.73	0.71			0.78	0.74	0.70	0.68	0.70	
V-R	0.72	0.70	0.71	0.71	0.70			0.75	0.73	0.70	0.68	0.69	
V-I	1.28	1.25	1.26	1.25	1.23			1.32	1.29	1.24	1.21	1.22	
V-J	1.82	1.78	1.78	1.78	1.75			1.87	1.83	1.77	1.74	1.74	
V-K	2.56	2.51	2.51	2.51	2.48			2.62	2.57	2.51	2.47	2.46	
% MS	.317	.303	.298	.313	.309			.325	.310	.306	.318	.310	
% SGB	.119	.122	.119	.088	.085			.122	.125	.122	.089	.086	
% RGB	.370	.350	.332	.319	.307			.379	.360	.340	.323	.308	
% HB	.058	.070	.078	.080	.078			.034	.044	.055	.068	.076	
% AGB	.132	.153	.170	.198	.218			.135	.157	.174	.200	.219	
% PAGB	.004	.004	.003	.002	.002			.004	.004	.003	.002	.002	
M/Lbol	2.90	2.60	2.20	1.90	1.70			3.00	2.70	2.20	1.90	1.70	
M/Lb	4.81	4.08	3.55	3.04	2.65			5.46	4.65	3.52	2.88	2.60	
M/Lv	4.43	3.79	3.21	2.77	2.46			4.75	4.20	3.30	2.75	2.43	
M/Lk	1.58	1.42	1.20	1.03	0.94			1.60	1.48	1.23	1.06	0.95	
					Z	[Fe/H]	Y	s	η				
					0.0010	-1.27	0.23	2.35	0.50				
Mto	0.76	0.79	0.83	0.89	0.94			0.76	0.79	0.83	0.89	0.94	
Mrt	0.55	0.62	0.68	0.76	0.83			0.55	0.62	0.68	0.76	0.83	
Mpn	0.47	0.49	0.50	0.53	0.55			0.47	0.49	0.50	0.53	0.55	
B	1.94	1.87	1.81	1.78	1.73			1.99	1.93	1.85	1.79	1.74	
Bol	0.17	0.00	-0.16	-0.34	-0.52			0.16	0.00	-0.17	-0.36	-0.55	
Bol-V	-0.51	-0.45	-0.46	-0.45	-0.44			-0.54	-0.52	-0.47	-0.44	-0.44	
U-V	0.77	0.77	0.79	0.78	0.76			0.84	0.78	0.73	0.74	0.75	
B-V	0.71	0.69	0.72	0.72	0.70			0.76	0.72	0.68	0.68	0.69	
V-R	0.70	0.68	0.70	0.70	0.68			0.73	0.71	0.68	0.67	0.68	
V-I	1.25	1.21	1.23	1.22	1.21			1.29	1.25	1.21	1.19	1.20	
V-J	1.77	1.72	1.75	1.74	1.71			1.82	1.78	1.72	1.70	1.70	
V-K	2.49	2.42	2.45	2.44	2.42			2.54	2.49	2.43	2.40	2.40	
% MS	.339	.320	.314	.331	.324			.350	.330	.321	.334	.325	
% SGB	.127	.129	.125	.093	.089			.131	.133	.128	.094	.090	
% RGB	.396	.370	.349	.336	.321			.408	.382	.358	.339	.322	
% HB	.065	.078	.085	.085	.082			.038	.049	.062	.076	.081	
% AGB	.064	.097	.123	.152	.180			.066	.100	.126	.154	.180	
% PAGB	.008	.006	.005	.004	.003			.008	.006	.005	.004	.003	
M/Lbol	3.10	2.80	2.30	2.00	1.80			3.20	2.80	2.40	2.00	1.80	
M/Lb	5.00	4.20	3.58	3.08	2.70			5.56	4.60	3.63	2.94	2.67	
M/Lv	4.65	3.97	3.29	2.84	2.53			4.93	4.24	3.47	2.81	2.53	
M/Lk	1.77	1.61	1.30	1.13	1.03			1.79	1.61	1.39	1.16	1.05	

TABLE 6—*Continued*

F.

					Z 0.0010	[Fe/H] −1.27	Y 0.23	s 1.35	η 0.30			
		I-HB							B-HB			
Age (Gyr)	18.0	15.0	12.5	10.0	8.0			18.0	15.0	12.5	10.0	8.0
Mto	0.76	0.79	0.83	0.89	0.94			0.76	0.79	0.83	0.89	0.94
Mrt	0.65	0.71	0.76	0.82	0.89			0.65	0.71	0.76	0.82	0.89
Mpn	0.52	0.53	0.55	0.57	0.59			0.52	0.53	0.55	0.57	0.59
B	2.00	1.94	1.88	1.84	1.81			2.05	2.00	1.93	1.87	1.82
Bol	0.21	0.00	−0.21	−0.46	−0.70			0.21	0.00	−0.22	−0.48	−0.73
Bol-V	−0.51	−0.46	−0.47	−0.47	−0.46			−0.55	−0.53	−0.49	−0.45	−0.45
U-V	0.79	0.79	0.80	0.80	0.78			0.86	0.80	0.75	0.75	0.76
B-V	0.71	0.70	0.73	0.73	0.71			0.77	0.73	0.69	0.68	0.70
V-R	0.71	0.69	0.70	0.71	0.69			0.74	0.72	0.69	0.68	0.69
V-I	1.25	1.22	1.24	1.24	1.22			1.30	1.26	1.22	1.20	1.21
V-J	1.78	1.74	1.76	1.76	1.73			1.83	1.80	1.75	1.72	1.72
V-K	2.51	2.46	2.48	2.49	2.46			2.57	2.53	2.48	2.44	2.44
% MS	.247	.234	.233	.251	.244			.254	.242	.239	.255	.244
% SGB	.130	.132	.129	.095	.092			.133	.136	.132	.096	.093
% RGB	.408	.384	.364	.348	.337			.420	.396	.374	.353	.338
% HB	.065	.077	.085	.087	.086			.038	.048	.061	.074	.083
% AGB	.146	.168	.186	.216	.239			.150	.173	.192	.219	.240
% PAGB	.005	.004	.003	.003	.002			.005	.004	.003	.003	.002
M/Lbol	1.20	1.00	0.90	0.80	0.60			1.20	1.10	0.90	0.80	0.60
M/Lb	1.94	1.53	1.43	1.27	0.93			2.12	1.84	1.40	1.19	0.91
M/Lv	1.80	1.43	1.30	1.16	0.86			1.87	1.68	1.33	1.14	0.85
M/Lk	0.67	0.56	0.50	0.44	0.34			0.66	0.62	0.51	0.45	0.34
					Z 0.0010	[Fe/H] −1.27	Y 0.23	s 1.35	η 0.50			
Mto	0.76	0.79	0.83	0.89	0.94			0.76	0.79	0.83	0.89	0.94
Mrt	0.55	0.62	0.68	0.76	0.83			0.55	0.62	0.68	0.76	0.83
Mpn	0.47	0.49	0.50	0.53	0.55			0.47	0.49	0.50	0.53	0.55
B	2.16	2.07	1.99	1.95	1.91			2.23	2.14	2.04	1.97	1.91
Bol	0.23	0.00	−0.22	−0.47	−0.71			0.22	0.00	−0.23	−0.49	−0.74
Bol-V	−0.48	−0.42	−0.44	−0.44	−0.43			−0.51	−0.49	−0.45	−0.42	−0.42
U-V	0.75	0.76	0.78	0.78	0.76			0.82	0.76	0.72	0.73	0.75
B-V	0.69	0.68	0.72	0.71	0.70			0.75	0.71	0.67	0.68	0.69
V-R	0.69	0.67	0.69	0.69	0.68			0.72	0.70	0.67	0.66	0.67
V-I	1.21	1.18	1.21	1.21	1.19			1.26	1.22	1.18	1.17	1.18
V-J	1.72	1.68	1.71	1.71	1.69			1.77	1.74	1.69	1.67	1.68
V-K	2.42	2.37	2.41	2.41	2.39			2.48	2.44	2.39	2.36	2.37
% MS	.267	.249	.246	.267	.257			.275	.259	.253	.269	.257
% SGB	.140	.141	.136	.101	.097			.145	.146	.139	.102	.097
% RGB	.441	.409	.384	.368	.354			.455	.424	.395	.372	.355
% HB	.072	.086	.093	.093	.091			.042	.054	.068	.083	.089
% AGB	.072	.107	.136	.167	.198			.074	.111	.139	.169	.198
% PAGB	.008	.007	.005	.004	.003			.009	.007	.006	.004	.003
M/Lbol	1.30	1.10	0.90	0.80	0.70			1.40	1.20	1.00	0.80	0.70
M/Lb	2.00	1.59	1.37	1.21	1.04			2.34	1.90	1.47	1.16	1.02
M/Lv	1.90	1.52	1.27	1.12	0.98			2.10	1.77	1.42	1.10	0.97
M/Lk	0.77	0.64	0.52	0.46	0.41			0.81	0.70	0.59	0.47	0.41

TABLE 6—*Continued*

G.

	Z	[Fe/H]	Y	s	η			
	0.0100	−0.25	0.25	3.35	0.30			
	I-HB				B-HB			
Age (Gyr)	15.0	12.5	10.0	8.0	15.0	12.5	10.0	8.0
Mto	0.87	0.91	0.97	1.02	0.87	0.91	0'.97	1.02
Mrt	0.75	0.82	0.89	0.97	0.75	0.82	0.89	0.97
Mpn	0.53	0.55	0.57	0.59	0.53	0.55	0.57	0.59
B	1.43	1.38	1.38	1.35	1.46	1.39	1.38	1.35
Bol	0.00	−0.11	−0.21	−0.32	0.00	−0.13	−0.23	−0.34
Bol-V	−0.88	−0.88	−0.84	−0.80	−0.97	−0.88	−0.84	−0.80
U-V	1.11	1.21	1.15	1.09	1.14	1.19	1.14	1.09
B-V	0.83	0.90	0.88	0.85	0.88	0.90	0.87	0.85
V-R	0.85	0.88	0.86	0.83	0.89	0.87	0.85	0.83
V-I	1.55	1.59	1.55	1.51	1.62	1.58	1.54	1.51
V-J	2.25	2.27	2.22	2.17	2.33	2.26	2.22	2.16
V-K	3.18	3.20	3.14	3.07	3.28	3.19	3.13	3.07
% MS	.459	.441	.429	.410	.469	.442	.429	.410
% SGB	.078	.088	.084	.093	.080	.089	.084	.093
% RGB	.279	.263	.256	.244	.285	.263	.256	.244
% HB	.057	.066	.066	.064	.039	.065	.065	.064
% AGB	.123	.139	.165	.187	.125	.139	.165	.187
% PAGB	.003	.002	.002	.002	.003	.002	.002	.002
M/Lbol	11.00	10.60	8.80	8.10	11.20	10.60	8.80	8.10
M/Lb	27.89	28.66	22.52	19.43	32.30	28.66	22.31	19.43
M/Lv	23.19	22.35	17.88	15.87	25.66	22.35	17.88	15.87
M/Lk	4.67	4.42	3.74	3.54	4.71	4.46	3.77	3.54
	Z	[Fe/H]	Y	s	η			
	0.0100	−0.25	0.25	3.35	0.50			
Mto	0.87	0.91	0.97	1.02	0.87	0.91	0.97	1.02
Mrt	0.63	0.71	0.80	0.89	0.63	0.71	0.80	0.89
Mpn	0.48	0.50	0.51	0.53	0.48	0.50	0.51	0.53
B	1.52	1.45	1.45	1.43	1.55	1.45	1.45	1.43
Bol	0.00	−0.12	−0.22	−0.33	0.00	−0.14	−0.24	−0.35
Bol-V	−0.83	−0.84	−0.80	−0.76	−0.92	−0.84	−0.79	−0.76
U-V	1.09	1.20	1.13	1.08	1.11	1.19	1.13	1.07
B-V	0.82	0.90	0.87	0.84	0.86	0.89	0.87	0.84
V-R	0.83	0.87	0.84	0.82	0.87	0.86	0.84	0.82
V-I	1.52	1.56	1.52	1.48	1.58	1.56	1.52	1.48
V-J	2.19	2.23	2.17	2.12	2.28	2.23	2.17	2.12
V-K	3.10	3.13	3.06	3.00	3.20	3.13	3.06	3.00
% MS	.487	.464	.452	.432	.498	.464	.452	.433
% SGB	.083	.093	.088	.098	.084	.093	.088	.098
% RGB	.296	.276	.270	.256	.302	.276	.270	.256
% HB	.063	.070	.070	.068	.043	.070	.069	.067
% AGB	.066	.093	.116	.143	.068	.093	.116	.143
% PAGB	.005	.004	.004	.003	.005	.004	.004	.003
M/Lbol	11.70	11.10	9.30	8.50	11.90	11.10	9.30	8.50
M/Lb	28.07	28.93	22.72	19.47	32.18	28.66	22.52	19.47
M/Lv	23.56	22.56	18.22	16.05	26.03	22.56	18.05	16.05
M/Lk	5.11	4.76	4.10	3.81	5.15	4.76	4.06	3.81

TABLE 6—*Continued*

H.

				Z 0.0100	[Fe/H] -0.25	Y 0.25	s 2.35	η 0.30			
Age (Gyr)	I-HB 15.0	12.5	10.0	8.0				B-HB 15.0	12.5	10.0	8.0
Mto	0.87	0.91	0.97	1.02				0.87	0.91	0.97	1.02
Mrt	0.75	0.82	0.89	0.97				0.75	0.82	0.89	0.97
Mpn	0.53	0.55	0.57	0.59				0.53	0.55	0.57	0.59
B	1.82	1.76	1.72	1.67				1.87	1.76	1.72	1.67
Bol	0.00	-0.17	-0.35	-0.54				0.00	-0.20	-0.38	-0.57
Bol-V	-0.76	-0.77	-0.76	-0.73				-0.86	-0.77	-0.75	-0.73
U-V	1.05	1.16	1.11	1.06				1.07	1.15	1.10	1.06
B-V	0.79	0.88	0.86	0.84				0.84	0.87	0.85	0.83
V-R	0.80	0.84	0.83	0.81				0.84	0.83	0.82	0.81
V-I	1.46	1.50	1.48	1.45				1.53	1.50	1.48	1.45
V-J	2.10	2.15	2.12	2.08				2.19	2.14	2.11	2.08
V-K	3.00	3.03	3.00	2.96				3.11	3.02	3.00	2.96
% MS	.311	.294	.291	.279				.320	.294	.291	.279
% SGB	.098	.110	.102	.112				.101	.110	.102	.112
% RGB	.357	.333	.318	.299				.366	.334	.318	.299
% HB	.073	.084	.081	.079				.050	.083	.081	.078
% AGB	.157	.176	.205	.229				.161	.177	.205	.229
% PAGB	.004	.003	.002	.002				.004	.003	.002	.002
M/Lbol	3.40	3.00	2.50	2.20				3.50	3.00	2.50	2.20
M/Lb	7.44	7.20	5.83	4.90				8.79	7.13	5.73	4.86
M/Lv	6.42	5.72	4.72	4.04				7.25	5.72	4.68	4.04
M/Lk	1.53	1.32	1.12	1.00				1.56	1.33	1.11	1.00
				Z 0.0100	[Fe/H] -0.25	Y 0.25	s 2.35	η 0.50			
Mto	0.87	0.91	0.97	1.02				0.87	0.91	0.97	1.02
Mrt	0.63	0.71	0.80	0.89				0.63	0.71	0.80	0.89
Mpn	0.48	0.50	0.51	0.53				0.48	0.50	0.51	0.53
B	1.96	1.87	1.84	1.77				2.02	1.87	1.84	1.78
Bol	0.00	-0.18	-0.36	-0.55				0.00	-0.21	-0.39	-0.58
Bol-V	-0.69	-0.72	-0.70	-0.67				-0.80	-0.72	-0.69	-0.67
U-V	1.03	1.15	1.10	1.05				1.04	1.15	1.09	1.05
B-V	0.78	0.87	0.85	0.83				0.82	0.87	0.84	0.82
V-R	0.78	0.82	0.81	0.79				0.82	0.82	0.81	0.79
V-I	1.41	1.47	1.44	1.42				1.48	1.47	1.44	1.42
V-J	2.03	2.09	2.06	2.03				2.12	2.09	2.05	2.02
V-K	2.89	2.95	2.91	2.87				3.00	2.94	2.90	2.87
% MS	.336	.312	.312	.297				.345	.312	.312	.297
% SGB	.106	.117	.109	.119				.109	.117	.109	.119
% RGB	.384	.355	.341	.318				.395	.355	.341	.319
% HB	.082	.090	.088	.084				.056	.090	.087	.084
% AGB	.086	.119	.146	.177				.088	.119	.146	.177
% PAGB	.007	.005	.005	.004				.007	.005	.005	.004
M/Lbol	3.70	3.20	2.70	2.30				3.80	3.20	2.70	2.30
M/Lb	7.52	7.26	5.91	4.81				8.87	7.26	5.80	4.76
M/Lv	6.55	5.82	4.82	4.00				7.44	5.82	4.78	4.00
M/Lk	1.72	1.45	1.25	1.07				1.77	1.46	1.25	1.07

TABLE 6—*Continued*

I.

				Z	[Fe/H]	Y	s	η	
				0.0100	−0.25	0.25	1.35	0.30	
	I-HB						B-HB		
Age (Gyr)	15.0	12.5	10.0	8.0		15.0	12.5	10.0	8.0
Mto	0.87	0.91	0.97	1.02		0.87	0.91	0.97	1.02
Mrt	0.75	0.82	0.89	0.97		0.75	0.82	0.89	0.97
Mpn	0.53	0.55	0.57	0.59		0.53	0.55	0.57	0.59
B	2.02	1.93	1.87	1.81		2.07	1.94	1.87	1.81
Bol	0.00	−0.23	−0.48	−0.74		0.00	−0.25	−0.51	−0.77
Bol-V	−0.74	−0.76	−0.75	−0.73		−0.85	−0.76	−0.75	−0.73
U-V	1.03	1.16	1.11	1.07		1.05	1.14	1.10	1.06
B-V	0.78	0.88	0.86	0.84		0.83	0.87	0.85	0.84
V-R	0.79	0.83	0.82	0.81		0.83	0.83	0.82	0.81
V-I	1.43	1.49	1.48	1.46		1.51	1.48	1.47	1.45
V-J	2.07	2.13	2.11	2.08		2.17	2.12	2.11	2.08
V-K	2.97	3.01	3.00	2.97		3.08	3.00	2.99	2.96
% MS	.241	.225	.226	.217		.248	.225	.226	.217
% SGB	.107	.119	.110	.120		.110	.119	.110	.120
% RGB	.394	.367	.348	.326		.405	.367	.348	.326
% HB	.081	.092	.089	.086		.055	.091	.088	.085
% AGB	.173	.194	.224	.250		.178	.194	.225	.250
% PAGB	.004	.003	.003	.002		.005	.003	.003	.002
M/Lbol	1.30	1.20	0.90	0.80		1.40	1.20	0.90	0.80
M/Lb	2.77	2.85	2.08	1.78		3.45	2.83	2.06	1.78
M/Lv	2.41	2.27	1.68	1.47		2.87	2.27	1.68	1.47
M/Lk	0.59	0.53	0.40	0.36		0.63	0.54	0.40	0.36
				Z	[Fe/H]	Y	s	η	
				0.0100	−0.25	0.25	1.35	0.50	
Mto	0.87	0.91	0.97	1.02		0.87	0.91	0.97	1.02
Mrt	0.63	0.71	0.80	0.89		0.63	0.71	0.80	0.89
Mpn	0.48	0.50	0.51	0.53		0.48	0.50	0.51	0.53
B	2.19	2.07	2.02	1.94		2.26	2.07	2.02	1.94
Bol	0.00	−0.24	−0.49	−0.75		0.00	−0.27	−0.52	−0.79
Bol-V	−0.66	−0.70	−0.69	−0.67		−0.78	−0.70	−0.68	−0.67
U-V	1.01	1.15	1.09	1.05		1.02	1.14	1.09	1.05
B-V	0.76	0.87	0.85	0.83		0.81	0.86	0.84	0.83
V-R	0.76	0.82	0.81	0.79		0.81	0.82	0.80	0.79
V-I	1.38	1.46	1.44	1.42		1.46	1.45	1.43	1.41
V-J	1.99	2.07	2.04	2.02		2.09	2.06	2.04	2.02
V-K	2.84	2.92	2.89	2.87		2.96	2.91	2.89	2.86
% MS	.262	.241	.244	.233		.270	.241	.244	.233
% SGB	.116	.127	.118	.128		.120	.128	.118	.128
% RGB	.428	.393	.375	.349		.441	.393	.375	.349
% HB	.091	.100	.096	.092		.062	.100	.096	.092
% AGB	.096	.132	.162	.194		.099	.132	.162	.194
% PAGB	.008	.006	.005	.004		.008	.006	.005	.004
M/Lbol	1.50	1.20	1.00	0.80		1.50	1.20	1.00	0.80
M/Lb	2.91	2.67	2.17	1.67		3.40	2.65	2.13	1.67
M/Lv	2.58	2.14	1.77	1.39		2.88	2.14	1.75	1.39
M/Lk	0.71	0.55	0.47	0.37		0.71	0.55	0.46	0.38

TABLE 6—*Continued*

J.

				Z	[Fe/H]	Y	s	η	
				0.0170	-0.02	0.25	3.35	0.30	
	I-HB						B-HB		
Age (Gyr)	15.0	12.5	10.0	8.0		15.0	12.5	10.0	8.0
Mto	0.94	0.98	1.02	1.08		0.94	0.98	1.02	1.08
Mrt	0.81	0.87	0.95	1.03		0.81	0.87	0.95	1.03
Mpn	0.54	0.56	0.58	0.59		0.54	0.56	0.58	0.59
B	1.31	1.32	1.31	1.30		1.33	1.32	1.31	1.30
Bol	0.00	-0.07	-0.18	-0.28		0.00	-0.09	-0.19	-0.30
Bol-V	-1.00	-0.99	-0.94	-0.90		-1.10	-0.98	-0.94	-0.89
U-V	1.22	1.33	1.26	1.19		1.25	1.32	1.26	1.18
B-V	0.87	0.94	0.91	0.88		0.92	0.94	0.91	0.88
V-R	0.89	0.92	0.89	0.87		0.94	0.91	0.89	0.87
V-I	1.64	1.66	1.61	1.57		1.71	1.65	1.61	1.57
V-J	2.38	2.38	2.32	2.27		2.46	2.37	2.32	2.26
V-K	3.37	3.35	3.28	3.22		3.46	3.34	3.27	3.21
% MS	.506	.478	.441	.427		.515	.479	.441	.427
% SGB	.058	.062	.085	.087		.059	.062	.085	.087
% RGB	.254	.251	.241	.235		.259	.251	.241	.235
% HB	.052	.062	.061	.060		.036	.061	.060	.060
% AGB	.127	.145	.170	.189		.129	.145	.170	.189
% PAGB	.003	.002	.002	.002		.003	.002	.002	.002
M/Lbol	12.50	11.10	10.20	9.40		12.70	11.10	10.30	9.40
M/Lb	36.72	34.46	29.42	25.42		42.84	34.14	29.71	25.18
M/Lv	29.44	25.90	22.73	20.19		32.79	25.66	22.95	20.00
M/Lk	4.98	4.46	4.17	3.92		5.10	4.46	4.25	3.92
				Z	[Fe/H]	Y	s	η	
				0.0170	-0.02	0.25	3.35	0.50	
Mto	0.94	0.98	1.02	1.08		0.94	0.98	1.02	1.08
Mrt	0.68	0.76	0.86	0.95		0.68	0.76	0.86	0.95
Mpn	0.49	0.50	0.52	0.54		0.49	0.50	0.52	0.54
B	1.39	1.39	1.38	1.37		1.42	1.39	1.38	1.37
Bol	0.00	-0.07	-0.18	-0.29		0.00	-0.09	-0.20	-0.30
Bol-V	-0.95	-0.94	-0.89	-0.85		-1.05	-0.93	-0.89	-0.84
U-V	1.20	1.32	1.25	1.18		1.23	1.31	1.25	1.17
B-V	0.86	0.94	0.91	0.88		0.91	0.93	0.90	0.87
V-R	0.88	0.90	0.88	0.85		0.92	0.90	0.88	0.85
V-I	1.61	1.63	1.59	1.54		1.68	1.63	1.58	1.54
V-J	2.33	2.33	2.28	2.22		2.42	2.33	2.27	2.22
V-K	3.29	3.28	3.21	3.14		3.39	3.27	3.21	3.14
% MS	.535	.504	.465	.451		.546	.504	.466	.451
% SGB	.062	.066	.090	.092		.063	.066	.090	.092
% RGB	.269	.265	.254	.247		.274	.265	.254	.247
% HB	.056	.066	.064	.064		.038	.065	.064	.063
% AGB	.074	.096	.124	.144		.075	.096	.124	.144
% PAGB	.004	.004	.003	.003		.005	.004	.003	.003
M/Lbol	13.20	11.80	10.80	9.90		13.40	11.80	10.80	9.90
M/Lb	36.69	34.99	29.75	25.56		42.77	34.35	29.47	25.10
M/Lv	29.69	26.30	22.98	20.31		33.04	26.05	22.98	20.12
M/Lk	5.40	4.83	4.50	4.24		5.48	4.83	4.50	4.20

TABLE 6—*Continued*

K.

				Z	[Fe/H]	Y	s	η	
				0.0170	-0.02	0.25	2.35	0.30	
	I-HB						B-HB		
Age (Gyr)	15.0	12.5	10.0	8.0		15.0	12.5	10.0	8.0
Mto	0.94	0.98	1.02	1.08		0.94	0.98	1.02	1.08
Mrt	0.81	0.87	0.95	1.03		0.81	0.87	0.95	1.03
Mpn	0.54	0.56	0.58	0.59		0.54	0.56	0.58	0.59
B	1.75	1.71	1.66	1.63		1.80	1.72	1.67	1.63
Bol	0.00	-0.15	-0.34	-0.53		0.00	-0.18	-0.37	-0.55
Bol-V	-0.86	-0.87	-0.84	-0.81		-0.97	-0.87	-0.84	-0.81
U-V	1.14	1.27	1.22	1.15		1.16	1.27	1.21	1.15
B-V	0.82	0.91	0.89	0.86		0.87	0.91	0.89	0.86
V-R	0.83	0.87	0.85	0.84		0.88	0.87	0.85	0.83
V-I	1.52	1.57	1.54	1.51		1.60	1.56	1.53	1.50
V-J	2.20	2.24	2.20	2.17		2.30	2.24	2.20	2.16
V-K	3.15	3.18	3.13	3.09		3.27	3.18	3.13	3.09
% MS	.341	.324	.291	.284		.349	.324	.291	.284
% SGB	.077	.079	.106	.107		.079	.079	.106	.107
% RGB	.340	.326	.307	.294		.348	.326	.307	.294
% HB	.069	.080	.077	.076		.048	.079	.077	.075
% AGB	.170	.189	.216	.238		.173	.189	.216	.238
% PAGB	.003	.003	.002	.002		.003	.003	.002	.002
M/Lbol	3.80	3.30	2.80	2.40		3.90	3.30	2.80	2.40
M/Lb	9.37	8.92	7.23	5.86		11.14	8.92	7.23	5.86
M/Lv	7.87	6.89	5.69	4.74		8.93	6.89	5.69	4.74
M/Lk	1.63	1.39	1.20	1.04		1.66	1.39	1.20	1.04
				Z	[Fe/H]	Y	s	η	
				0.0170	-0.02	0.25	2.35	0.50	
Mto	0.94	0.98	1.02	1.08		0.94	0.98	1.02	1.08
Mrt	0.68	0.76	0.86	0.95		0.68	0.76	0.86	0.95
Mpn	0.49	0.50	0.52	0.54		0.49	0.50	0.52	0.54
B	1.89	1.84	1.78	1.75		1.94	1.84	1.78	1.75
Bol	0.00	-0.16	-0.35	-0.53		0.00	-0.18	-0.38	-0.56
Bol-V	-0.79	-0.81	-0.78	-0.75		-0.90	-0.80	-0.78	-0.75
U-V	1.12	1.26	1.21	1.14		1.14	1.25	1.20	1.14
B-V	0.81	0.90	0.88	0.86		0.86	0.90	0.88	0.85
V-R	0.81	0.85	0.84	0.82		0.86	0.85	0.84	0.82
V-I	1.48	1.53	1.50	1.47		1.55	1.52	1.50	1.47
V-J	2.13	2.18	2.15	2.11		2.23	2.18	2.14	2.10
V-K	3.04	3.08	3.04	3.00		3.16	3.08	3.03	2.99
% MS	.367	.348	.311	.304		.377	.348	.311	.304
% SGB	.083	.085	.114	.114		.085	.085	.114	.114
% RGB	.366	.350	.328	.315		.376	.350	.328	.315
% HB	.076	.087	.083	.081		.053	.086	.083	.081
% AGB	.101	.126	.160	.183		.103	.126	.160	.184
% PAGB	.006	.005	.004	.003		.006	.005	.004	.003
M/Lbol	4.10	3.50	3.00	2.60		4.20	3.50	3.00	2.60
M/Lb	9.39	8.87	7.26	6.01		11.15	8.79	7.26	5.96
M/Lv	7.96	6.92	5.77	4.86		9.02	6.86	5.77	4.86
M/Lk	1.82	1.53	1.32	1.16		1.85	1.51	1.33	1.17

TABLE 6—*Continued*

L.

	Z	[Fe/H]	Y	s	η			
	0.0170	-0.02	0.25	1.35	0.30			
	I-HB				B-HB			
Age (Gyr)	15.0	12.5	10.0	8.0	15.0	12.5	10.0	8.0
Mto	0.94	0.98	1.02	1.08	0.94	0.98	1.02	1.08
Mrt	0.81	0.87	0.95	1.03	0.81	0.87	0.95	1.03
Mpn	0.54	0.56	0.58	0.59	0.54	0.56	0.58	0.59
B	1.96	1.89	1.83	1.79	2.01	1.90	1.83	1.79
Bol	0.00	-0.22	-0.48	-0.73	0.00	-0.24	-0.50	-0.75
Bol-V	-0.83	-0.86	-0.84	-0.82	-0.95	-0.86	-0.84	-0.82
U-V	1.11	1.26	1.21	1.15	1.13	1.26	1.21	1.15
B-V	0.80	0.91	0.89	0.87	0.86	0.91	0.89	0.86
V-R	0.82	0.87	0.85	0.84	0.87	0.86	0.85	0.84
V-I	1.49	1.55	1.53	1.51	1.58	1.55	1.53	1.51
V-J	2.17	2.23	2.20	2.17	2.27	2.22	2.19	2.16
V-K	3.12	3.17	3.13	3.10	3.24	3.16	3.13	3.10
% MS	.266	.253	.224	.219	.272	.253	.224	.219
% SGB	.085	.086	.114	.114	.087	.087	.114	.114
% RGB	.379	.360	.337	.322	.389	.361	.337	.322
% HB	.077	.088	.085	.083	.054	.088	.085	.082
% AGB	.189	.208	.237	.260	.194	.208	.237	.260
% PAGB	.004	.003	.002	.002	.004	.003	.002	.002
M/Lbol	1.50	1.30	1.00	0.90	1.50	1.30	1.00	0.90
M/Lb	3.53	3.48	2.58	2.24	4.17	3.48	2.58	2.22
M/Lv	3.02	2.69	2.03	1.80	3.37	2.69	2.03	1.80
M/Lk	0.64	0.55	0.43	0.39	0.64	0.55	0.43	0.39
	Z	[Fe/H]	Y	s	η			
	0.0170	-0.02	0.25	1.35	0.50			
Mto	0.94	0.98	1.02	1.08	0.94	0.98	1.02	1.08
Mrt	0.68	0.76	0.86	0.95	0.68	0.76	0.86	0.95
Mpn	0.49	0.50	0.52	0.54	0.49	0.50	0.52	0.54
B	2.13	2.05	1.97	1.92	2.19	2.06	1.97	1.92
Bol	0.00	-0.22	-0.48	-0.74	0.00	-0.25	-0.52	-0.77
Bol-V	-0.75	-0.79	-0.77	-0.75	-0.88	-0.79	-0.77	-0.75
U-V	1.09	1.25	1.20	1.14	1.11	1.24	1.19	1.13
B-V	0.79	0.90	0.88	0.86	0.84	0.90	0.88	0.85
V-R	0.79	0.85	0.84	0.82	0.84	0.84	0.83	0.82
V-I	1.44	1.51	1.49	1.47	1.52	1.51	1.49	1.47
V-J	2.09	2.16	2.13	2.10	2.19	2.15	2.13	2.10
V-K	2.99	3.05	3.03	3.00	3.11	3.05	3.02	2.99
% MS	.289	.274	.241	.236	.297	.274	.242	.236
% SGB	.092	.094	.123	.123	.095	.094	.123	.123
% RGB	.413	.390	.363	.347	.425	.390	.363	.347
% HB	.086	.097	.092	.089	.060	.096	.091	.089
% AGB	.113	.140	.177	.202	.117	.140	.177	.202
% PAGB	.007	.006	.005	.004	.007	.006	.005	.004
M/Lbol	1.60	1.40	1.10	0.90	1.70	1.40	1.10	0.90
M/Lb	3.47	3.48	2.64	2.08	4.35	3.48	2.64	2.06
M/Lv	2.99	2.72	2.10	1.68	3.58	2.72	2.10	1.68
M/Lk	0.72	0.62	0.48	0.40	0.77	0.62	0.49	0.40

TABLE 6—*Continued*

M.

			Z	[Fe/H]	Y	s	η	
			0.0300	0.23	0.25	3.35	0.30	
	I-HB					B-HB		
Age (Gyr)	15.0	12.5	10.0	8.0		15.0	12.5	10.0	8.0
Mto	1.00	1.04	1.08	1.14		1.00	1.04	1.08	1.14
Mrt	0.86	0.93	1.01	1.09		0.86	0.93	1.01	1.09
Mpn	0.54	0.56	0.58	0.60		0.54	0.56	0.58	0.60
B	1.29	1.26	1.30	1.29		1.30	1.26	1.30	1.29
Bol	0.00	−0.10	−0.16	−0.27		0.00	−0.11	−0.18	−0.28
Bol-V	−1.09	−1.09	−1.03	−0.98		−1.20	−1.08	−1.03	−0.98
U-V	1.30	1.44	1.37	1.29		1.34	1.42	1.36	1.29
B-V	0.89	0.97	0.94	0.91		0.94	0.96	0.94	0.91
V-R	0.92	0.94	0.91	0.89		0.96	0.94	0.91	0.89
V-I	1.69	1.71	1.66	1.62		1.76	1.70	1.66	1.61
V-J	2.45	2.46	2.40	2.34		2.55	2.45	2.39	2.33
V-K	3.49	3.49	3.40	3.34		3.59	3.48	3.40	3.33
% MS	.517	.500	.441	.427		.524	.501	.441	.427
% SGB	.052	.052	.082	.083		.053	.052	.082	.083
% RGB	.248	.240	.239	.232		.251	.240	.239	.232
% HB	.050	.057	.059	.059		.035	.057	.059	.058
% AGB	.132	.149	.177	.198		.134	.149	.177	.198
% PAGB	.002	.002	.002	.001		.002	.002	.002	.001
M/Lbol	14.40	14.20	12.20	10.90		14.60	14.20	12.20	10.90
M/Lb	46.81	49.69	39.30	32.62		55.00	48.79	39.30	32.62
M/Lv	36.84	36.33	29.54	25.20		41.34	36.00	29.54	25.20
M/Lk	5.58	5.50	4.86	4.38		5.71	5.50	4.86	4.42
			Z	[Fe/H]	Y	s	η	
			0.0300	0.23	0.25	3.35	0.50	
Mto	1.00	1.04	1.08	1.14		1.00	1.04	1.08	1.14
Mrt	0.72	0.81	0.91	1.00		0.72	0.81	0.91	1.00
Mpn	0.49	0.51	0.52	0.54		0.49	0.51	0.52	0.54
B	1.36	1.33	1.37	1.36		1.38	1.33	1.37	1.36
Bol	0.00	−0.10	−0.16	−0.27		0.00	−0.12	−0.18	−0.28
Bol-V	−1.04	−1.04	−0.97	−0.93		−1.14	−1.04	−0.97	−0.92
U-V	1.29	1.44	1.36	1.29		1.32	1.43	1.36	1.28
B-V	0.88	0.97	0.94	0.91		0.93	0.97	0.94	0.90
V-R	0.90	0.93	0.90	0.88		0.95	0.93	0.90	0.87
V-I	1.66	1.69	1.64	1.59		1.73	1.68	1.63	1.59
V-J	2.41	2.43	2.35	2.29		2.50	2.42	2.35	2.29
V-K	3.41	3.42	3.33	3.26		3.52	3.42	3.33	3.26
% MS	.546	.528	.467	.451		.556	.528	.467	.452
% SGB	.055	.055	.087	.088		.056	.055	.087	.088
% RGB	.262	.253	.253	.245		.266	.253	.253	.245
% HB	.053	.061	.063	.062		.037	.061	.062	.062
% AGB	.079	.101	.128	.150		.080	.101	.128	.150
% PAGB	.004	.003	.003	.003		.004	.003	.003	.003
M/Lbol	15.20	14.90	12.90	11.50		15.50	14.90	12.90	11.50
M/Lb	46.76	49.80	39.32	32.86		54.74	49.80	39.32	32.26
M/Lv	37.14	36.41	29.55	25.39		41.53	36.41	29.55	25.16
M/Lk	6.05	5.88	5.18	4.75		6.11	5.88	5.18	4.71

TABLE 6—*Continued*

N.

	Z 0.0300	[Fe/H] 0.23	Y 0.25	s 2.35	η 0.30			
	I-HB				B-HB			
Age (Gyr)	15.0	12.5	10.0	8.0	15.0	12.5	10.0	8.0
Mto	1.00	1.04	1.08	1.14	1.00	1.04	1.08	1.14
Mrt	0.86	0.93	1.01	1.09	0.86	0.93	1.01	1.09
Mpn	0.54	0.56	0.58	0.60	0.54	0.56	0.58	0.60
B	1.72	1.68	1.65	1.61	1.75	1.68	1.65	1.61
Bol	0.00	-0.16	-0.33	-0.52	0.00	-0.18	-0.35	-0.54
Bol-V	-0.95	-0.96	-0.93	-0.90	-1.07	-0.95	-0.93	-0.90
U-V	1.22	1.38	1.33	1.26	1.25	1.35	1.32	1.25
B-V	0.84	0.94	0.92	0.89	0.89	0.93	0.92	0.89
V-R	0.85	0.89	0.88	0.86	0.90	0.89	0.88	0.86
V-I	1.57	1.61	1.59	1.56	1.65	1.60	1.58	1.55
V-J	2.28	2.32	2.29	2.25	2.39	2.31	2.28	2.24
V-K	3.28	3.30	3.27	3.23	3.40	3.29	3.26	3.22
% MS	.353	.339	.292	.286	.360	.339	.292	.286
% SGB	.069	.068	.102	.102	.071	.068	.102	.102
% RGB	.332	.318	.304	.290	.339	.318	.304	.290
% HB	.067	.076	.075	.073	.047	.075	.075	.073
% AGB	.176	.197	.225	.248	.180	.197	.225	.248
% PAGB	.003	.003	.002	.002	.003	.003	.002	.002
M/Lbol	4.30	3.80	3.20	2.70	4.30	3.80	3.20	2.70
M/Lb	11.73	11.48	9.23	7.37	13.72	11.27	9.23	7.37
M/Lv	9.67	8.63	7.07	5.80	10.80	8.55	7.07	5.80
M/Lk	1.78	1.56	1.31	1.12	1.78	1.56	1.32	1.13
	Z 0.0300	[Fe/H] 0.23	Y 0.25	s 2.35	η 0.50			
Mto	1.00	1.04	1.08	1.14	1.00	1.04	1.08	1.14
Mrt	0.72	0.81	0.91	1.00	0.72	0.81	0.91	1.00
Mpn	0.49	0.51	0.52	0.54	0.49	0.51	0.52	0.54
B	1.85	1.80	1.78	1.73	1.90	1.80	1.78	1.73
Bol	0.00	-0.16	-0.33	-0.52	0.00	-0.19	-0.36	-0.55
Bol-V	-0.87	-0.89	-0.86	-0.83	-0.99	-0.89	-0.86	-0.83
U-V	1.21	1.38	1.32	1.25	1.23	1.37	1.31	1.24
B-V	0.83	0.94	0.91	0.89	0.88	0.93	0.91	0.88
V-R	0.84	0.88	0.86	0.84	0.89	0.88	0.86	0.84
V-I	1.53	1.58	1.55	1.52	1.61	1.58	1.55	1.52
V-J	2.22	2.26	2.23	2.19	2.32	2.26	2.22	2.18
V-K	3.17	3.21	3.17	3.13	3.30	3.21	3.16	3.12
% MS	.381	.363	.314	.306	.390	.363	.314	.306
% SGB	.075	.073	.109	.109	.076	.073	.109	.109
% RGB	.358	.341	.327	.312	.366	.341	.327	.312
% HB	.073	.082	.081	.079	.051	.082	.080	.078
% AGB	.108	.136	.165	.191	.110	.136	.165	.191
% PAGB	.006	.005	.004	.003	.006	.005	.004	.003
M/Lbol	4.60	4.10	3.40	2.90	4.70	4.10	3.40	2.90
M/Lb	11.55	11.61	9.11	7.42	13.81	11.50	9.11	7.35
M/Lv	9.61	8.73	7.04	5.84	10.97	8.73	7.04	5.84
M/Lk	1.95	1.71	1.43	1.23	1.98	1.71	1.44	1.24

TABLE 6—*Continued*

O

				Z [Fe/H] Y s η 0.0300 0.23 0.25 1.35 0.30				
	I-HB				B-HB			
Age (Gyr)	15.0	12.5	10.0	8.0	15.0	12.5	10.0	8.0
Mto	1.00	1.04	1.08	1.14	1.00	1.04	1.08	1.14
Mrt	0.86	0.93	1.01	1.09	0.86	0.93	1.01	1.09
Mpn	0.54	0.56	0.58	0.60	0.54	0.56	0.58	0.60
B	1.93	1.86	1.82	1.77	1.97	1.87	1.82	1.77
Bol	0.00	−0.22	−0.47	−0.72	0.00	−0.24	−0.49	−0.74
Bol-V	−0.93	−0.95	−0.94	−0.92	−1.06	−0.94	−0.93	−0.91
U-V	1.18	1.36	1.32	1.25	1.21	1.34	1.31	1.25
B-V	0.82	0.93	0.92	0.89	0.88	0.92	0.91	0.89
V-R	0.84	0.89	0.88	0.86	0.89	0.88	0.87	0.86
V-I	1.54	1.60	1.58	1.56	1.63	1.59	1.58	1.56
V-J	2.24	2.30	2.28	2.25	2.36	2.28	2.28	2.25
V-K	3.25	3.29	3.27	3.24	3.38	3.27	3.27	3.24
% MS	.276	.265	.223	.220	.283	.266	.223	.220
% SGB	.076	.074	.109	.108	.078	.074	.109	.108
% RGB	.372	.354	.334	.318	.381	.354	.334	.318
% HB	.075	.085	.083	.080	.053	.084	.082	.080
% AGB	.197	.219	.248	.272	.202	.219	.248	.272
% PAGB	.004	.003	.002	.002	.004	.003	.002	.002
M/Lbol	1.60	1.40	1.10	1.00	1.70	1.40	1.10	1.00
M/Lb	4.21	4.15	3.20	2.78	5.33	4.08	3.14	2.75
M/Lv	3.53	3.15	2.45	2.19	4.23	3.12	2.43	2.17
M/Lk	0.67	0.57	0.45	0.42	0.71	0.58	0.45	0.41
				Z [Fe/H] Y s η 0.0300 0.23 0.25 1.35 0.50				
Mto	1.00	1.04	1.08	1.14	1.00	1.04	1.08	1.14
Mrt	0.72	0.81	0.91	1.00	0.72	0.81	0.91	1.00
Mpn	0.49	0.51	0.52	0.54	0.49	0.51	0.52	0.54
B	2.10	2.02	1.96	1.91	2.16	2.02	1.97	1.91
Bol	0.00	−0.22	−0.48	−0.73	0.00	−0.25	−0.50	−0.75
Bol-V	−0.84	−0.87	−0.86	−0.84	−0.97	−0.87	−0.86	−0.84
U-V	1.17	1.36	1.31	1.24	1.19	1.35	1.30	1.24
B-V	0.81	0.93	0.91	0.89	0.87	0.93	0.91	0.88
V-R	0.82	0.87	0.86	0.85	0.87	0.87	0.86	0.84
V-I	1.49	1.56	1.55	1.52	1.58	1.56	1.54	1.52
V-J	2.17	2.24	2.22	2.19	2.28	2.23	2.21	2.18
V-K	3.12	3.18	3.16	3.13	3.26	3.18	3.16	3.13
% MS	.301	.287	.242	.238	.309	.287	.243	.238
% SGB	.083	.080	.118	.117	.085	.080	.118	.117
% RGB	.406	.383	.362	.344	.416	.383	.362	.344
% HB	.082	.092	.090	.087	.058	.092	.089	.086
% AGB	.121	.152	.184	.210	.124	.152	.184	.211
% PAGB	.006	.005	.004	.004	.007	.005	.004	.004
M/Lbol	1.80	1.50	1.20	1.00	1.80	1.50	1.20	1.00
M/Lb	4.32	4.13	3.22	2.58	5.14	4.13	3.22	2.56
M/Lv	3.66	3.13	2.48	2.03	4.12	3.13	2.48	2.03
M/Lk	0.78	0.63	0.51	0.43	0.77	0.63	0.51	0.43

NOTE.—See Note to Table 5.

TABLE 7

DISTINCTIVE PARAMETERS FOR SELECTED SSPs[a]

Number	Z	Y	t	s	η	HB[b]
1.....	0.0001	0.23	15	2.35	0.3	B-HB
2.....	0.0001	0.23	15	2.35	0.3	I-HB
3.....	0.001	0.23	15	2.35	0.3	I-HB
4.....	0.001	0.23	15	2.35	0.3	R-HB
5.....	0.01	0.25	5	2.35	0.3	R-HB
6.....	0.01	0.25	15	2.35	0.3	R-HB
7.....	0.017	0.25	5	2.35	0.3	R-HB
8.....	0.017	0.25	15	2.35	0.3	R-HB
9.....	0.03	0.25	5	2.35	0.3	R-HB
10.....	0.03	0.25	15	2.35	0.3	R-HB

[a]Selected SSPs are those for which synthetic SEDs are presented in Tables 8A and 8B.

[b]See Note to Table 5.

TABLE 8A

SYNTHETIC SEDs OF SELECTED SSPs[a]

λ_A	(1)	(2)	(3)	(4)	λ	(1)	(2)	(3)	(4)	λ	(1)	(2)	(3)	(4)	λ	(1)	(2)	(3)	(4)
229.	4.896	4.883	4.912	4.906	1062.	5.419	3.748	3.703	3.694	2187.	5.396	5.312	5.154	5.008	3287.	5.746	5.755	5.669	5.635
234.	4.901	4.888	4.919	4.913	1087.	5.407	3.888	3.673	3.661	2212.	5.395	5.319	5.143	5.000	3312.	5.752	5.762	5.675	5.642
243.	4.907	4.894	4.929	4.922	1112.	5.447	4.132	3.825	3.629	2237.	5.418	5.351	5.198	5.069	3337.	5.749	5.758	5.668	5.636
252.	4.910	4.896	4.935	4.928	1137.	5.455	4.085	3.790	3.597	2262.	5.396	5.330	5.119	4.974	3362.	5.752	5.762	5.663	5.629
256.	4.910	4.896	4.937	4.930	1162.	5.460	3.904	3.738	3.566	2287.	5.417	5.356	5.167	5.030	3387.	5.758	5.768	5.678	5.646
260.	4.910	4.896	4.938	4.931	1187.	5.363	3.551	3.599	3.535	2312.	5.431	5.380	5.194	5.065	3412.	5.740	5.751	5.653	5.615
266.	4.908	4.895	4.939	4.932	1210.	4.800	3.412	3.517	3.507	2337.	5.410	5.360	5.049	4.893	3437.	5.759	5.770	5.673	5.642
275.	4.905	4.891	4.938	4.931	1229.	5.225	3.404	3.504	3.484	2362.	5.428	5.388	5.101	4.958	3462.	5.770	5.781	5.684	5.656
283.	4.900	4.886	4.936	4.929	1254.	5.406	3.672	3.699	3.455	2387.	5.403	5.361	4.995	4.835	3487.	5.771	5.782	5.674	5.647
293.	4.892	4.878	4.930	4.924	1285.	5.453	4.047	4.016	3.419	2412.	5.427	5.391	5.091	4.954	3512.	5.773	5.784	5.678	5.650
301.	4.884	4.870	4.925	4.918	1312.	5.408	4.196	4.095	3.389	2437.	5.468	5.439	5.249	5.142	3537.	5.778	5.790	5.692	5.663
309.	4.875	4.862	4.918	4.911	1337.	5.425	4.293	4.176	3.362	2462.	5.461	5.432	5.221	5.109	3562.	5.777	5.789	5.672	5.642
325.	4.855	4.842	4.902	4.895	1362.	5.384	4.326	4.169	3.335	2487.	5.455	5.427	5.155	5.026	3587.	5.779	5.791	5.663	5.634
342.	4.831	4.817	4.881	4.874	1387.	5.364	4.369	4.200	3.309	2506.	5.493	5.469	5.246	5.134	3612.	5.781	5.794	5.669	5.643
351.	4.817	4.803	4.869	4.862	1410.	5.361	4.401	4.209	3.285	2519.	5.456	5.427	5.107	4.957	3636.	5.794	5.806	5.698	5.673
356.	4.809	4.795	4.861	4.855	1433.	5.364	4.420	4.220	3.263	2537.	5.451	5.427	5.187	5.078	3661.	5.803	5.815	5.710	5.688
365.	4.794	4.780	4.848	4.841	1457.	5.343	4.445	4.248	3.240	2562.	5.507	5.488	5.292	5.197	3687.	5.806	5.818	5.711	5.692
375.	4.777	4.763	4.833	4.826	1482.	5.316	4.462	4.242	3.218	2587.	5.509	5.490	5.234	5.126	3712.	5.811	5.831	5.710	5.683
384.	4.761	4.748	4.819	4.812	1507.	5.282	4.520	4.272	3.198	2612.	5.518	5.503	5.213	5.099	3737.	5.831	5.858	5.719	5.680
400.	4.732	4.719	4.792	4.785	1532.	5.301	4.755	4.389	3.331	2637.	5.551	5.539	5.375	5.292	3762.	5.839	5.866	5.747	5.710
415.	4.705	4.691	4.766	4.760	1557.	5.260	4.715	4.312	3.266	2662.	5.573	5.564	5.448	5.377	3787.	5.875	5.907	5.803	5.754
425.	4.686	4.672	4.749	4.742	1582.	5.280	4.775	4.373	3.305	2687.	5.581	5.573	5.441	5.370	3812.	5.895	5.930	5.819	5.762
445.	4.648	4.634	4.713	4.706	1608.	5.307	4.837	4.400	3.339	2712.	5.570	5.562	5.396	5.320	3837.	5.870	5.901	5.773	5.730
472.	4.596	4.582	4.663	4.657	1635.	5.302	4.854	4.380	3.344	2737.	5.554	5.547	5.327	5.240	3862.	5.921	5.959	5.856	5.793
494.	4.553	4.539	4.622	4.616	1663.	5.284	4.840	4.337	3.315	2762.	5.581	5.576	5.366	5.285	3887.	5.885	5.914	5.809	5.770
506.	4.532	4.516	4.600	4.593	1688.	5.293	4.868	4.660	4.243	2787.	5.555	5.550	5.273	5.178	3912.	5.930	5.966	5.857	5.798
516.	4.515	4.496	4.581	4.575	1712.	5.272	4.888	4.670	4.280	2812.	5.592	5.588	5.369	5.287	3937.	5.916	5.953	5.786	5.730
540.	4.470	4.450	4.537	4.530	1737.	5.289	4.930	4.733	4.378	2837.	5.620	5.619	5.456	5.389	3962.	5.894	5.924	5.787	5.751
564.	4.425	4.404	4.492	4.486	1762.	5.296	4.959	4.749	4.398	2862.	5.610	5.609	5.444	5.377	3987.	5.941	5.975	5.882	5.833
587.	4.382	4.360	4.450	4.443	1787.	5.303	5.009	4.821	4.513	2887.	5.633	5.634	5.492	5.432	4012.	5.953	5.989	5.905	5.852
612.	4.338	4.313	4.404	4.398	1815.	5.285	5.013	4.750	4.427	2912.	5.656	5.657	5.553	5.500	4037.	5.954	5.989	5.901	5.849
640.	4.289	4.261	4.354	4.347	1840.	5.284	5.040	4.792	4.476	2937.	5.654	5.657	5.542	5.489	4062.	5.955	5.989	5.898	5.848
671.	4.236	4.205	4.299	4.293	1862.	5.293	5.067	4.844	4.558	2962.	5.660	5.663	5.546	5.493	4087.	5.947	5.978	5.892	5.851
705.	4.181	4.145	4.241	4.234	1892.	5.308	5.102	4.886	4.619	2987.	5.669	5.673	5.554	5.502	4112.	5.928	5.956	5.875	5.842
736.	4.133	4.091	4.188	4.181	1920.	5.320	5.144	4.940	4.695	3012.	5.669	5.673	5.546	5.493	4137.	5.958	5.992	5.905	5.858
770.	4.084	4.034	4.132	4.125	1940.	5.330	5.151	4.918	4.665	3037.	5.685	5.691	5.576	5.527	4162.	5.963	5.996	5.916	5.869
810.	4.029	3.968	4.067	4.060	1964.	5.337	5.169	4.939	4.689	3062.	5.693	5.698	5.591	5.545	4187.	5.959	5.993	5.906	5.859
850.	3.978	3.904	4.004	3.998	1989.	5.343	5.193	4.986	4.764	3087.	5.694	5.700	5.600	5.555	4212.	5.960	5.993	5.910	5.863
890.	3.937	3.842	3.944	3.937	2012.	5.339	5.190	4.946	4.718	3112.	5.703	5.710	5.616	5.574	4237.	5.958	5.991	5.900	5.854
920.	3.975	3.797	3.899	3.892	2037.	5.345	5.207	4.974	4.758	3137.	5.714	5.721	5.626	5.585	4262.	5.957	5.990	5.901	5.855
940.	4.466	3.768	3.870	3.863	2063.	5.356	5.230	4.970	4.757	3162.	5.721	5.728	5.638	5.599	4287.	5.963	5.996	5.913	5.869
962.	4.948	3.736	3.838	3.832	2088.	5.362	5.247	5.104	4.937	3187.	5.708	5.715	5.604	5.563	4312.	5.963	5.994	5.909	5.869
987.	5.278	3.702	3.803	3.796	2112.	5.368	5.257	5.089	4.919	3212.	5.723	5.731	5.634	5.595	4337.	5.932	5.957	5.878	5.856
1012.	5.245	3.666	3.769	3.762	2137.	5.363	5.258	5.070	4.904	3237.	5.718	5.727	5.616	5.576	4362.	5.967	5.997	5.923	5.887
1037.	5.260	3.633	3.734	3.727	2162.	5.370	5.273	5.075	4.910	3262.	5.738	5.747	5.660	5.625	4387.	5.970	6.001	5.923	5.886

TABLE 8A—*Continued*

λ_8	(1)	(2)	(3)	(4)	λ	(1)	(2)	(3)	(4)	λ	(1)	(2)	(3)	(4)	λ	(1)	(2)	(3)	(4)
4412.	5.973	6.004	5.927	5.892	6075.	5.966	5.983	5.952	5.950	9550.	5.743	5.749	5.757	5.768	14050.	5.464	5.466	5.507	5.520
4437.	5.975	6.006	5.932	5.897	6125.	5.964	5.980	5.948	5.946	9650.	5.738	5.745	5.753	5.763	14150.	5.459	5.461	5.503	5.515
4462.	5.977	6.007	5.935	5.902	6175.	5.961	5.977	5.946	5.944	9750.	5.730	5.737	5.747	5.757	14250.	5.455	5.456	5.499	5.511
4487.	5.979	6.009	5.943	5.911	6225.	5.959	5.974	5.943	5.942	9850.	5.723	5.730	5.741	5.751	14350.	5.450	5.452	5.495	5.507
4512.	5.981	6.010	5.948	5.917	6275.	5.956	5.972	5.941	5.940	9950.	5.716	5.722	5.734	5.745	14450.	5.446	5.447	5.490	5.503
4537.	5.982	6.010	5.940	5.912	6325.	5.954	5.969	5.938	5.938	10050.	5.706	5.712	5.725	5.737	14544.	5.441	5.442	5.487	5.500
4562.	5.984	6.012	5.951	5.923	6375.	5.951	5.966	5.936	5.936	10150.	5.702	5.708	5.721	5.732	14644.	5.437	5.438	5.482	5.495
4587.	5.985	6.013	5.954	5.927	6425.	5.949	5.963	5.933	5.933	10250.	5.695	5.701	5.715	5.726	14750.	5.432	5.433	5.478	5.491
4612.	5.986	6.014	5.955	5.928	6475.	5.946	5.960	5.931	5.931	10350.	5.688	5.694	5.709	5.720	14850.	5.427	5.428	5.473	5.487
4637.	5.987	6.014	5.957	5.931	6525.	5.943	5.957	5.930	5.931	10450.	5.681	5.687	5.703	5.714	14950.	5.423	5.423	5.470	5.483
4662.	5.988	6.015	5.959	5.934	6575.	5.931	5.943	5.917	5.922	10550.	5.674	5.679	5.696	5.708	15100.	5.416	5.416	5.463	5.477
4687.	5.989	6.016	5.960	5.936	6625.	5.938	5.952	5.926	5.928	10650.	5.667	5.672	5.689	5.701	15300.	5.405	5.405	5.455	5.468
4712.	5.990	6.016	5.958	5.935	6675.	5.935	5.949	5.924	5.926	10750.	5.660	5.665	5.684	5.695	15500.	5.393	5.393	5.444	5.458
4737.	5.990	6.017	5.960	5.938	6725.	5.933	5.946	5.923	5.925	10850.	5.652	5.658	5.677	5.688	15700.	5.382	5.382	5.433	5.447
4762.	5.991	6.017	5.963	5.941	6775.	5.930	5.943	5.920	5.923	10950.	5.642	5.647	5.668	5.680	15900.	5.370	5.369	5.422	5.435
4787.	5.992	6.018	5.964	5.943	6825.	5.927	5.940	5.918	5.921	11050.	5.638	5.643	5.665	5.676	16100.	5.356	5.356	5.410	5.424
4812.	5.991	6.017	5.962	5.942	6875.	5.924	5.937	5.915	5.918	11150.	5.632	5.637	5.659	5.670	16300.	5.348	5.347	5.403	5.417
4837.	5.989	6.014	5.960	5.942	6925.	5.921	5.934	5.912	5.915	11250.	5.625	5.630	5.652	5.664	16500.	5.329	5.329	5.385	5.399
4862.	5.962	5.981	5.925	5.920	6975.	5.918	5.931	5.909	5.913	11350.	5.618	5.623	5.646	5.658	16700.	5.317	5.316	5.373	5.387
4887.	5.988	6.012	5.956	5.938	7025.	5.915	5.927	5.906	5.910	11450.	5.612	5.617	5.640	5.651	16900.	5.297	5.296	5.354	5.368
4912.	5.990	6.014	5.957	5.938	7075.	5.912	5.924	5.903	5.907	11550.	5.605	5.610	5.634	5.646	18000.	5.214	5.213	5.273	5.286
4937.	5.990	6.014	5.959	5.940	7150.	5.908	5.919	5.898	5.903	11650.	5.599	5.603	5.628	5.639	27000.	4.638	4.635	4.708	4.720
4962.	5.989	6.013	5.957	5.939	7250.	5.901	5.913	5.894	5.899	11750.	5.592	5.597	5.622	5.634	40000.	4.028	4.025	4.112	4.123
4987.	5.990	6.014	5.955	5.937	7350.	5.895	5.906	5.890	5.895	11850.	5.586	5.590	5.616	5.627	50000.	3.666	3.662	3.760	3.770
5025.	5.989	6.013	5.954	5.936	7450.	5.889	5.900	5.884	5.890	11950.	5.580	5.584	5.611	5.622	65000.	3.238	3.234	3.337	3.347
5075.	5.988	6.012	5.956	5.939	7550.	5.883	5.893	5.880	5.887	12050.	5.574	5.578	5.605	5.617	100000.	2.527	2.523	2.628	2.637
5125.	5.987	6.010	5.955	5.939	7650.	5.876	5.886	5.875	5.881	12150.	5.568	5.572	5.600	5.612	200000.	1.363	1.358	1.461	1.469
5175.	5.985	6.007	5.949	5.934	7750.	5.869	5.879	5.869	5.876	12250.	5.562	5.566	5.595	5.606					
5225.	5.985	6.007	5.952	5.938	7850.	5.863	5.872	5.864	5.871	12350.	5.556	5.560	5.590	5.601					
5275.	5.985	6.007	5.952	5.939	7950.	5.856	5.866	5.857	5.865	12450.	5.550	5.553	5.584	5.596					
5325.	5.985	6.006	5.954	5.942	8050.	5.849	5.859	5.851	5.859	12550.	5.544	5.548	5.579	5.591					
5375.	5.985	6.005	5.958	5.947	8152.	5.842	5.851	5.845	5.853	12650.	5.539	5.542	5.574	5.585					
5425.	5.983	6.004	5.957	5.947	8252.	5.836	5.844	5.839	5.847	12750.	5.532	5.535	5.568	5.580					
5475.	5.984	6.004	5.961	5.951	8350.	5.829	5.837	5.833	5.842	12850.	5.523	5.525	5.559	5.572					
5525.	5.984	6.003	5.963	5.955	8450.	5.822	5.830	5.826	5.835	12950.	5.522	5.524	5.559	5.571					
5575.	5.983	6.002	5.960	5.953	8550.	5.814	5.822	5.817	5.827	13050.	5.516	5.519	5.554	5.566					
5625.	5.981	6.000	5.961	5.953	8650.	5.807	5.814	5.812	5.821	13150.	5.511	5.513	5.549	5.561					
5675.	5.979	5.998	5.959	5.953	8750.	5.800	5.808	5.808	5.817	13250.	5.505	5.508	5.544	5.556					
5725.	5.978	5.996	5.958	5.952	8850.	5.793	5.801	5.801	5.811	13350.	5.500	5.502	5.539	5.551					
5775.	5.976	5.994	5.956	5.950	8950.	5.787	5.796	5.797	5.806	13450.	5.495	5.497	5.534	5.547					
5825.	5.974	5.992	5.955	5.950	9050.	5.779	5.786	5.789	5.799	13550.	5.490	5.492	5.530	5.542					
5875.	5.971	5.989	5.951	5.946	9150.	5.773	5.781	5.785	5.794	13650.	5.484	5.486	5.525	5.537					
5925.	5.971	5.988	5.952	5.949	9250.	5.764	5.771	5.776	5.787	13750.	5.479	5.481	5.521	5.533					
5975.	5.969	5.986	5.953	5.949	9350.	5.759	5.767	5.773	5.782	13850.	5.474	5.476	5.516	5.529					
6025.	5.968	5.985	5.952	5.950	9450.	5.752	5.759	5.766	5.776	13950.	5.469	5.471	5.511	5.524					

[a] Models are referred to with the sequence number of Table 7.

TABLE 8B

SYNTHETIC SEDs OF SELECTED SSPs[a]

λ_R	(5)	(6)	(7)	(8)	(9)	(10)	λ	(5)	(6)	(7)	(8)	(9)	(10)	λ	(5)	(6)	(7)	(8)	(9)	(10)
229.	4.651	4.928	4.577	4.899	4.557	4.887	1062.	2.928	3.783	2.791	3.652	2.754	3.612	2187.	4.813	4.358	4.622	4.073	4.409	3.782
234.	4.642	4.937	4.566	4.905	4.546	4.892	1087.	2.893	3.750	2.755	3.618	2.718	3.579	2212.	4.759	4.319	4.554	4.032	4.330	3.741
243.	4.626	4.950	4.546	4.913	4.525	4.898	1112.	2.858	3.718	2.720	3.586	2.683	3.546	2237.	4.882	4.486	4.710	4.237	4.523	3.978
252.	4.608	4.959	4.525	4.917	4.503	4.902	1137.	2.824	3.686	2.685	3.554	2.648	3.514	2262.	4.635	4.142	4.381	3.794	4.099	3.454
256.	4.599	4.962	4.515	4.918	4.493	4.902	1162.	2.791	3.656	2.652	3.522	2.615	3.482	2287.	4.738	4.244	4.503	3.903	4.239	3.564
260.	4.590	4.965	4.505	4.919	4.482	4.902	1187.	2.758	3.625	2.619	3.492	2.582	3.451	2312.	4.766	4.293	4.535	3.961	4.275	3.629
266.	4.577	4.967	4.490	4.919	4.467	4.901	1210.	2.728	3.598	2.589	3.464	2.552	3.423	2337.	4.377	3.954	4.075	3.616	3.758	3.303
275.	4.556	4.969	4.466	4.917	4.443	4.898	1229.	2.704	3.575	2.564	3.441	2.527	3.400	2362.	4.491	4.074	4.212	3.743	3.916	3.427
283.	4.536	4.969	4.445	4.913	4.421	4.893	1254.	2.673	3.546	2.533	3.411	2.496	3.370	2387.	4.284	3.896	3.986	3.576	3.682	3.284
293.	4.512	4.966	4.418	4.906	4.393	4.886	1285.	2.635	3.510	2.495	3.375	2.457	3.334	2412.	4.523	4.117	4.267	3.801	3.996	3.497
301.	4.492	4.962	4.396	4.900	4.370	4.878	1312.	2.603	3.479	2.462	3.344	2.425	3.303	2437.	4.831	4.431	4.618	4.131	4.382	3.830
309.	4.471	4.957	4.373	4.892	4.348	4.870	1337.	2.574	3.452	2.433	3.316	2.395	3.275	2462.	4.758	4.324	4.521	3.996	4.258	3.672
325.	4.429	4.944	4.329	4.874	4.302	4.850	1362.	2.546	3.424	2.404	3.288	2.365	3.247	2487.	4.605	4.128	4.329	3.768	4.027	3.429
342.	4.384	4.927	4.281	4.851	4.253	4.827	1387.	2.519	3.397	2.375	3.261	2.337	3.220	2506.	4.734	4.258	4.461	3.893	4.157	3.544
351.	4.360	4.916	4.255	4.838	4.227	4.813	1410.	2.495	3.373	2.350	3.236	2.311	3.195	2519.	4.488	3.969	4.173	3.605	3.834	3.280
356.	4.347	4.910	4.241	4.831	4.213	4.805	1433.	2.471	3.349	2.325	3.212	2.285	3.171	2537.	4.742	4.372	4.534	4.092	4.310	3.815
365.	4.323	4.898	4.216	4.817	4.187	4.790	1457.	2.449	3.324	2.300	3.187	2.259	3.145	2562.	4.952	4.678	4.800	4.488	4.643	4.296
375.	4.297	4.884	4.188	4.800	4.159	4.773	1482.	2.426	3.298	2.274	3.161	2.232	3.120	2587.	4.754	4.449	4.547	4.208	4.334	3.969
384.	4.273	4.871	4.163	4.785	4.134	4.758	1507.	2.406	3.273	2.250	3.136	2.206	3.094	2612.	4.650	4.339	4.410	4.073	4.166	3.817
400.	4.230	4.846	4.119	4.758	4.089	4.730	1532.	2.498	3.250	2.273	3.111	2.202	3.069	2637.	5.129	4.907	5.020	4.772	4.912	4.635
415.	4.191	4.823	4.078	4.731	4.047	4.702	1557.	2.456	3.225	2.247	3.086	2.176	3.044	2662.	5.283	5.094	5.204	4.991	5.129	4.886
425.	4.165	4.806	4.050	4.713	4.020	4.684	1582.	2.490	3.202	2.248	3.062	2.163	3.020	2687.	5.237	5.031	5.142	4.908	5.047	4.781
445.	4.114	4.772	3.997	4.676	3.966	4.646	1608.	2.522	3.178	2.254	3.038	2.152	2.995	2712.	5.134	4.896	5.012	4.740	4.888	4.583
472.	4.045	4.725	3.927	4.625	3.895	4.594	1635.	2.535	3.154	2.256	3.013	2.141	2.970	2737.	4.924	4.633	4.744	4.404	4.555	4.176
494.	3.991	4.686	3.871	4.583	3.839	4.551	1663.	2.523	3.129	2.247	2.987	2.124	2.944	2762.	4.961	4.696	4.784	4.479	4.601	4.262
506.	3.962	4.665	3.841	4.561	3.808	4.528	1688.	3.695	3.230	3.209	3.005	2.703	2.931	2787.	4.792	4.518	4.593	4.284	4.388	4.055
516.	3.938	4.647	3.816	4.542	3.783	4.509	1712.	3.719	3.230	3.234	2.993	2.724	2.912	2812.	4.963	4.690	4.784	4.470	4.597	4.250
540.	3.881	4.604	3.758	4.496	3.725	4.463	1737.	3.893	3.273	3.432	2.995	2.919	2.895	2837.	5.144	4.867	4.994	4.657	4.831	4.444
564.	3.826	4.561	3.701	4.451	3.668	4.417	1762.	3.884	3.263	3.412	2.981	2.892	2.876	2862.	5.160	4.889	5.023	4.693	4.875	4.496
587.	3.774	4.519	3.648	4.408	3.614	4.373	1787.	4.028	3.332	3.572	3.002	3.054	2.866	2887.	5.280	5.083	5.184	4.955	5.086	4.824
612.	3.719	4.475	3.592	4.362	3.558	4.327	1815.	3.794	3.255	3.315	2.963	2.810	2.844	2912.	5.408	5.246	5.339	5.153	5.274	5.058
640.	3.659	4.426	3.531	4.311	3.497	4.275	1840.	3.885	3.265	3.400	2.955	2.874	2.826	2937.	5.363	5.185	5.281	5.071	5.197	4.955
671.	3.595	4.373	3.466	4.255	3.431	4.219	1862.	4.024	3.322	3.551	2.973	3.017	2.818	2962.	5.365	5.171	5.277	5.047	5.187	4.919
705.	3.527	4.315	3.396	4.196	3.361	4.159	1892.	4.084	3.365	3.614	2.991	3.081	2.811	2987.	5.364	5.166	5.272	5.035	5.176	4.902
736.	3.466	4.263	3.335	4.142	3.300	4.105	1920.	4.164	3.430	3.703	3.025	3.175	2.812	3012.	5.328	5.084	5.214	4.916	5.091	4.746
770.	3.403	4.208	3.270	4.086	3.235	4.048	1940.	4.095	3.395	3.625	3.005	3.098	2.800	3037.	5.395	5.199	5.306	5.070	5.212	4.938
810.	3.330	4.145	3.197	4.021	3.161	3.983	1964.	4.124	3.402	3.648	3.004	3.111	2.790	3062.	5.424	5.249	5.343	5.135	5.261	5.020
850.	3.260	4.083	3.126	3.957	3.090	3.919	1989.	4.292	3.531	3.870	3.083	3.379	2.809	3087.	5.434	5.261	5.352	5.147	5.269	5.031
890.	3.193	4.023	3.058	3.896	3.022	3.857	2012.	4.170	3.466	3.726	3.046	3.226	2.795	3112.	5.490	5.357	5.433	5.279	5.379	5.201
920.	3.144	3.979	3.008	3.851	2.972	3.812	2037.	4.227	3.512	3.792	3.077	3.296	2.802	3137.	5.496	5.364	5.437	5.285	5.382	5.206
940.	3.112	3.950	2.976	3.822	2.940	3.783	2063.	4.188	3.517	3.755	3.091	3.269	2.812	3162.	5.512	5.385	5.456	5.308	5.403	5.233
962.	3.077	3.919	2.941	3.790	2.905	3.751	2088.	4.776	4.270	4.580	3.971	4.360	3.666	3187.	5.439	5.292	5.365	5.195	5.293	5.096
987.	3.039	3.884	2.902	3.754	2.866	3.715	2112.	4.709	4.187	4.492	3.867	4.248	3.548	3212.	5.489	5.349	5.422	5.258	5.357	5.167
1012.	3.001	3.850	2.864	3.720	2.828	3.680	2137.	4.661	4.148	4.435	3.822	4.182	3.498	3237.	5.447	5.300	5.373	5.199	5.298	5.098
1037.	2.964	3.816	2.827	3.685	2.790	3.646	2162.	4.642	4.120	4.407	3.782	4.144	3.449	3262.	5.541	5.423	5.489	5.350	5.440	5.279

TABLE 8B—*Continued*

λ_{air}	(5)	(6)	(7)	(8)	(9)	(10)	λ	(5)	(6)	(7)	(8)	(9)	(10)	λ	(5)	(6)	(7)	(8)	(9)	(10)
3287.	5.552	5.439	5.502	5.370	5.455	5.302	4412.	5.809	5.729	5.763	5.674	5.724	5.623	6075.	5.889	5.864	5.861	5.831	5.837	5.800
3312.	5.552	5.435	5.499	5.361	5.448	5.288	4437.	5.817	5.739	5.772	5.684	5.734	5.635	6125.	5.881	5.856	5.852	5.822	5.826	5.789
3337.	5.542	5.428	5.488	5.354	5.438	5.280	4462.	5.821	5.743	5.776	5.688	5.737	5.638	6175.	5.880	5.856	5.851	5.822	5.826	5.790
3362.	5.519	5.397	5.458	5.315	5.399	5.233	4487.	5.839	5.767	5.798	5.717	5.765	5.673	6225.	5.876	5.853	5.847	5.819	5.821	5.787
3387.	5.543	5.421	5.484	5.339	5.427	5.257	4512.	5.847	5.778	5.808	5.731	5.776	5.688	6275.	5.874	5.852	5.846	5.820	5.821	5.788
3412.	5.511	5.375	5.447	5.284	5.383	5.193	4537.	5.823	5.749	5.775	5.692	5.734	5.639	6325.	5.870	5.850	5.842	5.817	5.817	5.786
3437.	5.533	5.399	5.468	5.306	5.403	5.213	4562.	5.850	5.781	5.809	5.731	5.774	5.686	6375.	5.869	5.850	5.842	5.818	5.818	5.788
3462.	5.546	5.422	5.485	5.334	5.425	5.246	4587.	5.857	5.791	5.818	5.744	5.786	5.701	6425.	5.866	5.847	5.839	5.815	5.814	5.784
3487.	5.517	5.392	5.449	5.298	5.381	5.206	4612.	5.857	5.791	5.817	5.743	5.784	5.699	6475.	5.864	5.845	5.836	5.813	5.811	5.782
3512.	5.526	5.402	5.460	5.311	5.396	5.221	4637.	5.862	5.798	5.824	5.751	5.792	5.709	6525.	5.867	5.850	5.841	5.820	5.818	5.791
3537.	5.557	5.442	5.501	5.362	5.448	5.284	4662.	5.865	5.802	5.828	5.757	5.797	5.715	6575.	5.855	5.842	5.829	5.812	5.806	5.782
3562.	5.523	5.390	5.462	5.301	5.401	5.215	4687.	5.869	5.809	5.833	5.765	5.804	5.726	6625.	5.865	5.850	5.840	5.820	5.817	5.791
3587.	5.496	5.353	5.425	5.253	5.353	5.157	4712.	5.861	5.802	5.822	5.755	5.790	5.713	6675.	5.865	5.850	5.840	5.821	5.817	5.792
3612.	5.506	5.364	5.434	5.263	5.361	5.166	4737.	5.865	5.806	5.826	5.759	5.794	5.717	6725.	5.864	5.850	5.839	5.821	5.817	5.793
3636.	5.556	5.432	5.494	5.343	5.433	5.258	4762.	5.871	5.812	5.833	5.767	5.802	5.726	6775.	5.861	5.847	5.836	5.818	5.813	5.789
3661.	5.579	5.480	5.526	5.409	5.479	5.342	4787.	5.872	5.815	5.835	5.770	5.804	5.730	6825.	5.860	5.847	5.835	5.818	5.812	5.790
3687.	5.573	5.474	5.519	5.399	5.470	5.328	4812.	5.869	5.812	5.831	5.767	5.800	5.726	6875.	5.857	5.845	5.833	5.817	5.810	5.789
3712.	5.546	5.424	5.479	5.333	5.416	5.247	4837.	5.869	5.813	5.832	5.768	5.801	5.727	6925.	5.854	5.842	5.830	5.815	5.807	5.787
3737.	5.522	5.359	5.434	5.243	5.346	5.134	4862.	5.830	5.787	5.793	5.740	5.762	5.698	6975.	5.850	5.840	5.826	5.812	5.803	5.784
3762.	5.574	5.446	5.504	5.353	5.437	5.264	4887.	5.860	5.805	5.822	5.759	5.790	5.717	7025.	5.846	5.836	5.822	5.808	5.799	5.780
3787.	5.652	5.530	5.592	5.452	5.539	5.379	4912.	5.859	5.803	5.820	5.757	5.787	5.714	7075.	5.844	5.834	5.819	5.806	5.797	5.779
3812.	5.650	5.505	5.579	5.414	5.512	5.328	4937.	5.863	5.808	5.825	5.763	5.793	5.722	7150.	5.840	5.831	5.815	5.803	5.792	5.775
3837.	5.576	5.426	5.489	5.317	5.404	5.216	4962.	5.863	5.810	5.826	5.765	5.796	5.726	7250.	5.839	5.830	5.815	5.803	5.792	5.776
3862.	5.696	5.552	5.628	5.466	5.566	5.387	4987.	5.855	5.801	5.816	5.755	5.783	5.712	7350.	5.840	5.832	5.817	5.806	5.796	5.780
3887.	5.653	5.532	5.588	5.447	5.528	5.368	5025.	5.851	5.798	5.812	5.751	5.778	5.707	7450.	5.837	5.829	5.815	5.804	5.793	5.778
3912.	5.676	5.536	5.599	5.444	5.527	5.359	5075.	5.861	5.811	5.824	5.768	5.794	5.729	7550.	5.837	5.831	5.817	5.807	5.797	5.782
3937.	5.531	5.392	5.425	5.283	5.329	5.185	5125.	5.858	5.809	5.820	5.764	5.789	5.724	7650.	5.832	5.826	5.812	5.803	5.792	5.778
3962.	5.586	5.464	5.500	5.368	5.422	5.281	5175.	5.843	5.792	5.801	5.741	5.764	5.694	7750.	5.828	5.823	5.808	5.800	5.788	5.776
3987.	5.733	5.621	5.672	5.548	5.618	5.480	5225.	5.854	5.807	5.816	5.761	5.783	5.719	7850.	5.825	5.822	5.807	5.801	5.788	5.778
4012.	5.773	5.669	5.722	5.606	5.679	5.550	5275.	5.853	5.807	5.814	5.761	5.781	5.719	7950.	5.819	5.817	5.801	5.795	5.782	5.772
4037.	5.761	5.652	5.706	5.583	5.657	5.521	5325.	5.860	5.817	5.823	5.774	5.792	5.734	8050.	5.815	5.813	5.797	5.792	5.778	5.770
4062.	5.755	5.644	5.697	5.573	5.647	5.509	5375.	5.873	5.832	5.839	5.792	5.810	5.755	8152.	5.811	5.810	5.793	5.790	5.775	5.767
4087.	5.760	5.664	5.709	5.600	5.665	5.543	5425.	5.871	5.830	5.836	5.788	5.805	5.749	8252.	5.805	5.805	5.788	5.785	5.770	5.764
4112.	5.748	5.665	5.702	5.605	5.663	5.549	5475.	5.880	5.842	5.847	5.802	5.818	5.766	8350.	5.800	5.801	5.783	5.781	5.766	5.760
4137.	5.769	5.669	5.718	5.606	5.674	5.548	5525.	5.887	5.851	5.855	5.813	5.828	5.778	8450.	5.794	5.796	5.778	5.776	5.760	5.755
4162.	5.792	5.702	5.749	5.648	5.713	5.599	5575.	5.881	5.843	5.847	5.803	5.817	5.765	8550.	5.785	5.787	5.768	5.767	5.750	5.746
4187.	5.773	5.678	5.724	5.616	5.683	5.561	5625.	5.883	5.849	5.851	5.811	5.824	5.776	8650.	5.781	5.784	5.765	5.765	5.747	5.743
4212.	5.785	5.691	5.739	5.633	5.701	5.581	5675.	5.879	5.846	5.846	5.807	5.818	5.772	8750.	5.780	5.784	5.765	5.766	5.749	5.747
4237.	5.765	5.668	5.715	5.604	5.670	5.547	5725.	5.879	5.847	5.846	5.809	5.819	5.774	8850.	5.774	5.779	5.759	5.762	5.744	5.742
4262.	5.766	5.666	5.714	5.601	5.668	5.541	5775.	5.874	5.843	5.840	5.804	5.812	5.768	8950.	5.772	5.777	5.758	5.761	5.743	5.742
4287.	5.784	5.692	5.735	5.631	5.692	5.575	5825.	5.875	5.846	5.843	5.809	5.816	5.776	9050.	5.765	5.771	5.751	5.755	5.736	5.736
4312.	5.784	5.694	5.735	5.634	5.694	5.580	5875.	5.865	5.835	5.830	5.794	5.800	5.757	9150.	5.763	5.769	5.751	5.755	5.736	5.737
4337.	5.764	5.697	5.723	5.643	5.688	5.594	5925.	5.876	5.848	5.843	5.812	5.817	5.779	9250.	5.755	5.763	5.743	5.748	5.729	5.731
4362.	5.813	5.737	5.772	5.687	5.739	5.642	5975.	5.882	5.855	5.851	5.820	5.826	5.789	9350.	5.754	5.761	5.742	5.748	5.729	5.731
4387.	5.806	5.724	5.761	5.669	5.723	5.620	6025.	5.886	5.859	5.856	5.825	5.831	5.793	9450.	5.748	5.755	5.736	5.742	5.723	5.725

TABLE 8B—*Continued*

λ_R	(5)	(6)	(7)	(8)	(9)	(10)	λ	(5)	(6)	(7)	(8)	(9)	(10)
9550.	5.742	5.751	5.731	5.738	5.719	5.723	14050.	5.541	5.563	5.549	5.570	5.552	5.572
9650.	5.738	5.747	5.728	5.735	5.715	5.719	14150.	5.537	5.559	5.545	5.566	5.548	5.568
9750.	5.734	5.742	5.724	5.731	5.712	5.716	14250.	5.533	5.556	5.542	5.563	5.545	5.565
9850.	5.729	5.738	5.719	5.727	5.707	5.712	14350.	5.531	5.553	5.540	5.561	5.543	5.564
9950.	5.724	5.734	5.714	5.723	5.703	5.709	14450.	5.527	5.549	5.536	5.557	5.539	5.560
10050.	5.716	5.728	5.708	5.718	5.697	5.705	14544.	5.524	5.548	5.534	5.556	5.538	5.559
10150.	5.713	5.724	5.706	5.716	5.695	5.702	14644.	5.521	5.543	5.530	5.552	5.535	5.555
10250.	5.709	5.721	5.703	5.713	5.693	5.700	14750.	5.518	5.541	5.528	5.550	5.533	5.554
10350.	5.704	5.716	5.697	5.707	5.687	5.695	14850.	5.513	5.535	5.523	5.544	5.528	5.548
10450.	5.699	5.712	5.692	5.704	5.683	5.692	14950.	5.511	5.535	5.522	5.544	5.527	5.548
10550.	5.695	5.707	5.688	5.699	5.679	5.688	15100.	5.505	5.528	5.517	5.538	5.522	5.542
10650.	5.688	5.701	5.682	5.693	5.673	5.682	15300.	5.500	5.524	5.513	5.535	5.519	5.540
10750.	5.684	5.697	5.678	5.690	5.669	5.679	15500.	5.492	5.516	5.504	5.527	5.511	5.533
10850.	5.677	5.691	5.672	5.684	5.663	5.673	15700.	5.481	5.505	5.494	5.517	5.502	5.523
10950.	5.670	5.685	5.666	5.679	5.658	5.670	15900.	5.471	5.495	5.485	5.507	5.492	5.514
11050.	5.669	5.684	5.665	5.678	5.658	5.669	16100.	5.462	5.487	5.477	5.500	5.485	5.508
11150.	5.663	5.678	5.660	5.673	5.653	5.665	16300.	5.459	5.483	5.474	5.497	5.483	5.506
11250.	5.658	5.673	5.654	5.668	5.648	5.660	16500.	5.442	5.467	5.458	5.482	5.468	5.491
11350.	5.653	5.669	5.650	5.665	5.644	5.657	16700.	5.431	5.456	5.448	5.471	5.458	5.480
11450.	5.648	5.664	5.645	5.660	5.640	5.653	16900.	5.415	5.440	5.432	5.456	5.443	5.466
11550.	5.643	5.660	5.641	5.657	5.636	5.650	18000.	5.339	5.365	5.359	5.383	5.372	5.396
11650.	5.637	5.654	5.635	5.651	5.630	5.644	27000.	4.814	4.842	4.848	4.874	4.875	4.901
11750.	5.633	5.650	5.632	5.648	5.627	5.641	40000.	4.247	4.276	4.291	4.318	4.329	4.356
11850.	5.627	5.644	5.626	5.642	5.621	5.635	50000.	3.907	3.937	3.956	3.983	3.998	4.026
11950.	5.623	5.640	5.623	5.639	5.619	5.633	65000.	3.497	3.528	3.550	3.578	3.597	3.626
12050.	5.618	5.636	5.618	5.635	5.615	5.629	100000.	2.802	2.832	2.859	2.887	2.911	2.941
12150.	5.615	5.633	5.615	5.633	5.612	5.628	200000.	1.646	1.678	1.708	1.737	1.764	1.795
12250.	5.610	5.629	5.612	5.629	5.609	5.625							
12350.	5.606	5.625	5.608	5.626	5.605	5.621							
12450.	5.602	5.621	5.604	5.622	5.602	5.618							
12550.	5.597	5.617	5.600	5.618	5.598	5.615							
12650.	5.593	5.613	5.596	5.615	5.595	5.612							
12750.	5.589	5.609	5.592	5.612	5.591	5.609							
12850.	5.581	5.602	5.585	5.604	5.584	5.602							
12950.	5.581	5.602	5.585	5.605	5.585	5.603							
13050.	5.577	5.598	5.582	5.601	5.582	5.600							
13150.	5.573	5.594	5.578	5.598	5.578	5.596							
13250.	5.569	5.590	5.574	5.594	5.575	5.593							
13350.	5.565	5.586	5.571	5.591	5.572	5.590							
13450.	5.562	5.583	5.568	5.588	5.569	5.588							
13550.	5.558	5.580	5.565	5.585	5.566	5.585							
13650.	5.554	5.576	5.561	5.582	5.563	5.582							
13750.	5.551	5.573	5.558	5.579	5.560	5.579							
13850.	5.547	5.569	5.555	5.575	5.557	5.576							
13950.	5.543	5.565	5.551	5.571	5.553	5.572							

[a] Models are referred to with the sequence number of Table 7.

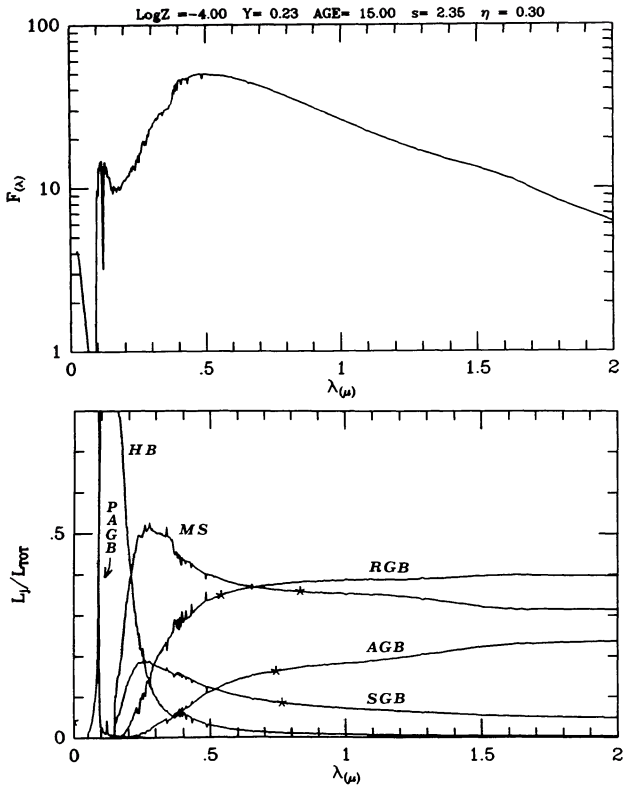

FIG. 11.—Synthetic model for a $Z = 0.0001$, $t = 15$ Gyr SSP. Above the figure are noted the other distinctive parameters adopted. The upper panel displays the integral SED, while the lower panel plots the relative monochromatic contributions from the different stellar evolutionary phases. Here asterisks mark the wavelengths at which monochromatic and bolometric percentages for each phase are equal. A B-HB morphology is assumed. See text for details.

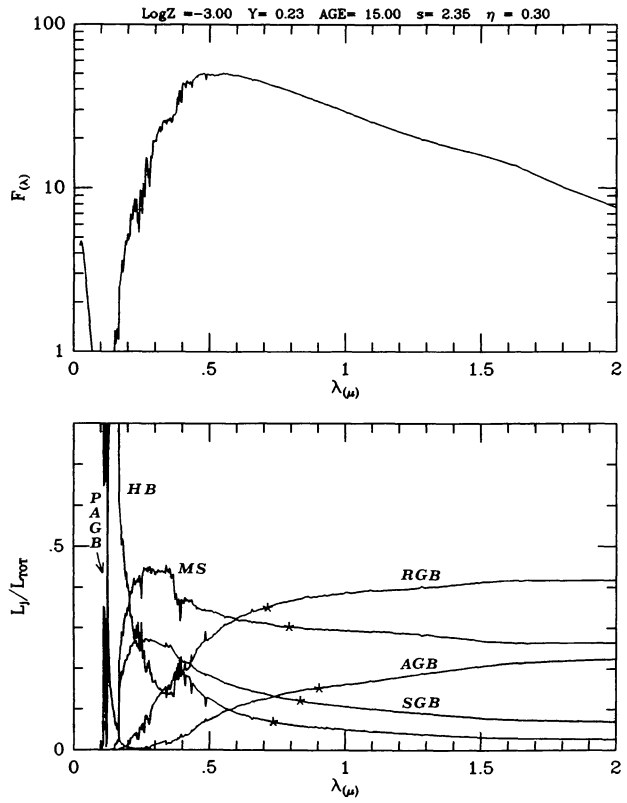

FIG. 13.—Same as Fig. 11, but for $Z = 0.001$. An I-HB morphology is adopted.

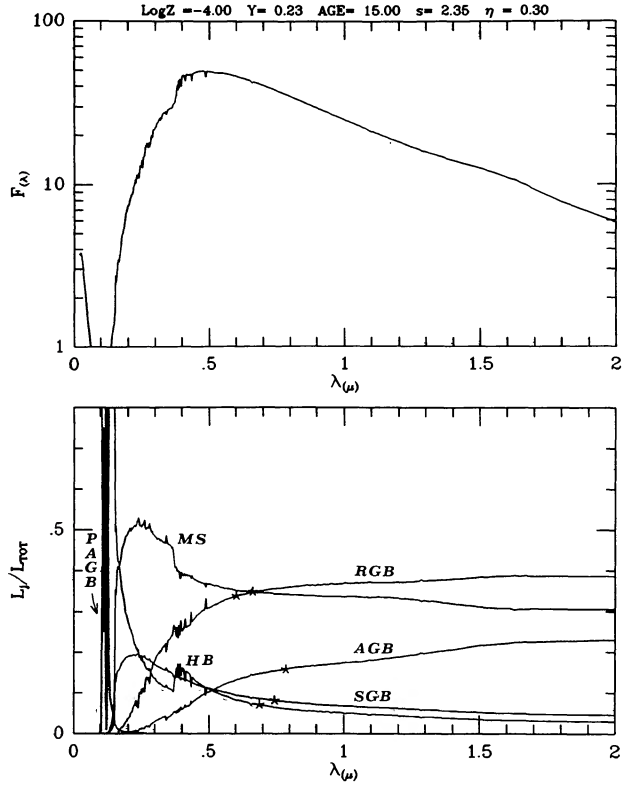

FIG. 12.—Same as Fig. 11, but for an I-HB morphology

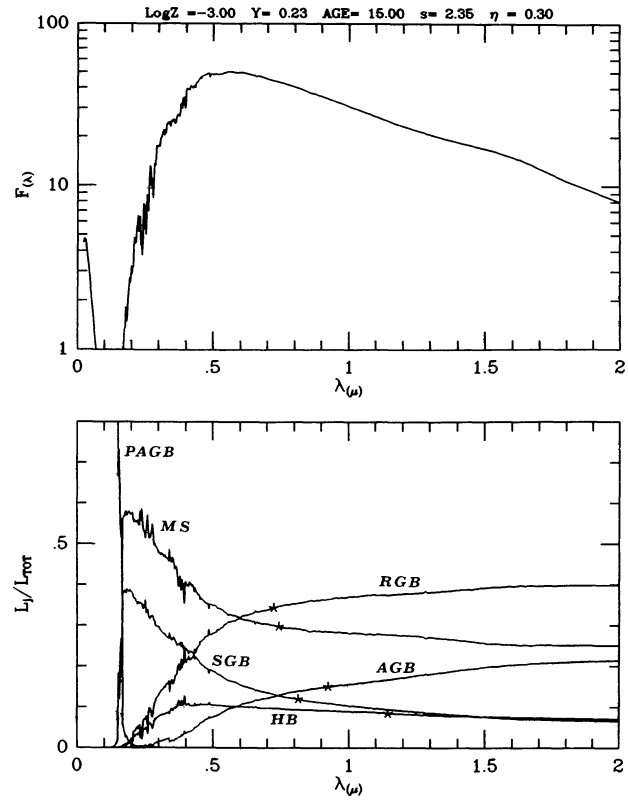

FIG. 14.—Same as Fig. 13, but for an R-HB morphology

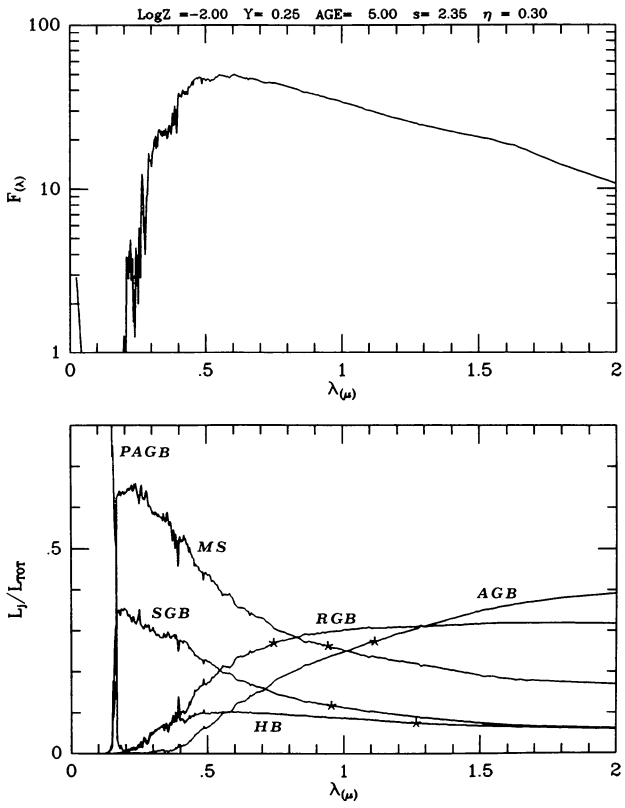

FIG. 15.—Same as Fig. 11, but for $Z = 0.01$ and $t = 5$ Gyr. An evolved R-HB morphology is adopted.

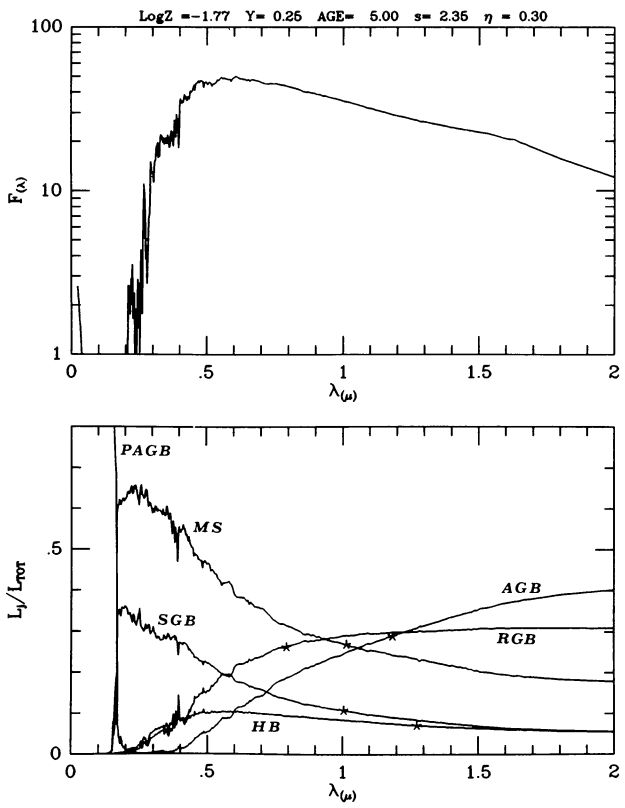

FIG. 17.—Same as Fig. 11, but for $Z = 0.017$ and $t = 5$ Gyr. An evolved R-HB morphology is adopted.

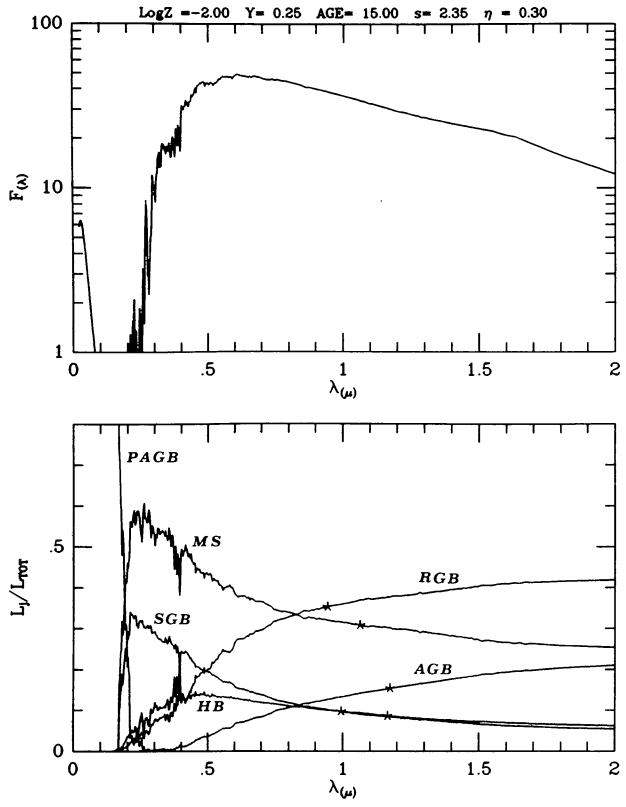

FIG. 16.—Same as Fig. 15, but for $t = 15$ Gyr and an R-HB morphology.

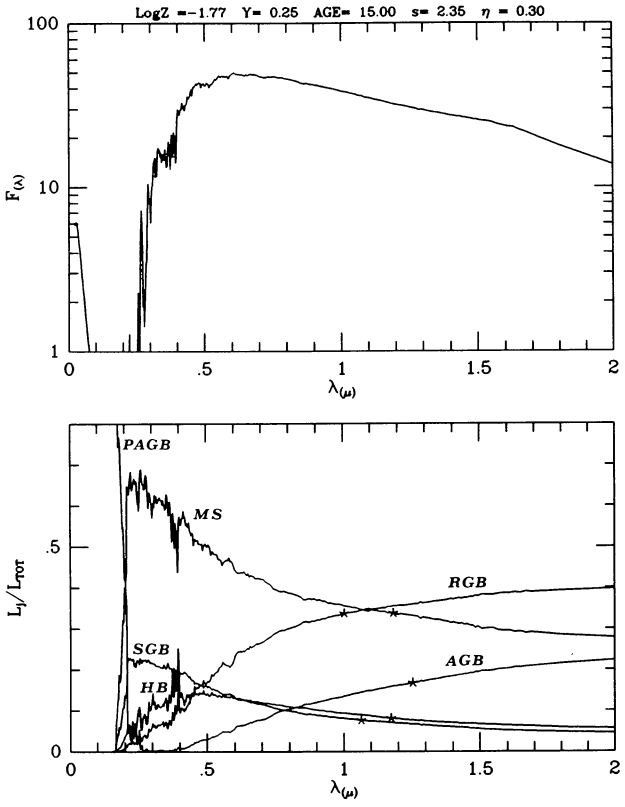

FIG. 18.—Same as Fig. 17, but for $t = 15$ Gyr and an R-HB morphology.

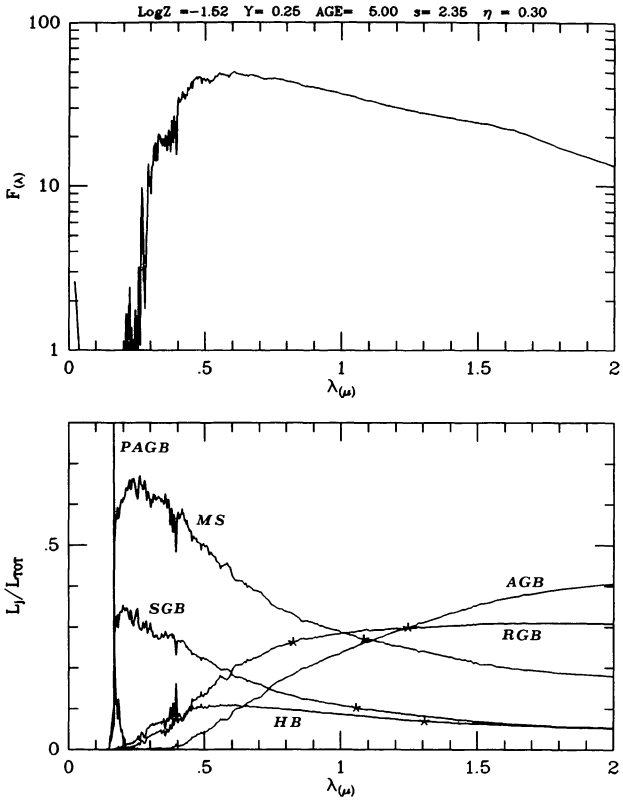

FIG. 19.—Same as Fig. 11, but for $Z = 0.03$ and $t = 5$ Gyr. An evolved R-HB morphology is adopted.

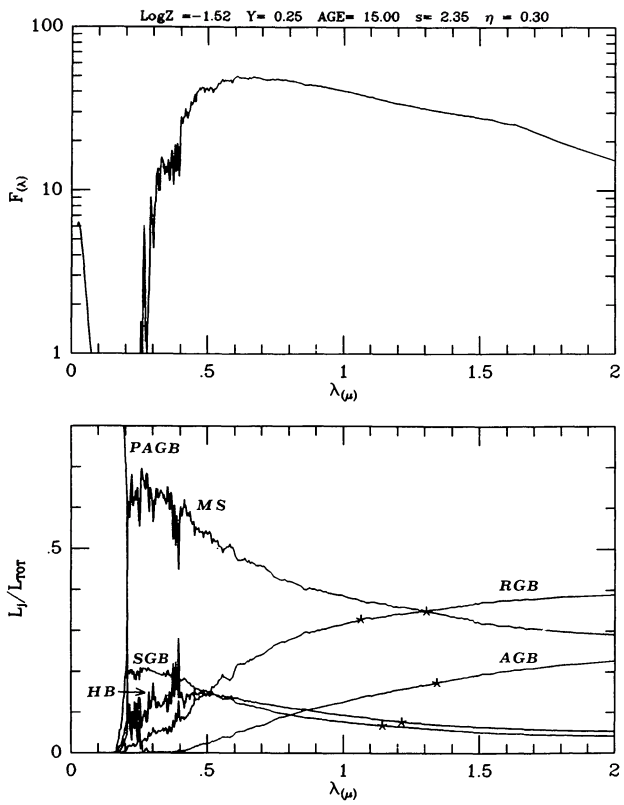

FIG. 20.—Same as Fig. 19, but for $t = 15$ Gyr and an R-HB morphology.

Among the many people who directly or indirectly contributed to the ideas on which this work rests, I wish to mention Flavio Fusi Pecci and Alvio Renzini: their patience and professional competence helped greatly in refining my feeling about the topics here approached. It is a pleasure also to thank Guido Chincarini for useful comments on the draft, and Andrew Pickles, the referee of this paper, for his pertinent and helpful suggestions.

I cannot avoid a posthumous word of thankful appreciation to Beatrice Tinsley: her brilliant intuitions provided the fruitful background on which most of this has grown.

Finally, I wish to dedicate this work to my father and my mother: their support has been invaluable to me throughout the many years spent on this project.

This research has been supported by the GNA of the Italian Consiglio Nazionale delle Ricerche and by the Ministero della Pubblica Istruzione.

REFERENCES

Aaronson, M., Frogel, J. A., and Persson, S. E. 1978, *Ap. J.*, **220**, 442.
Arimoto, N., and Yoshii, Y. 1986, *Astr. Ap.*, **164**, 260.
Ažusienis, A., and Straižys, V. 1969, *Soviet Astr.*, **13**, 316.
Barbaro, G., and Olivi, F. 1989, *Ap. J.*, **337**, 125.
Bell, R. A., and Gustafsson, B. 1978, *Astr. Ap. Suppl.*, **34**, 229 (BG78).
Bertelli G., Chiosi, and C., and Bertola, F. 1989, preprint.
Bertola, F. 1988, invited paper presented at the Goddard Space Flight Center Symposium on A Decade of UV Astronomy with the *IUE* Satellite.
Boesgaard, A. M., and Steigman, G. 1985, *Ann. Rev. Astr. Ap.*, **23**, 319.
Boulade, O., Rose, J. A., and Vigroux, L. 1988, *A.J.*, **96**, 1319.
Bruzual, A. G. 1983, *Ap. J.*, **273**, 105.
Burstein, D. 1979, *Ap. J.*, **232**, 74.
Burstein, D., Bertola, F., Buson, L. M., Faber, S. M., and Lauer, T. R. 1988, *Ap. J.*, **328**, 440.
Buser, R. 1978*a*, *Astr. Ap.*, **62**, 411.
_____. 1978*b*, *Astr. Ap.*, **62**, 425.
Buser, R., and Kurucz, R. L. 1978, *Astr. Ap.*, **70**, 555.
Buzzoni, A. 1982, thesis dissertation, Bologna University.
_____. 1988, in *Proc. Erice Workshop, Toward Understanding Galaxies at Large Redshift*, ed. R. G. Kron and A. Renzini (Dordrecht: Kluwer), p. 61.
Buzzoni, A., Fusi Pecci, F., Buonanno, R., and Corsi, C. E. 1983, *Astr. Ap.*, **128**, 94.
Cameron, L. M. 1985, *Astr. Ap.*, **146**, 59.
Campins, H., Rieke, G. H., and Lebofsky, M. J. 1985, *A.J.*, **90**, 896.
Caputo, F. 1983, *Astr. Ap.*, **128**, 190.
Carney, B. W. 1979, *Ap. J.*, **233**, 211.
Ciardullo, R. B., and Demarque, P. 1977, *Trans. Astr. Obs. Yale Univ.*, **35**, 1.
Code, A. D., Davis, J., Bless, R. C., and Hanbury Brown, R. 1976, *Ap. J.*, **203**, 417.
Cohen, J. G., Frogel, J. A., Persson, S. E., and Elias, J. H. 1981, *Ap. J.*, **249**, 481.
Copeland, H., Jensen, J. O., and Jørgensen, H. E. 1970, *Astr. Ap.*, **5**, 12.
Crocker, D. A., Rood, R. T., and O'Connell, R. W. 1988, *Ap. J.*, **332**, 236.
D'Antona, F., and Mazzitelli, I. 1985, *Ap. J.*, **296**, 502.
Drukier, G. A., Fahlman, G. G., and Richer, H. B. 1988, *A.J.*, **95**, 1415.
Faber, S. M. 1973, *Ap. J.*, **179**, 731.
Faber, S. M., Burstein, D., and Dressler, A. 1977, *A.J.*, **82**, 941.
Flower, P. J. 1977, *Astr. Ap.*, **54**, 31.
Frogel, J. A., Persson, S. E., Aaronson, M., and Matthews, K. 1978, *Ap. J.*, **220**, 75.

Frogel, J. A., Persson, S. E., and Cohen, J. G. 1980, *Ap. J.*, **239**, 495.
Fusi Pecci, F., and Renzini, A. 1976, *Astr. Ap.*, **46**, 447.
_____. 1978, in *IAU Symposium 80, The HR Diagram*, ed. A. G. D. Philip and D. S. Hayes (Dordrecht: Reidel), p. 225.
Gingold, R. A. 1974, *Ap. J.*, **193**, 177.
_____. 1976, *Ap. J.*, **204**, 116.
Golay, M. 1974, *Introduction to Astronomical Photometry* (Dordrecht: Reidel), p. 11.
Gunn, J. E., Stryker, L. L., and Tinsley, B. M 1981, *Ap. J.*, **249**, 48.
Hardorp, J. 1978, *Astr. Ap.*, **63**, 383.
_____. 1980, *Astr. Ap.*, **88**, 334.
Hayes, D. S., and Latham, D. W. 1975, *Ap. J.*, **197**, 593.
Hejlesen, P. M., Jørgensen, H. E., Otzen Petersen, J., and Rømcke, L. 1972, in *IAU Colloquium 17, Stellar Ages*, ed. C. Cayrel de Strobel and A. M. Delplace (Paris: Meudon Observatory), p. 36.
Iben, I., Jr. 1982, *Ap. J.*, **260**, 821.
Iben, I., Jr., and Renzini, A. 1982*a*, *Ap. J. (Letters)*, **259**, L79.
_____. 1982*b*, *Ap. J. (Letters)*, **263**, L188.
_____. 1983, *Ann. Rev. Astr. Ap.*, **21**, 271.
Iben, I., Jr., and Rood, R. T. 1970, *Ap. J.*, **161**, 587.
Iben, I., Jr., and Truran, J. W. 1978, *Ap. J.*, **220**, 980.
Jacoby, G. H., Hunter, D. A., and Christian, C. A. 1984, *Ap. J. Suppl.*, **56**, 257.
Johnson, H. L. 1965, *Ap. J.*, **141**, 923.
_____. 1966, *Ann. Rev. Astr. Ap.*, **4**, 193.
Kurucz, R. L. 1979, *Ap. J. Suppl.*, **40**, 1.
Labs, D., and Neckel, H. 1970, *Solar Phys.*, **15**, 79.
Lee, T. A. 1970, *Ap. J.*, **162**, 217.
Magain, P. 1983, *Astr. Ap.*, **122**, 225.
Matthews, T. A., and Sandage, A. R. 1963, *Ap. J.*, **138**, 30.
Mendoza V., E. E., and Johnson, H. L. 1965, *Ap. J.*, **141**, 161.
Mengel, J. G., Sweigart, A. V., Demarque, P., and Gross, P. G. 1979, *Ap. J. Suppl.*, **40**, 733.
Neece, G. D. 1984, *Ap. J.*, **277**, 738.
Nissen, P. E. 1970, *Astr. Ap.*, **6**, 138.
Nissen, P. E., and Gustafsson, B. 1978, in *Important Advances in Twentieth Century Astronomy*, ed. A. Reiz and T. Andersen (Copenhagen: Royal Danish Academy of Science and Letters), p. 43.
O'Connell, R. W. 1973, *A.J.*, **78**, 1074.
_____. 1980, *Ap. J.*, **236**, 430.
Oke, J. B., and Schild, R. 1970, *Ap. J.*, **161**, 1015.
Paczyński, B. 1970, *Acta Astr.*, **20**, 47.
_____. 1971, *Acta Astr.*, **21**, 47.
_____. 1975, *Ap. J.*, **202**, 558.
Pickles, A. J. 1985*a*, *Ap. J.*, **296**, 340.
_____. 1985*b*, *Ap. J. Suppl.*, **59**, 33.
Pickles, A. J., and Van der Kruit, P. C. 1988, in *Proc. Erice Workshop, Toward Understanding Galaxies at Large Redshift*, ed. R. G. Kron and A. Renzini (Dordrecht: Kluwer), p. 29.
Reimers, D. 1975, *Mém. Soc. Roy. Sci. Liège*, 6th Ser., **8**, 369.
Renzini, A. 1981, *Ann. de Phys.* **6**, 87.
Renzini, A., and Buzzoni, A. 1983*a*, in *Proc. RAL Workshop, Spectral Evolution of Galaxies*, ed. P. M. Gondhalekar (Chilton: Rutherford Appleton Laboratory), p. 86.
_____. 1983*b*, *Mem. Soc. Astr. Italiana*, **54**, 739.
_____. 1986, in *Proc. Erice Workshop, Spectral Evolution of Galaxies*, ed. C. Chiosi and A. Renzini (Dordrecht: Reidel), p. 195 (RB86).
Renzini, A., and Voli, M. 1981, *Astr. Ap.*, **94**, 175.
Richer, H. 1981, *Ap. J.*, **243**, 744.
Ridgway, S. T., Joyce, R. R., White, N. M., and Wing, R. F. 1980, *Ap. J.*, **235**, 126.
Rood, R. T. 1983, *Ap. J.*, **184**, 815.
Rose, J. A. 1985, *A.J.*, **90**, 1927.
Sandage, A. R. 1969, *Ap. J.*, **158**, 1115.
Sandage, A. R., and Fouts, G. 1988, *A.J.*, **93**, 74.
Sandage, A. R., and Wildey, R. 1967, *Ap. J.*, **150**, 469.
Schönberner, D. 1979, *Astr. Ap.*, **94**, 175.
_____. 1981, *Astr. Ap.*, **103**, 119.
Seidel, E., Demarque, P., and Weinberg, D. 1987, *Ap. J. Suppl.*, **63**, 917.
Sienkiewicz, R. 1982, *Acta Astr.*, **32**, 275.
Sil'chenko, O. K. 1983, *Soviet Astr. Letters*, **9**, 145.
Spinrad, H., and Taylor, B. J. 1969*a*, *Ap. J.*, **157**, 1279.
_____. 1969*b*, *Ap. J. Suppl.*, **22**, 445.
Straižys, V., and Sviderskiene, Z. 1972, *Bull. Vilnius Astr. Obs.*, **35**, 1.
Sweigart, A. V. 1987, *Ap. J. Suppl.*, **65**, 95.
Seigart, A. V., and Gross, P. G. 1976, *Ap. J. Suppl.*, **32**, 367.
_____. 1978, *Ap. J. Suppl.*, **36**, 405.
Tinsley, B. M. 1978, *Ap. J.*, **222**, 14.
Tinsley, B. M., and Gunn, J. E. 1976, *Ap. J.*, **203**, 52 (TG76).
Tsuji, T. 1978, *Pub. Astr. Soc. Japan*, **30**, 435.
Tüg, H., White, N. M., and Lockwood, G. W. 1977, *Astr. Ap.*, **61**, 679.
VandenBerg, D. A. 1983, *Ap. J. Suppl.*, **51**, 29.
_____. 1985, *Ap. J. Suppl.*, **58**, 711.
VandenBerg, D. A., and Bell, R. A. 1985, *Ap. J. Suppl*, **58**, 561.
VandenBerg, D. A., Hartwick, F. D. A., and Alexander, D. R. 1983, *Ap. J.*, **266**, 747.
VandenBerg, D. A., and Laskarides, P. G. 1987, *Ap. J. Suppl.*, **64**, 103.
Wagoner, R. V. 1973, *Ap. J.*, **179**, 343.
Whitford, A. E. 1973, in *IAU Symposium 58, The Formation and Dynamic of Galaxies*, ed. J. R. Shakeshaft (Dordrecht: Reidel), p. 169.
_____. 1977, *Ap. J.*, **211**, 527.
Wood, P. R., and Cahn, J. H. 1977, *Ap. J.*, **211**, 499.

ALBERTO BUZZONI: Osservatorio Astronomico di Brera, Via Brera, 28, 20121 Milano, Italy